

## TWO-DIMENSIONAL QUANTUM ANTIFERROMAGNETS

Grégoire MISGUICH

*Service de Physique Théorique, CEA/DSM/SPhT  
Unité de recherche associée au CNRS  
CEA/Saclay 91191 Gif-sur-Yvette Cédex, France  
E-mail: gmisguich@cea.fr*

Claire LHUILLIER

*Laboratoire de Physique Théorique des Liquides  
Université P. et M. Curie and UMR 7600 of CNRS  
Case 121, 4 Place Jussieu, 75252 Paris Cédex, France  
E-mail: claire.lhuillier@lptl.jussieu.fr*

### Contents

1	Introduction . . . . .	3
2	$J_1$ - $J_2$ model on the square lattice . . . . .	4
2.1	Classical ground-state and spin-wave analysis . . . . .	5
2.2	Order by disorder ( $J_2 > J_1/2$ ) . . . . .	6
2.3	Non-magnetic region ( $J_2 \simeq J_1/2$ ) . . . . .	7
2.3.1	Series expansions . . . . .	8
2.3.2	Exact diagonalizations . . . . .	10
2.3.3	Quantum Monte Carlo . . . . .	10
3	Valence-bond crystals . . . . .	12
3.1	Definitions . . . . .	12
3.2	One-dimensional and quasi one-dimensional examples (spin- $\frac{1}{2}$ systems) . . . . .	13
3.3	Valence Bond Solids . . . . .	14
3.4	Two-dimensional examples of VBC . . . . .	15
3.4.1	Without spontaneous lattice symmetry breaking . . . . .	15
3.4.2	With spontaneous lattice symmetry breaking . . . . .	17
3.5	Methods . . . . .	19

3.6	Summary of the properties of VBC phases . . . . .	20
4	Large- $N$ methods . . . . .	21
4.1	Bond variables . . . . .	22
4.2	$SU(N)$ . . . . .	23
4.3	$Sp(N)$ . . . . .	23
4.3.1	Gauge invariance . . . . .	25
4.3.2	Mean-field ( $N = \infty$ limit) . . . . .	25
4.3.3	Fluctuations about the mean-field solution . . . . .	26
4.3.4	Topological effects - instantons and spontaneous dimerization . . . . .	28
4.3.5	Deconfined phases . . . . .	29
5	Quantum Dimer Models . . . . .	30
5.1	Hamiltonian . . . . .	30
5.2	Relation with spin- $\frac{1}{2}$ models . . . . .	31
5.3	Square lattice . . . . .	33
5.3.1	Transition graphs and topological sectors . . . . .	33
5.3.2	Staggered VBC for $V/J > 1$ . . . . .	34
5.3.3	Columnar crystal for $V < 0$ . . . . .	34
5.3.4	Plaquette phase . . . . .	35
5.3.5	Rokhsar-Kivelson point . . . . .	35
5.4	Hexagonal lattice . . . . .	36
5.5	Triangular lattice . . . . .	37
5.5.1	RVB liquid at the RK point . . . . .	38
5.5.2	Topological order . . . . .	39
5.6	Solvable QDM on the kagome lattice . . . . .	40
5.6.1	Hamiltonian . . . . .	40
5.6.2	RK ground-state . . . . .	40
5.6.3	Ising pseudo-spin variables . . . . .	42
5.6.4	Dimer-dimer correlations . . . . .	43
5.6.5	Visons excitations . . . . .	43
5.6.6	Spinons deconfinement . . . . .	45
5.6.7	$\mathbb{Z}_2$ gauge theory . . . . .	46
5.7	A QDM with an extensive ground-state entropy . . . . .	47
6	Multiple-spin exchange models . . . . .	48
6.1	Physical realizations of multiple-spin interactions . . . . .	48
6.1.1	Nuclear magnetism of solid $^3\text{He}$ . . . . .	48
6.1.2	Wigner crystal . . . . .	50
6.1.3	Cuprates . . . . .	50
6.2	Two-leg ladders . . . . .	50
6.3	MSE model on the square lattice . . . . .	52
6.4	RVB phase of the triangular $J_2$ - $J_4$ MSE . . . . .	52
6.4.1	Non-planar classical ground-states . . . . .	53
6.4.2	Absence of Néel LRO . . . . .	53
6.4.3	Local singlet-singlet correlations - absence of lattice symmetry breaking . . . . .	54
6.4.4	Topological degeneracy and Lieb-Schultz-Mattis Theorem . . . . .	55
6.4.5	Deconfined spinons . . . . .	56

6.5	Other models with MSE interactions . . . . .	57
7	Antiferromagnets on the kagome (and related) lattices . . . . .	58
7.1	Miscellaneous models on the kagome lattice . . . . .	58
7.2	Spin- $\frac{1}{2}$ Heisenberg model on the kagome lattice: an extreme play-ground for “quantum fluctuations” . . . . .	59
7.2.1	Ground-state energy per spin . . . . .	59
7.2.2	Correlations . . . . .	60
7.2.3	Spin-gap . . . . .	60
7.2.4	An exceptional density of low lying excitations in the singlet sector . . . . .	61
7.2.5	Absence of gap in the singlet sector . . . . .	64
7.2.6	Anomalous density of states in other spin sectors . . . . .	65
7.3	Next-neighbor RVB description of the spin- $\frac{1}{2}$ kagome antiferromagnet . . . . .	66
7.4	Experiments in compounds with kagome-like lattices . . . . .	67
7.5	”Haldane’s conjecture” . . . . .	67
8	Conclusions . . . . .	68
9	Acknowledgments . . . . .	70
	References . . . . .	70

## 1. Introduction

In this review we present some theoretical advances in the field of quantum magnetism in two-dimensional (2D) systems. The spin- $\frac{1}{2}$  next neighbor 2-dimensional Heisenberg model on Bravais lattices (square, triangular) is Néel ordered<sup>a</sup> at  $T = 0$ .<sup>1,2</sup> Frustration, small coordination number, competition between interactions can lead to specific quantum phases without magnetic long-ranged order. Since a decade this subject is a highly debated issue in the field of quantum magnetism. It was revived by the discovery of high- $T_c$  superconductivity in the doped cuprates and fueled by numerous experimental studies of 2D antiferromagnetic insulators.<sup>3</sup>

Section 2 is devoted to the first academic model of quantum frustration: the spin- $\frac{1}{2}$  Heisenberg model on the square lattice with first- and second-neighbor interactions ( $J_1$ - $J_2$  model). This model is one of the most studied in the field and this section is a short guide to the literature, with a special emphasis on the various methods used for this problem.

Section 3 deals with general properties of valence-bond crystals (VBC) and related states, the simplest phase which is commonly realized in frus-

<sup>a</sup>This generic kind of order, with a macroscopic sublattice magnetization is called in the following *magnetic* long-ranged order (LRO), in contrast to other ordered phases where the long-ranged ordered correlations concern  $S = 0$  scalar observables (on dimers, quadrumers...)

trated spin systems without magnetic LRO.

In section 4 we present large- $N$  generalizations of the Heisenberg model. This approach was extensively developed by Read and Sachdev from the early 90's and has been the first to give an insight into the alternative between VBC and related phases, which have long ranged order in local singlet patterns (whence the name of crystals), and resonating valence-bond (RVB) spin-liquids (SL) which are translationally invariant phases where the quantum coherence is a central issue.

Section 5 presents some results of quantum dimer models (QDM). These models are effective approaches to the quantum phases of antiferromagnets which are dominated by short-range valence-bonds (or singlets). They have received recently some special attention and provide useful insights onto the phenomenology of VBC and RVB SL.

In Section 6 we review some results concerning models with multiple-spin exchange (MSE) (also called ring exchange) interactions. These interactions are now recognized to be present in several physical systems and appear to play an important role in the stabilization of RVB liquid ground-states.

The last section is devoted to the Heisenberg model on the kagome lattice (and related models). Despite of an important activity on this subject, the understanding of the low-energy physics of the spin- $\frac{1}{2}$  kagome antiferromagnet remains a challenging problem and we discuss some of the important results and questions.

We should warn the readers that this review is quite “inhomogeneous” and cannot, of course, replace textbooks.<sup>4,5,6,7</sup> While some parts deal with some rather recent works (QDM or MSE for instance), some others are devoted to older results which we think are still of importance for current research (beginning of the section  $J_1$ - $J_2$ , large- $N$ ). The final part devoted to kagome reflects our own views and some unpublished material on still unsettled issues. Some parts are intended to be more pedagogical and concrete (QDM and beginning of large- $N$  section) while some others contain more qualitative discussions of the physical issues (end of the section  $J_1$ - $J_2$ , VBC, kagome).

## 2. $J_1$ - $J_2$ model on the square lattice

We consider the following Heisenberg model on the square lattice:

$$\mathcal{H} = 2J_1 \sum_{\langle ij \rangle} \vec{S}_i \cdot \vec{S}_j + 2J_2 \sum_{\langle\langle ij \rangle\rangle} \vec{S}_i \cdot \vec{S}_j \quad (1)$$

where  $\langle ij \rangle$  and  $\langle\langle ij \rangle\rangle$  denote pairs of nearest and next-nearest neighbors respectively. Although quite simple in appearance, this spin model realizes several interesting phenomena which are relevant to a large class of 2D frustrated quantum magnets: classical degeneracy, order by disorder, destruction of some long-ranged order by quantum fluctuations, break down of the spin-wave expansion, opening of a spin gap and (possibly ?) spontaneous translation symmetry breaking, etc. For this reason we start with a general overview of some important results concerning this system. We will focus on the properties related to *frustration*. A review on the non-frustrated model ( $J_2 = 0$ ) can be found in Ref.<sup>1</sup>

### 2.1. Classical ground-state and spin-wave analysis

It is easy to find *some* classical ground-state of a translation invariant Heisenberg model on a Bravais lattice because the energy can always be minimized by a planar helix

$$\vec{S}_{\mathbf{r}} = \vec{e}_1 \cos(\mathbf{q} \cdot \mathbf{r}) + \vec{e}_2 \sin(\mathbf{q} \cdot \mathbf{r}) \quad (2)$$

provided that the pitch  $\mathbf{q}$  minimizes the Fourier transform  $J(\mathbf{q})$  of the coupling.<sup>8</sup> In the case of the  $J_1$ - $J_2$  model one has

$$J(\mathbf{q}) = 2J_1 (\cos(q_x) + \cos(q_y)) + 2J_2 (\cos(q_x + q_y) + \cos(q_x - q_y)) \quad (3)$$

- $J_2 < 0.5J_1$ :  $J(\mathbf{q})$  has a single minimum at  $(\pi, \pi)$ . It corresponds to the “usual” Néel state.
- $J_2 > 0.5J_1$ :  $J(\mathbf{q})$  has two isolated minima at  $(0, \pi)$  and  $(\pi, 0)$ . They correspond to ferromagnetic lines (resp. columns) arranged in an antiferromagnetic way. These states are sometimes called *collinear* (in *real* space). From these planar helix states one can build many other ground-states by rotating globally all the spins of one sublattice with respect to the other. Although this costs no energy for classical spins at zero temperature, it is known (order from disorder, see below) that configurations where both sublattices have their staggered magnetization *collinear in spin space* are selected by thermal or quantum fluctuations.
- $J_2 = 0.5J_1$ :  $J(\mathbf{q})$  has lines of minima around the edges of the Brillouin zone. At this point the classical ground-state is highly degenerate : We can write  $\mathcal{H} = \text{cst} + J_2 \sum (S_1 + S_2 + S_3 + S_4)^2$  where the sum runs over all square plaquettes and any state where each plaquette has a vanishing total spin minimizes the classical energy.

Even at the lowest order in  $1/S$ , zero-temperature quantum corrections to the sublattice magnetization (order parameter) diverge around  $J_2 = 0.5J_1$  (Chandra and Douçot<sup>9</sup>). Such large- $S$  approximation usually tends to overestimate the stability of magnetic phases, therefore this breakdown around  $J_2 \sim 0.5J_1$  is a strong evidence for the existence of quantum disordered phase(s) in this region of parameter space.

## 2.2. Order by disorder ( $J_2 > J_1/2$ )

The concept of “order by disorder” was introduced in 1980 by Villain and co-workers<sup>10</sup> in the study of a frustrated Ising model on the square lattice. In this model the next neighbor couplings along the rows are ferromagnetic as well as those on the odd columns (named  $A$  in the following). The couplings on the even columns (named  $B$ ) are antiferromagnetic. At  $T = 0$  the ground-state has no average magnetization and is disordered. This changes when thermal fluctuations are introduced: a  $B$ -chain sandwiched between two  $A$  chains with parallel spins has *lower excitations* than a  $B$  chain between two  $A$ -chains with anti-parallel spins. This gives a larger Boltzmann weight to ferrimagnetically ordered states. Villain *et al.* have exactly shown that the system is indeed ferrimagnetic at low temperature. They were also able to show that site dilution (non-magnetic sites) selects the same ordered pattern, whence the name of “order by disorder”.

A somewhat less drastic phenomenon has been observed in quantum systems. It is the selection of particular long-ranged ordered quantum states among a larger family of ordered solutions which are classically degenerate at  $T = 0$ .<sup>b</sup> Consider a spin system in which the molecular field created by the spins of one sublattice on the other cancels, which is the case when  $J_2 > 0.5J_1$ . Shender<sup>11</sup> showed that if fluctuations are included, the system will select states in which all spins are collinear to each other. This follows from the fact that (moderate) fluctuations at one site are orthogonal to the mean value of the magnetization at that site and the system can gain some magnetic exchange energy by making such fluctuations coplanar on neighboring sites, that is to making the spins collinear. Such a selection of

<sup>b</sup>In Villain’s model the system is truly disordered at  $T = 0$  and an ordered solution is entropically selected at finite temperature. In the quantum  $J_1$ - $J_2$  model above, the classical solutions can adopt various ordered patterns: quantum fluctuations select among these patterns the most ordered one, that is the situation with the highest symmetry and the smallest degeneracy. The ultimate effect of these quantum fluctuations can be the destruction of the Néel order in favor of a fully quantum ground-state with  $\mathcal{O}(1)$  degeneracy.

order by quantum fluctuations (and dilution) was discussed by Henley<sup>12</sup> and appears also quite straightly in a spin-wave expansion.<sup>13</sup>

This selection of the  $(\pi, 0)$  or  $(0, \pi)$  order spontaneously breaks a four-fold lattice symmetry. An Ising order parameter is thus generated. It takes two values depending whether the ferromagnetic correlations are locally arranged horizontally or vertically. Chandra and co-workers<sup>14</sup> have studied this mechanism and predicted the existence of a finite temperature Ising phase transition independent of the subsequent development of a sublattice magnetization. This result has been questioned recently<sup>15</sup> and the transition has not been observed so far in the spin- $\frac{1}{2}$  model.<sup>16,15</sup> It has however been confirmed by some recent Monte Carlo simulations of the *classical* Heisenberg model.<sup>17</sup> Very similar phenomena are present in the  $J_1$ - $J_2$  quantum Heisenberg model on the *triangular* lattice.<sup>18,19,20,21</sup>

Melzi *et al.*<sup>22,23</sup> have studied a quasi 2D spin- $\frac{1}{2}$  system which is believed to be a  $J_1$ - $J_2$  square lattice Heisenberg antiferromagnet. They found some evidence (splitting of NMR lines) for a collinear  $((\pi, 0)$  or  $(0, \pi))$  magnetic ordering. Several estimates<sup>23,24,25,16</sup> indeed point to  $J_2 > J_1$  in this compound.

### 2.3. Non-magnetic region ( $J_2 \simeq J_1/2$ )

Consider the two classical “Ising states” corresponding to the wave vectors  $(\pi, \pi)$  and  $(\pi, 0)$ . They can be taken as (crude) variational states for the Hamiltonian Eq. 1. Their energies (per site) are  $E_{\pi, \pi} = -J_1 + J_2$  and  $E_{\pi, 0} = -J_2$ . As discussed above, these states cross at  $J_2 = \frac{1}{2}J_1$ . However, one can also consider any first-neighbor singlet (or valence-bond) covering of the lattice as another variational state. In such a completely dimerized state the expectation value of the energy per site is  $E_{dimer} = -\frac{3}{4}J_1$ , which is below the two Ising states around  $J_2 \simeq J_1/2$ . Of course this very simple argument does not prove anything since “dressing” these classical states with quantum fluctuations (spin flips in the Néel-like states or valence-bond motions in the dimerized wave-functions) will lower the energies of all these trial states and it is absolutely not clear which one may eventually win. Nevertheless, this shows in a simple way why non-magnetic states (*i.e.* rotationally invariant or spin singlet) such as dimerized states can be a route to minimize the energy in a frustrated magnet.<sup>c</sup>

<sup>c</sup>Klein<sup>26</sup> introduced a general procedure to generate local and  $SU(2)$  symmetric Hamiltonians for which any first-neighbor dimerized state is an exact ground-state. These

### 2.3.1. Series expansions

High-order series expansions can be a powerful technique to investigate frustrated quantum magnets. The general method to generate zero-temperature perturbation expansions in quantum many-body systems was described by Singh *et al.*<sup>28</sup> and Gelfand *et al.*<sup>29</sup> For instance, one can consider the following anisotropic model:

$$\begin{aligned} \mathcal{H}(\lambda) = & 2J_1 \sum_{\langle ij \rangle} [S_i^z S_j^z + \lambda (S_i^x S_j^x + S_i^y S_j^y)] \\ & + 2J_2 \sum_{\langle\langle ij \rangle\rangle} [S_i^z S_j^z + \lambda (S_i^x S_j^x + S_i^y S_j^y)] \end{aligned} \quad (4)$$

$\mathcal{H}(\lambda = 0)$  is a classical Ising model which ground-state is known. The series expansion about the Ising limit amounts to compute expectation values in the ground-state  $|\lambda\rangle$  of  $\mathcal{H}(\lambda)$  in powers of  $\lambda$ :

$$\frac{\langle \lambda | \hat{O} | \lambda \rangle}{\langle \lambda | \lambda \rangle} = \sum_n a_n \lambda^n, \quad (5)$$

(energy gaps, dispersion relations and susceptibilities can also be computed in the same approach). The calculation of  $a_n$  requires the enumeration and evaluation of the *connected clusters* of size  $\sim n$ , whose number grows exponentially with  $n$ . Depending on the quantity  $\hat{O}$  and on the model, orders from 7 to 20 can typically be obtained on present computers. The series is then extrapolated to  $\lambda = 1$  by standard Padé, Dlog Padé or integrated differential approximations. Such a series expansion about the Ising limit was done by Weihong *et al.*<sup>30</sup> for the first neighbor square-lattice antiferromagnet. Oitmaa and Weihong<sup>31</sup> extended the series to the  $J_1$ – $J_2$  model, where each  $a_n$  is now a polynomial in  $J_1$  and  $J_2$ . The disappearance of Néel order in the Heisenberg model manifests itself by a vanishing sublattice magnetization as well as some singular behavior of the series for  $\lambda_c < 1$ . The results indicate the absence of Néel long-ranged order in the strongly frustrated region  $0.4 \leq J_2/J_1 \leq 0.6$ . Such an expansion can locate with a reasonable accuracy the phase boundary of the Néel ordered regions but provides no direct information on the nature of the non-magnetic phase.

To study the model around  $J_2 \simeq J_1/2$ , several other expansions have been carried out. A dimer expansion about an exactly dimerized model was done by Gelfand *et al.*,<sup>32</sup> Gelfand,<sup>33</sup> Singh *et al.*<sup>34</sup> and Kotov *et al.*<sup>35</sup> In

---

Hamiltonians are simply defined as sums of projectors which annihilate all dimer coverings. The Majumdar-Gosh<sup>27</sup> chain is the simplest example of a “Klein model”.



this approach  $J_1$  and  $J_2$  are set to zero everywhere except on isolated bonds arranged in a columnar way and all the other couplings are treated perturbatively. At zeroth order the ground-state is simply a product of singlets. In these calculations the dimerized phase remains stable in the intermediate region. Singh *et al.*<sup>34</sup> also performed a different kind of zero-temperature series expansion. They started from a model of isolated 4-spin plaquettes in order to check a prediction made by Zhitomirsky and Ueda<sup>36</sup> that such plaquettes could spontaneously form around  $J_2 \simeq J_1/2$  to produce a state which is invariant under  $\pi/4$  lattice rotations. Although the ground-state energy they obtained is very close to the one obtained from the dimerized limit (within error bars of the extrapolation procedure) they observed an instability in the plaquette scenario (the triplet gap vanishes before reaching the isotropic square-lattice model) which suggests that plaquette order is not the issue (the analysis of the exact numerical spectra for 36 sites confirmed this result<sup>37</sup>).

Sushkov *et al.*<sup>38</sup> (improved numerical results compared to Ref.<sup>39</sup>) computed the susceptibility  $\chi_D$  associated with the appearance of columnar dimer order in the  $(\pi, \pi)$  Néel phase by a series expansion about the Ising limit. Such a susceptibility seems to diverge at  $J_2/J_1 = g_{c1} \simeq 0.405 \pm 0.04$ . On the other hand the disappearance of the magnetic LRO is observed (through the Néel order parameter or through the anisotropy in spin space of the spin-spin correlations) at  $J_2/J_1 = g_{c2} \simeq 0.39 \pm 0.02$ . This point could a priori be *different* from  $g_{c1}$ . In such a case the system would first break the  $\pi/4$  lattice rotation symmetry at  $g_{c1}$ , while magnetic LRO remains (gapless spin waves). Only at  $g_{c2} > g_{c1}$  the  $SU(2)$  rotation symmetry is restored and the magnetic excitations acquire a gap. From field theoretical arguments based on effective actions valid close to the critical points, Sushkov *et al.*<sup>38</sup> argue that the proximity (or possible equality) of  $g_{c1}$  and  $g_{c2}$  is a general feature in frustrated magnets which originate from the coupling of triplet and singlet excitations.

Sushkov *et al.*<sup>39</sup> computed susceptibility  $\chi_P$  associated to plaquette order by an expansion around the dimerized limit, assuming that the system has columnar dimer LRO. The result shows a divergence of  $\chi_P$  when  $J_2/J_1 \rightarrow g_{c3} = 0.5 \pm 0.02$ . From these results Sushkov *et al.* suggested that the translation symmetry along the columns is broken down at  $g_{c3}$  (giving rise to an eight-fold degenerate ground-state in the thermodynamic limit) before the  $(\pi, 0) - (0, \pi)$  magnetically ordered phase appears at  $g_{c4} \simeq 0.6$ . This picture is qualitatively consistent with the spin-spin correlations computed in a  $10 \times 10$  system with a density matrix renormalization group

(DMRG) algorithm.<sup>40</sup>

Due to the relatively short series (typically of order 7) involved and the uncertainties in the extrapolation procedures, such results should be confirmed by other methods but this succession of quantum phase transitions represents a very interesting scenario. We note that if the model has a fully symmetric liquid ground-state in some parameter range, it should be difficult to capture from series expansions about limits where some lattice symmetries are explicitly broken.

### 2.3.2. *Exact diagonalizations*

Exact diagonalizations have a priori no bias, and were used very early in this field.<sup>41,42,43</sup> Large-size computations and sophisticated finite size scaling analysis are nevertheless needed to extract significant information. Schulz *et al.*<sup>44</sup> performed extensive exact diagonalizations of the  $J_1$ - $J_2$  model for system sizes up to 36 sites. They analyzed the behavior of several quantities such as structure factors (Néel order parameter), ground-state energy, spin-wave velocities (obtained from the finite size corrections to the ground-state energy), spin stiffness and uniform susceptibility. Their analysis, including quantitative comparisons with non-linear sigma model predictions,<sup>45</sup> concluded to the absence of Néel long-ranged order in the strongly frustrated region  $0.4 \leq J_2/J_1 \leq 0.6$ . There, they show enhanced columnar dimer-dimer correlations as well as chiral ones but the size effects were not clear enough to discriminate between short or long-ranged order for these order parameters.

### 2.3.3. *Quantum Monte Carlo*

Quantum Monte Carlo (QMC) methods have been extensively applied to the  $J_1$ - $J_2$  model in the low frustration regime giving an highly accurate description of the Néel phase (Sandvik<sup>46</sup> and Refs. therein). In the non-magnetic and highly frustrated regime a simple QMC approach is ineffective due to the so-called sign problem. The fixed node approach is the first answer to this problem: the exact imaginary time propagator  $e^{-\tau\mathcal{H}}$  used to filter out the ground-state from a variational guess  $|\psi_g\rangle$  is replaced by an approximate propagator, which has the same nodes as  $|\psi_g\rangle$ . The quality of the result depends on the quality of the nodal regions of  $|\psi_g\rangle$ . Various schemes have been used to try to go beyond this limitation: stochastic reconfiguration (Sorella<sup>47</sup>), eventually associated to a few Lanczos iterations.<sup>48,37</sup> An alternative method has been devised by du Croo de Jongh *et al.*,<sup>40</sup> where

the guiding function is replaced by the result of a DMRG calculation.<sup>49,50</sup> Both methods have their own bias. Using the first of them, Capriotti and Sorella<sup>37</sup> concluded that for  $J_2/J_1 \sim 0.45$  a Gutzwiller-projected BCS wave-function  $|p \text{ BCS}\rangle$  was an excellent guiding wave-function:

$$|p \text{ BCS}\rangle = \hat{\Pi} |BCS\rangle \quad (6)$$

$$|BCS\rangle = \exp \left( \sum_{i,j} f_{i,j} c_{i\uparrow}^\dagger c_{j\downarrow}^\dagger \right) |0\rangle \quad (7)$$

where  $|0\rangle$  is the fermion vacuum,  $c_{i\uparrow}^\dagger c_{j\downarrow}^\dagger$  creates a valence-bond on sites  $(i, j)$  and  $\hat{\Pi}$  projects out states with double occupancy. The pairing amplitude  $f_{i,j}$  (often called gap function  $\Delta_k$ )<sup>d</sup> is optimized with a Monte Carlo algorithm in order to minimize the energy. Capriotti and Sorella gave convincing indications that their wave-function is quite accurate. The best variational energies are obtained in the frustrated region with a pairing amplitude which mixes  $d_{x^2-y^2}$  and  $d_{xy}$  symmetries. In particular it reproduces the correct nodal structure of the ground-state in the frustrated region at least for moderate system sizes where the variational result can be checked against the exact result. This is a subtle and non-trivial information for systems which do not obey the Marshall's sign rule as this frustrated model. They concluded from these results that the system probably had no long-ranged order neither in dimer-dimer correlations nor in four-spin plaquette correlations. On the other hand, du Croo de Jongh *et al.* argued in favor of columnar dimerized phase which also break the translation symmetry along the columns (plaquette-like correlations similar to those found by series expansions<sup>39</sup>).

The comparison of the results of these different approaches shows that this problem remains a very challenging one. The model in the frustrated regime is probably never very far from a quantum critical point and in these conditions none of the available methods seems able to discriminate between a VBC with tiny gaps both in the singlet and triplet sectors, a critical phase with a quasi order in dimers and gapless singlet excitations, or a true SL with gaps in any sector of spin but no long ranged order in any observable. As we will explain in the following sections some other frustrated models are happily deeper in the strong coupling regime and exhibit quantum phases which are easier to characterize.

<sup>d</sup>After the Gutzwiller projection  $\Delta_k$  is no longer the observable gap.<sup>51</sup>

### 3. Valence-bond crystals

#### 3.1. Definitions

Among the different quantum solutions to overcome frustration the VBC is the simplest scenario. In this phase, neighboring spins arrange themselves in a regular pattern of singlets: dimers,<sup>a</sup> quadrumers or  $2n$ -mers  $S = 0$  plaquettes. The stability of this phase comes from the extreme stability of small  $S = 0$  clusters (recall that the energy of a singlet of two spins  $\frac{1}{2}$  is  $-3/4$  to be compared to the energy of two classical (or Ising) spins which is only  $-1/4$ ), and eventually from the fact that frustrated bonds between two different singlets do not contribute to the total energy.

In a VBC phase there is no  $SU(2)$  symmetry breaking, no long-ranged order in spin-spin correlations, but long-ranged order in dimer-dimer or larger singlet units. Except at a quantum critical point, all excitations of a VBC are gapped. Depending on the lattice geometry, such a wave function can spontaneously break some lattice symmetry (*spontaneous VBC*) or can remain fully symmetric (*explicit VBC*). In a strict sense, the name VBC should be reserved for systems with a spontaneous lattice symmetry breaking. However, since these two kinds of systems share many similarities we will discuss both in this section.

When the Hamiltonian has some inequivalent bonds and an integer spin in the unit cell (even number of spin- $\frac{1}{2}$  for instance) the system can take full advantage of the strong bonds and minimize the effects of the frustrating ones. In that case the *explicit* VBC is the “natural” strong coupling solution. One can build a simple Hamiltonian in which the bonds which are not occupied by the singlet objects are turned off. The resulting model is a set of small decoupled clusters (dimers or larger plaquettes) and the ground-state is a trivial product of singlets. Importantly, this strong coupling limit has the same lattice symmetry as the original one. Going back to the original Hamiltonian *no quantum phase transition is encountered when going from the trivial singlet product up to real interacting ground-state*. Models with an half-odd-integer spin in the unit cell cannot realize a VBC unless they *spontaneously* enlarge their unit cell. In these situations there is no unique elected position for the  $2n$ -mers and a symmetry breaking must take place in order to form a VBC. Examples of these two kinds of VBC will be given below.

<sup>a</sup>whence the name Spin Peierls phase sometimes given to the VBC phase.

### 3.2. One-dimensional and quasi one-dimensional examples (spin- $\frac{1}{2}$ systems)

One of the simplest example of (spontaneous) VBC is observed in the  $J_1$ - $J_2$  model on the chain for  $J_2/J_1 > (J_2/J_1)_c \sim 0.24$ .<sup>27,52,53,54,55</sup> For  $J_2/J_1 = 0.5$  the doubly degenerate ground-states are exact products of dimers:<sup>27,5</sup>

$$|MG_{\pm}\rangle = \prod_{n=1}^{N/2} |(2n, 2n \pm 1)\rangle. \quad (8)$$

Here and in the following we call “dimer” a pair of spins in a singlet state, and note it:

$$|(i, j)\rangle = \frac{1}{\sqrt{2}} [|i, +\rangle |j, -\rangle - |i, -\rangle |j, +\rangle]. \quad (9)$$

For all  $J_2/J_1 > (J_2/J_1)_c$ , the ground-states are products of dimers, dressed by fluctuations of valence bonds, dimer long-ranged order persists in all the range of parameters. This model has gapful excitations which can be described as pairs of scattering spin- $\frac{1}{2}$  solitons separating the two exact ground-states<sup>52</sup> (these fractionalized excitations are specific of the 1D chain).

The Heisenberg chain with alternating strong and weak bonds (Spin Peierls instability), has indeed a unique ground-state where the dimers are mainly located on the strong bonds. In that case, the spin- $\frac{1}{2}$  excitations are confined by the underlying potential and the true excitations are gapful integer magnons (<sup>56,57</sup> and refs. therein). It is an explicit VBC.

A two-leg ladder with AF rung exchange has also a unique VBC ground-state and gapped magnons as excitations.<sup>58</sup> On the other hand Nersesyan and Tsvelik<sup>59,60</sup> have proposed an example of frustrated ladder, with a spontaneously dimerized ground-state, and gapful excitations. Excitations of this last model are identified as pairs of singlet and triplet domain walls connecting the two ground-states, they form a continuum.

As can be seen from this rapid and non exhaustive enumeration, VBC ground-states are relatively frequent in frustrated one-dimensional spin- $\frac{1}{2}$  models. All these systems are gapful but the excitations could be of different nature emerging as modes (associated to integer spin excitations) or continuum of pairs of excitations that could be fractionalized (it is then specific of one dimensional systems) or not.

### 3.3. Valence Bond Solids

The VBS wave-function was introduced by Affleck, Kennedy, Lieb and Tasaki (AKLT).<sup>61,62</sup> It can be constructed whenever the spin  $S$  on a site is a multiple of one half the coordination number  $z$ :  $2S = 0 \bmod z$ . Let us consider the simplest case  $2S = z$ . In that case the local spin  $S$  can be seen as the symmetric combination of  $2S$  (fictitious) spin- $\frac{1}{2}$ . Now on each bond of the lattice one can make a singlet between two fictitious spins- $\frac{1}{2}$ . Such a product of singlets does not belong to the physical Hilbert space of the original spin- $S$  model but to a much larger space. The VBS wave-function is defined as the projection of the singlet-product state onto the physical space. This projection amounts to symmetrize (for all lattice sites) the wave-function with respect to the fictitious spins to force them into a physical spin- $S$  state. A VBS can be viewed as an *explicit VBC of the fictitious spins*. Simple Hamiltonians with short ranged and  $SU(2)$ -symmetric interactions for which the VBS is an exact ground-state can be constructed (sum of projectors<sup>61,62</sup>). By construction the VBS wave-function is a spin singlet and *breaks no lattice symmetry*. By extension we may say that a system is in a VBS *phase* if its ground-state can be adiabatically transformed into the VBS wave-function without crossing a phase transition. As the VBC, models in the VBS phase have a gap to all excitations<sup>b</sup> but their wave-functions are slightly more complex and their order parameter is non-local. The order of VBS is associated to long-ranged singlet-singlet correlations in the *fictitious spins*. Expressing such observable in terms of the physical spins leads to a non-local quantity called *string order parameter*.<sup>63,64</sup> Contrary to explicit VBC, VBS have fractionalized degrees of freedom at the edges of the system with open boundary conditions. These are simply associated to the unpaired fictitious spins. To our knowledge these properties have not been explored in quantum 2D systems.

The spin-1 Heisenberg chain is the prototype of VBS in 1D.<sup>c</sup> Such a state has a unique ground-state, a gap in the excitations and exponentially decreasing spin-spin and dimer-dimer<sup>65</sup> correlations. See the chapter by P. Lecheminant in this volume for more details about the VBS phase of the spin-1 chain.

<sup>b</sup>This may however not always be true when the coordination number of the lattice is large.<sup>61</sup> In such cases the VBS wave-function is still a spin singlet but has long-ranged spin-spin correlations. We do not consider such cases here.

<sup>c</sup>In 1D, some authors call “Haldane systems” all the spin-gapped phases, whatever their true nature: VBC or VBS.

A spin- $\frac{3}{2}$  specific  $SU(2)$ -invariant model on the honeycomb lattice<sup>61,62</sup> is another example of 2D VBS. The spin-1 Heisenberg model on the kagome lattice was proposed to realize a VBS-like ground-state<sup>66</sup> in which singlets form on every hexagon without any spontaneous symmetry breaking (hexagonal singlet solid).<sup>d</sup> A similar approach was carried out for the spin-1 pyrochlore Heisenberg model.<sup>67</sup> In that case a lattice distortion was invoked to lift the degeneracy between the two singlet states of each tetrahedron.

### 3.4. Two-dimensional examples of VBC

#### 3.4.1. Without spontaneous lattice symmetry breaking

Two spin- $\frac{1}{2}$  experimental examples of 2D (explicit) VBC have recently attracted attention:  $\text{CaV}_4\text{O}_9$ <sup>68,69,70,71,72,73,74</sup> and  $\text{SrCu}_2(\text{BO}_3)_2$ .<sup>75,76,77,78,79,80,81,82,83,84</sup> Both of them have a lattice derived from the square lattice: in  $\text{CaV}_4\text{O}_9$  the  $\text{V}^{4+}$  ions are on a  $1/5$  depleted square lattice and  $\text{SrCu}_2(\text{BO}_3)_2$  is an illustration of the Shastry Sutherland model<sup>85</sup>. A lattice embedding the main couplings of these two physical problems is drawn in Fig. 1. Interactions are of the Heisenberg type.<sup>e</sup>

VBC are obvious ground-states in the strong coupling limits of each problem.

The exact ground-state of the Shastry Sutherland model is built from singlets on the  $J'$  bonds.<sup>85,77</sup> For  $J'/J \gtrsim 1.55 \pm 0.05$  the model has a gap in the spectrum of excitations and is in a dimerized VBC phase.<sup>f</sup> For  $J'/J \lesssim 1.15 \pm 0.05$  the system is in the  $(\pi, \pi)$  Néel state of the square lattice (results of zero-temperature series expansion<sup>87</sup>). The possibility of an intermediate phase, possibly with helical short-ranged correlations, has been actively discussed in the literature.<sup>88,79,89</sup> S. Miyahara and K. Ueda have recently written a review of the theory of the orthogonal dimer Heisenberg spin model for  $\text{SrCu}_2(\text{BO}_3)_2$ .<sup>84</sup>

<sup>d</sup>Each kagome site belongs to two hexagons. Each physical spin-1 can be split into two spin- $\frac{1}{2}$ , each of them being involved in the formation of a singlet on one neighboring hexagon.

<sup>e</sup>Small Dzyaloshinsky-Moriya interactions have been identified in  $\text{SrCu}_2(\text{BO}_3)_2$ .<sup>86</sup>

<sup>f</sup>Consider a decomposition of the Shastry-Sutherland lattice as edge- and corner-sharing triangles. For  $J' = 2J$  the Hamiltonian is accordingly written as a sum of  $J(\vec{S}_1 + \vec{S}_2 + \vec{S}_3)^2$  terms for each triangle ( $J'$ -bonds are shared by two triangles) and each such term is minimized by the dimerized state. This shows rigorously that the dimerized state is the ground-state as soon as  $J'/J \gtrsim 2$ .

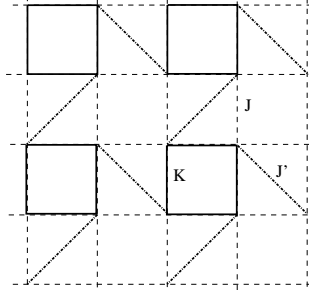


Fig. 1. The  $\frac{1}{5}$ -depleted lattice and the Shastry Sutherland lattice. The strong bonds of the Shastry Sutherland model are the bonds  $J'$  (dotted dashed lines): they can accommodate orthogonal dimers ( $J = K$  acts as a perturbation in the real  $\text{SrCu}_2(\text{BO}_3)_2$ ). The lattice formed by the strongest exchanges in  $\text{CaV}_4\text{O}_9$  is obtained with  $J = 0$ . The phase diagram of this model<sup>82</sup> contains collinear Néel phases, dimer and 4-spin plaquette VBC.

The  $\frac{1}{5}$ -depleted Heisenberg square lattice model ( $J = 0$ ) has been studied as a function of the ratio of the two different couplings: bonds within a plaquette ( $K$ ) and dimer bonds ( $J'$ ) between plaquettes. At isotropic coupling ( $J' = K$ ) collinear long-ranged Néel order survives the depletion, (the decrease in the order parameter is roughly 50%<sup>71</sup>). A small unbalance in couplings drives the system either in a 4-spin plaquette VBC ( $K > J'$ ) or in a dimer VBC ( $K < J'$ ). Both (explicit) VBC phases have a spin gap. A recent generalization of these models by Läuchli *et al* encompasses both the  $\frac{1}{5}$ -depleted Heisenberg square lattice model and the Shastry Sutherland model<sup>82</sup> (see Fig. 1). Its phase diagram exhibits collinear Néel phases ( $(\pi, \pi)$  or  $(0, \pi)$ ) separated from the VBC phases by second order phase transitions. Transition between the two VBC phases which have different symmetries occurs via a first order phase transition.<sup>g</sup>

Excitations in these models come from the promotion of local singlets to triplet excitations. In 2D the ordered dimer background provides a confining force for the spin- $\frac{1}{2}$  excitations. Indeed, separating two unpaired spins (that is two *spinons*) creates disruption in the ordered pattern all the way from the first to the second. The energy cost is thus proportional to the length of the string of defaults and both spin- $\frac{1}{2}$  excitations remains in fact

<sup>g</sup>A recent  $Sp(N)$  study of the Shastry Sutherland model<sup>89</sup> suggests that a spin liquid phase with deconfined spinons might appear in such a model. No evidence of such a phase has emerged from the  $SU(2)$  studies.



confined. Only integer spin excitations are expected. On the other hand in these strongly coupled models single-triplet hoppings can be difficult and correlated motions might be important, leading to a large zoology of excited modes (see Ref.<sup>81</sup> and Refs. therein). This potential frustration of the triplet motion favors the appearance of magnetization plateaus in VBC models.<sup>90,75,91,92,93,94</sup> This aspect was briefly discussed in the lecture notes published by the authors.<sup>95</sup>

#### 3.4.2. *With spontaneous lattice symmetry breaking*

In the previous models the (explicit) VBC phases do not break any lattice symmetry. They can be directly related to the geometry and relative strength of the couplings. In more symmetric situations with frustration, spontaneously symmetry breaking VBC can appear as a way to overcome this frustration by taking full advantage of the quantum fluctuations. This is probably the case in the  $J_1$ – $J_3$  model on the square lattice for intermediate  $J_3/J_1 \sim 0.6$ ,<sup>96</sup> in the  $J_1$ – $J_2$  model on the hexagonal lattice for intermediate  $J_2/J_1 \sim 0.4$ ,<sup>97</sup> and in the Heisenberg model on the checker-board lattice.<sup>98,99,100,101,102,103</sup> In the two first cases the ground-states are dressed columnar VBC of dimers. Translation and  $C_4$  (resp.  $C_3$  only) symmetries of the lattice are spontaneously broken. The ground-state is 4 (resp. 3) times degenerate. Spin-spin correlations decrease exponentially with the system size. All excitations are gapped. Contrary to the  $J_1$ – $J_2$  model on the square lattice, exact diagonalizations<sup>96,97,99</sup> give a rather straightforward information on these systems where the correlation lengths are small enough (far enough from the critical points which limit the boundary of the VBC phases).

The spin- $\frac{1}{2}$  Heisenberg model on the checker board lattice, which can also be seen as a planar lattice of corner sharing tetrahedrons (see Fig. 2), has received the largest attention for different reasons.<sup>104,105,98,101,100,99,102,103</sup> The problem has classically a continuous local degeneracy: the Hamiltonian can be rewritten as the sum of the squares of the total spin of each tetrahedron, and every configuration with a zero spin on each tetrahedron is a ground-state. Classically this problem shares this property with the Heisenberg model on the kagome, pyrochlore<sup>106,107</sup>, garnet<sup>108</sup> and pyrochlore slab<sup>109</sup> lattices (these lattices made of corner sharing “simplexes” with 2, 3 or 4 spins each were dubbed “bisimplex” lattices by Henley<sup>110</sup>).

The quantum spin- $\frac{1}{2}$  antiferromagnet on the kagome lattice has been

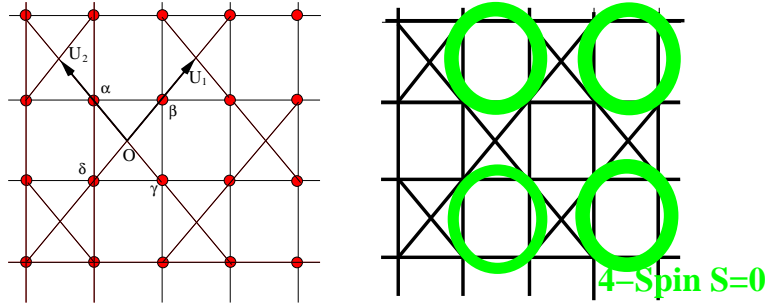


Fig. 2. Left: the checkerboard lattice. The spins sit at the vertices shown by bullets, all couplings are identical,  $\mathbf{u}_1$ ,  $\mathbf{u}_2$  are the unit vectors of the Bravais lattice. Right: the ground-states of the Heisenberg model on the checker board lattice are translational symmetry breaking VBC of 4-spin plaquettes on the uncrossed squares.

found to be quite specific with a small gap (if any) toward triplet excitations and an anomalous density of gapless low-lying singlets excitations (see §7).

The quantum scenario on the checkerboard lattice is quite different. The ground-state is a (dressed) product of 4-spin  $S = 0$  plaquettes on uncrossed squares: this state breaks translational symmetry but not  $C_4$  (the point group being defined at the center of an empty plaquette). It has a two fold degeneracy in the thermodynamic limit: this is easily seen in the symmetries and finite size scaling of the low lying levels of exact spectra.<sup>99</sup> The choice of the 4-spin  $S = 0$  states on the uncrossed squares corresponds to the most stable local configuration. The product of  $S = 0$  quadrumers is only weakly renormalized in the exact ground-state.<sup>99</sup>

Excitations of this model have been studied in different approaches, exact diagonalizations<sup>111</sup>, series expansions,<sup>101</sup> real space renormalization transformation.<sup>102</sup> All the excitations (singlet and triplet) are gapped. The triplet excitations originate from the triplet excitation of an uncrossed plaquette, they are weakly dispersive with a large gap. The singlet excitations cannot be described so simply: from exact diagonalizations data one can suspect that some of these excitations come from the reorganization of two adjacent triplet on crossed squares. The Contractor Renormalization (CORE) method of Berg *et al.*<sup>102</sup> on the other hand suggests that these excitations are domain walls between the two translated plaquette-VBC ground-states.

### 3.5. Methods

Spin waves<sup>69</sup> and Schwinger bosons<sup>88,70</sup> are simple approximations to study the phase diagram of a quantum frustrated magnet. But the first method only gives an approximate knowledge on the range of existence of the Néel phases, and it is rather difficult to include the effect of fluctuations beyond the mean-field approximation within the Schwinger-Boson formulation. As discussed in the section devoted to large- $N$  approaches (§4), spontaneous lattice symmetry breaking are very likely to be due to topological effects (Berry phase of instantons) which cannot be captured by the mean-field state. This probably explains why no spontaneous VBC has ever been found (to our knowledge) in Schwinger-Boson calculations.<sup>h</sup> For unfrustrated problems, as the Heisenberg model on the  $\frac{1}{5}$ -depleted square lattice,<sup>71</sup> QMC is considered as the method which can give benchmarks for other approaches.

Although VBC are naturally described with the help of spin- $\frac{1}{2}$  valence-bonds, the appearance of such states in the low-spin limit can sometimes be anticipated from an appropriate large- $S$  approach. An example is given in the work of Tchernyshyov *et al.*<sup>103</sup> (see also a previous paper by Henley<sup>110</sup>) on the checkerboard Heisenberg model. In this model, when both couplings (square lattice bonds and diagonal bonds) are equal, ground-state has a continuous local degeneracy. However leading  $1/S$  corrections select collinear states out of this huge manifold.<sup>110</sup> There remains an exponential number of such states and they do not have any magnetic order. However they exhibit long-ranged *bond* order and a spontaneous symmetry breaking<sup>103</sup> which is analogous to the one observed numerically in the spin- $\frac{1}{2}$  case.

For frustrated problems, exact diagonalizations can be useful tools in situations where the system is not too close from a critical point, that is when the correlations length is not too large. Successful applications of exact diagonalizations methods to 2D Heisenberg magnets realizing a VBC include studies of the  $J_1$ - $J_3$  model on the square lattice,<sup>96</sup>  $J_1$ - $J_2$  model on the hexagonal lattice,<sup>97</sup> Heisenberg model on the checkerboard lattice.<sup>99</sup> In such situations analysis of the quasi degeneracy of the low-lying levels of the spectra and of their finite-size scaling gives an unbiased and direct informations on the symmetry breakings in the thermodynamic limit.<sup>99</sup> However the boundaries of the phases and the quantum critical points cannot be

---

<sup>h</sup>It seems however that spontaneous VBC naturally arise in large- $N$  approaches with fermionic representation of  $SU(N)$  when  $1/N$  corrections are considered (see section 5.2).

accurately determined with this method. The series expansions described in the previous section appears to be a powerful approach to determine phase boundaries.<sup>112,74</sup> If the spin-spin correlation length is not very short, as it is the case in the  $J_1$ – $J_2$  model on the square lattice for  $J_2/J_1 \sim 0.5$ ,<sup>37</sup> it is very difficult to decide from exact diagonalizations between a VBC, a critical phase or an RVB SL.

Concerning excitations, exact diagonalizations give the gaps in each sector and provide a crude approximation of the dispersion laws of the first excitations. The large-scale nature of the excitations (as for examples domain walls excitations) can escape this method. The semi-analytical approaches which can be used for the study of the excitations of the VBC, all use as a basic departure point the excitations of a local cluster of spins conveniently renormalized by perturbation<sup>73,101</sup> or effective renormalization technique.<sup>102</sup> Contrary to exact diagonalizations these methods are not limited by finite-size effects but the results can be biased by the departure point.<sup>101,102</sup>

### 3.6. Summary of the properties of VBC phases

The generic features of VBC (whatever the dimensionality of the lattice) are:

- A spin gap, no  $SU(2)$  symmetry breaking and short-ranged spin-spin correlations,
- Long-ranged order in dimer-dimer and/or larger  $S = 0$  plaquettes. The coupling of this order to lattice distortions is probable in experimental realizations of spontaneous VBC.
- In *spontaneous* VBC phases the ground-state is degenerate. From the theoretical point of view the discrete symmetry of the order parameter of the VBC which spontaneously breaks a lattice symmetry may give birth to a finite temperature Ising-like transition.<sup>14</sup> Simultaneity between this transition and a possible structural transition is likely when the couplings of the spins to the lattice degrees of freedom (phonons) is considered.<sup>113</sup>
- VBC have gapped excitations, in the  $S = 0$  sector as well as in other  $S$  sectors. A wide zoology of modes is to be expected as well as continua associated to multi-particle excitations or scattering of domain walls (in the case of a spontaneous symmetry breaking of the ground-state). In two dimensions all these excitations have integer spins (the ordered back-ground inducing a confinement of

the spin- $\frac{1}{2}$  excitations)

Frustration on the square lattice or more generally on bipartite lattices is often overcome by VBC phases. No theorem forbids the appearance of VBC in triangular geometries but there is up to now no examples of such phases in pure spin- $\frac{1}{2}$  models (in Sec. 5 examples will be given within the framework of quantum dimer models).

It has been advocated in the large- $N$  approaches (see section 4) that, at least in two dimensions, collinear spin-spin correlations generically lead to VBC or VBS and only non-collinear spin-spin correlations can give birth to RVB SL with unconfined spin- $\frac{1}{2}$  excitations. The present knowledge of  $SU(2)$  phase diagrams supports this prediction. The VBC found so far numerically in  $SU(2)$  spin models appear to be in regions of parameter space where the spin-spin correlations are characterized by some short-ranged collinear order in the large- $S$  limit. The  $J_1$ - $J_2$  model on the honeycomb lattice has a classical incommensurate phase in the regime of high frustration and there are some evidences that in the quantum phase diagram the collinear phase is separated from the columnar VBC phase by a RVB SL.<sup>97</sup> The multiple-spin exchange (MSE) model on the triangular lattice is also believed to be a RVB SL<sup>114</sup> and the corresponding classical ground-states generically have non-coplanar spin configurations. Capriotti *et al.*<sup>37</sup> argued that the spin- $\frac{1}{2}$  square lattice  $J_1$ - $J_2$  model could be a RVB SL. If confirmed, this would be the first counter-example to the general rule explained above (The Heisenberg model on the pyrochlore lattice might be an other counter-example<sup>102</sup>).

#### 4. Large- $N$ methods

Introduced by Affleck,<sup>115</sup> Affleck and Marston,<sup>116</sup> Arovas and Auerbach<sup>117</sup> and Read and Sachdev<sup>118,119,120</sup> in the context of spin models, large- $N$  approaches are powerful methods to investigate quantum antiferromagnets. When  $N$  is taken to infinity many of these models can be solved by saddle point methods and finite- $N$  corrections can be, at least in principle, explored in a controlled way. A success of these approaches is that they can describe the phenomenology of a large variety of phases encountered in quantum magnets : Magnetic LRO (possibly with order by disorder selection) as well as phases dominated by short-ranged valence-bonds: VBC, VBS and RVB liquids. One crucial result (due to Read and Sachdev<sup>118,119,120,121,122</sup>) concerning these three later phases is that the analysis of finite- $N$  corrections to some large- $N$  formulations ( $Sp(N)$  for instance, see below) provides

a general criterion to decide which of these three phase should appear in a given model.

This criterion is the following in 2D: if the (large- $N$  equivalent of the) “spin”  $S$  at each site matches the lattice coordination number  $z$  by  $2S = 0 \bmod z$  a VBS is to be expected. If it is not the case (as for a spin- $\frac{1}{2}$  model on the square lattice) one should look at the local spin-spin correlations. If they are reminiscent of a collinear order, a VBC with spontaneous translation symmetry breaking is expected whereas non-collinear short-ranged correlation generically give rise to a RVB phase without any broken symmetry and deconfined spinon excitations. These results are of course based on a large- $N$  generalization of the original spin model and there is no guaranty at all that these rules should always apply to  $SU(2)$  models. To our knowledge they have however not been manifestly found in error up to now.<sup>i</sup> In the following we will present some of the important reasoning steps leading to this result.

#### 4.1. Bond variables

The  $SU(2)$  algebra of a spin  $S$  at one site can be represented by 2 species of particles  $a_\sigma^\dagger$  (with  $\sigma = \uparrow, \downarrow$ ), provided that the total number of particles on one site is constrained to be  $a_\uparrow^\dagger a_\uparrow + a_\downarrow^\dagger a_\downarrow = 2S$ . The raising operator  $S^+$  (resp.  $S^-$ ) is simply represented by  $a_\uparrow^\dagger a_\downarrow$  (resp.  $a_\downarrow^\dagger a_\uparrow$ ). These particles can be chosen to be fermions (Abrikosov fermions) or bosons (Schwinger bosons). These particles carry a magnetization  $\pm\frac{1}{2}$  since  $S^z = \frac{1}{2}(a_\uparrow^\dagger a_\uparrow - a_\downarrow^\dagger a_\downarrow)$ . For this reason they are often called *spinons*. The Heisenberg interaction is a quartic interaction for these particles:

$$\vec{S}_i \cdot \vec{S}_j = S^2 - \frac{1}{2} A_{ij}^\dagger A_{ij} \quad (10)$$

with the bond operator  $A_{ij}$  defined by:

$$A_{ij} = a_{j\downarrow} a_{i\uparrow} - a_{j\uparrow} a_{i\downarrow} \quad (11)$$

Acting on the vacuum,  $A_{ij}^\dagger$  creates a spin singlet on the bond  $(ij)$ . Physically  $A_{ij}^\dagger A_{ij}$  measures the number of singlets on that bond and Eq. 10 shows that the antiferromagnetic Heisenberg interaction just tries to maximize that number.

The idea of large- $N$  methods is to generalize the  $SU(2)$  symmetry of the spin- $S$  algebra to a larger group  $SU(N)$  (or  $Sp(N)$ ) by letting the index

<sup>i</sup>The spin- $\frac{1}{2}$  Kagome antiferromagnet might however be such an example. See section 7.

$\sigma$  go from 1 to  $N$  (or  $2N$ ). The  $SU(N)$  (or  $Sp(N)$ ) generalization of the Heisenberg model is solved by a saddle point calculation of the action. The  $N = \infty$  limit is very similar to a mean-field decoupling of the four-body interaction of the physical  $SU(2)$  model:  $A_{ij}^\dagger A_{ij} \simeq A_{ij}^\dagger \langle A_{ij} \rangle + \langle A_{ij}^\dagger \rangle A_{ij} - |\langle A_{ij} \rangle|^2$ .

#### 4.2. $SU(N)$

The generalization of the Heisenberg model to such a symmetry group depends only on the choice of the irreducible representation of  $SU(N)$  according to which the “spin” operators transform (and not on the choice of fermions or bosons to implement the representation). For  $SU(2)$  this amounts to specify the magnitude  $S$  of the spin. For  $SU(N)$  irreducible representations are labeled by Young tableaux. The case of a general rectangular tableau with  $n_c$  columns and  $m$  rows was discussed by Read and Sachdev<sup>123</sup> and  $n_c$  appears to continue to play a role similar to  $2S$  in the large- $N$  phase diagrams.<sup>j</sup> In this review we will focus on a slightly different large- $N$  generalization of the  $SU(2)$  model which is both able to deal with frustration and magnetic states.

#### 4.3. $Sp(N)$

To perform a large- $N$  extension of *frustrated* Heisenberg models one has to use either fermions<sup>116</sup> or bosons with an  $Sp(N)$  symmetry. The latter seems to produce phase diagrams that closely resemble the  $SU(2)$  problems and we will focus on this representation which was introduced by Read and Sachdev.<sup>120</sup> The presentation below is largely inspired from their papers.<sup>118,119,120,121,122</sup>

We now have  $2N$  flavors of bosons at each site:  $b_{i,\sigma}$  with  $\sigma = 1..2N$  and

<sup>j</sup>Taking the limit  $N \rightarrow \infty$  with  $m$  fixed of order 1 and  $n_c \sim N$  is most conveniently done with bosons  $b_{\alpha p}^\dagger$  where  $\alpha = 1 \dots N$  is the  $SU(N)$  index, while  $p = 1 \dots m$  label the different “colors”. There are therefore  $Nm$  kinds of bosons. On the other hand it is convenient to use  $n_c$  “colors” of fermions (still with an  $SU(N)$  index) to deal with the case  $n_c \sim \mathcal{O}(1)$  and  $m \sim N$ . Bosonic representations with  $n_c \sim N$  are appropriate to describe magnetically ordered phases<sup>117</sup> but cannot be used for frustrated models (such a representation is not self-conjugate). On the other hand fermionic representations, such as the  $m = N/2$  and  $n_c = 1$  one,<sup>116,124</sup> can be used on any lattice but they do not display magnetically ordered phases and tend to favor dimerized states.<sup>116,123,124</sup>

we define an  $Sp(N)$ -invariant bond operator:

$$A_{ij} = \sum_{\sigma, \sigma'=1..2N} \mathcal{J}_{\sigma, \sigma'} b_i^\sigma b_j^{\sigma'} \quad (12)$$

where the  $2N \times 2N$  antisymmetric tensor  $\mathcal{J}$  is block diagonal

$$\mathcal{J} = \begin{bmatrix} 0 & 1 & & \\ -1 & 0 & & \\ & & \ddots & \\ & & & 0 & 1 \\ & & & -1 & 0 \end{bmatrix} \quad (13)$$

and generalizes the  $SU(2)$  antisymmetric tensor  $\epsilon_{ij}$  ( $SU(2)$  is identical to  $Sp(1)$ ). Up to some constant the  $Sp(N)$  Hamiltonian is

$$\mathcal{H} = -\frac{1}{N} \sum_{ij} J_{ij} A_{ij}^\dagger A_{ij} \quad (14)$$

with the constraints

$$\forall i \quad \sum_{\sigma=1}^{2N} b_{i\sigma}^\dagger b_{i\sigma} = n_c \quad (15)$$

$n_c = 2S$  in the  $SU(2)$  case and  $n_c/N = \kappa$  will be kept constant when taking the large- $N$  limit. The partition function can be represented by an imaginary time functional integral:

$$Z = \int \mathcal{D}[\lambda_i, b_i^\sigma, b_i^{\dagger\sigma}] \exp \left( - \int_0^\beta (L_0 + \mathcal{H}) d\tau \right) \quad (16)$$

$$L_0 = \sum_{i\sigma} b_i^{\dagger\sigma} (\partial_\tau + i\lambda_i) b_{i\sigma} - iN\kappa \sum_i \lambda_i \quad (17)$$

The  $\lambda_i(\tau)$  are Lagrange multipliers that enforce the constraint Eq. 15 at every site. Bond degrees of freedom  $Q_{ij}$  are introduced in order to decouple the bosons (Hubbard-Stratonovitch). The partition function is now

$$Z = \int \mathcal{D}[Q_{ij}, \bar{Q}_{ij}, \lambda_i, b_i^\sigma, b_i^{\dagger\sigma}] \exp \left( - \int_0^\beta (L_0 + L_1) d\tau \right) \quad (18)$$

with

$$L_1 = \sum_{ij} \left[ N \frac{|Q_{ij}|^2}{J_{ij}} - (A_{ij}^\dagger Q_{ij} + \text{h.c.}) \right], \quad (19)$$



so that a Gaussian integration of the  $Q_{ij}$  gives back Eq. 16. The bond variables are  $Sp(N)$  invariant and they can take non-zero expectation values at a mean-field level without breaking the  $Sp(N)$  symmetry. As we explain below, they are however not *gauge-invariant*.

#### 4.3.1. Gauge invariance

An important property of Eq. 18 is the  $U(1)$  gauge invariance associated to the following transformations:

$$b_{i\sigma} \rightarrow b_{i\sigma} e^{i\phi_i} \quad (20)$$

$$Q_{ij} \rightarrow Q_{ij} e^{i(\phi_i + \phi_j)} \quad (21)$$

$$\lambda_i \rightarrow \lambda_i - \partial_\tau \phi_i \quad (22)$$

where  $\phi_i(\tau)$  are arbitrary site- and imaginary-time-dependent angles. This gauge invariance comes from the conservation of the local boson number and reflects the fact the magnitude of the spin is constant at each site. If we focus on the phase degrees of freedom of the bond variables, the Eq. 18 describes a system of charge-1 bosons coupled to a  $U(1)$  lattice gauge theory.<sup>125,126</sup> These gauge degrees of freedom play a crucial role in the analysis of the fluctuations about mean-field solutions.

*Effective action for the bond variables* — The boson degrees of freedom can be integrated out to give an effective action for the bond variables:

$$Z = \int \mathcal{D}[Q_{ij}, \bar{Q}_{ij}, \lambda_i] \exp(-S^{\text{eff}}) \quad (23)$$

$$S^{\text{eff}} = N \int_0^\beta \left[ \sum_{ij} \frac{|Q_{ij}|^2}{J_{ij}} - i\kappa \sum_i \lambda_i \right] - N \text{Tr} \log G \quad (24)$$

where  $G^{-1}$  is the quadratic form which couples the bosons in Eq. 18 (propagator). It depends on the bond variables and on  $\lambda_i$ . We may write formally  $G^{-1} = \partial_\tau - i\lambda - Q$ . The term  $N \text{Tr} \log G$  is the free energy of the bosons in presence of the bond fields. By construction the action  $S^{\text{eff}}$  is gauge-invariant with respect to the transformations of Eqs. 20–22. So far this is an exact formulation of the original model for arbitrary  $N$ .

#### 4.3.2. Mean-field ( $N = \infty$ limit)

Since  $N$  factorizes (no flavor index is left in Eq. 24),  $Z$  is dominated by the saddle point of  $S^{\text{eff}}$  when  $N$  is large. For simple models such as the

first-neighbor antiferromagnet on the cubic lattice (any space dimension), the saddle point can be determined analytically. The  $N = \infty$  limit is almost equivalent to the Schwinger-boson mean-field theory.<sup>127,128</sup> This can otherwise be done numerically.<sup>k</sup> In this large- $N$  limit, two kinds of mean-field solutions can appear. For large enough  $\kappa$  the bosons condense at some wave-vector, the spectrum of the mean-field Hamiltonian is gapless. This corresponds physically to Néel long-range order. On the other hand, for smaller  $\kappa$  (smaller “spin”) the mean field Hamiltonian is gapped and the ground-state preserves the  $Sp(N)$  symmetry. Fluctuations around the saddle point are not expected to change drastically the Néel ordered phases but they play an important role in the physics of  $Sp(N)$  symmetric phases. The following is a brief discussion of the effects of fluctuations in these non-magnetic phases.

#### 4.3.3. *Fluctuations about the mean-field solution*

At the mean-field level described above some  $Q_{ij}$  acquire a (static in all known cases) non-zero expectation value:  $\langle Q_{ij} \rangle = \bar{Q}_{ij}$ . For this reason such a state spontaneously breaks the local gauge invariance of Eqs. 20,21 and 22. However this does not mean that the gauge degrees are all gapped and do not play any role at low energy. In fact, as remarked by Read and Sachdev, depending on the *geometry* of the lattice defined by the bonds where  $Q_{ij} \neq 0$ , some long-wavelength gapless gauge excitations survive and the associated fluctuations must be taken into account. More precisely, the fluctuations of the bond variables about the saddle point are decomposed into an amplitude and a phase

$$Q_{ij} = (\bar{Q}_{ij} + q_{ij}) \exp(i\theta_{ij}) \quad (25)$$

and we expand  $S_{\text{eff}}$  with these new variables. Two cases must then be considered:

- i) The lattice made of the sites connected by non-zero  $\bar{Q}_{ij}$  bonds is bipartite. This is automatically the case if the original lattice

---

<sup>k</sup>To our knowledge, all the saddle points considered so far are static (expectation values of the  $Q_{ij}$  are time-independent) and the corresponding  $\langle Q_{ij} \rangle$  could all be made real with an appropriate gauge transformation. There is no chiral order and the time-reversal symmetry is unbroken. The (oriented) sum of the complex phases of the bond variables around a plaquette defines a  $U(1)$  flux. This flux is related to the solid angle formed by the spins and it vanishes in collinear as well as in coplanar states. In such cases the phases can be therefore be gauged away and the  $\langle Q_{ij} \rangle$  can be made real. For this reason complex bond variables are usually not observed.<sup>129</sup>

defined by bonds where the exchange  $J_{ij} \neq 0$  is bipartite. This can also be true if the original lattice is a non-bipartite lattice but some bonds have  $\bar{Q}_{ij} = 0$  so that the remaining lattice is bipartite. This is the case, for instance, in the  $J_1$ - $J_2$  model on the square lattice,<sup>120</sup> in some regions of the phase diagram of the Shastry-Sutherland model<sup>89</sup> and in on the checkerboard Heisenberg model.<sup>104</sup> Such configurations of the bond variables give *collinear* spin structures: spin-spin correlations can either be long-ranged (large  $\kappa$ , Néel phase) or short-ranged but in both cases the magnetic structure factor is peaked at a simple wave-vector  $\mathbf{k}_0$  such that  $2\mathbf{k}_0$  is a reciprocal lattice vector ( $k_0 = (\pi, 0)$ ,  $k_0 = (0, \pi)$  or  $k_0 = (\pi, \pi)$  in square geometries).

- ii) The lattice made of the sites connected by non-zero  $\bar{Q}_{ij}$  bonds is not bipartite. This happens in some phases of the  $J_1$ - $J_2$ - $J_3$  model on the square lattice,<sup>120</sup> on the triangular or kagome lattices<sup>130</sup>, in the Shastry-Sutherland model for some values of the exchange parameters<sup>89</sup> and on an anisotropic triangular lattice.<sup>131</sup> Such mean-field states generically have planar but non-collinear spin-spin correlations.

It is simple to check that case i) preserve a *global* continuous symmetry while such a symmetry is absent in ii). Consider the following *global* gauge transformation in case i) :

$$b_{i\sigma} \rightarrow b_{i\sigma} e^{i\phi} \quad b_{j\sigma} \rightarrow b_{j\sigma} e^{-i\phi} \quad (26)$$

$$Q_{ii'} \rightarrow Q_{ii'} e^{2i\phi} \quad Q_{jj'} \rightarrow Q_{jj'} e^{-2i\phi} \quad (27)$$

$$Q_{ij} \rightarrow Q_{ij} \quad (28)$$

where  $i, i'$  belongs to sublattice  $A$  and  $j, j'$  belongs to sublattice  $B$ . This transformation does not change the mean-field parameters  $\bar{Q}_{ij}$ . The only fields affected by this transformation are those connecting two sites on the same sublattice.<sup>1</sup> They have a zero expectation values in case i) (or do not even exist if the physical lattice is itself bipartite). For this reason it is possible to make low-energy (and long-wavelength) gapless gauge excitations about the saddle-point by replacing the global staggered phase shift  $\phi$  of Eq. 26 by a slowly varying (staggered)  $\theta_{ij}$  (Eq. 25). A gradient expansion

<sup>1</sup>In a gauge theory language the fields  $Q_{ii'}$  (resp.  $Q_{jj'}$ ) of Eq. 27 transform like a charge-2 scalar for the  $U(1)$  gauge field. Instead, from Eq. 26, the bosons (spinons) carry a charge 1.

of the effective action performed at the appropriate points in the Brillouin zone for the phase fluctuations only involves gradients of  $\theta$ . The corresponding action is that of  $U(1)$  lattice gauge theory coupled to charge-1 boson (spinons).

#### 4.3.4. Topological effects - instantons and spontaneous dimerization

So far only small fluctuations around the saddle point were considered and the contribution of topologically non-trivial gauge-field configurations were ignored. Consequently, the magnitude of the “spin”  $n_c/2$  was a continuous parameter and *the information about the integer or half-integer (for instance) character of  $S$  as disappeared*. From Haldane’s work on quantum spin chains and non-linear sigma models<sup>132</sup> it is well known that Berry phases in spin systems give rise to topological terms in the low-energy effective action which can play a crucial role depending on the parity of  $2S$ .

In non-linear sigma models in 2+1 dimensions the Berry phase vanishes for configurations which are smooth on the scale of the lattice spacing<sup>133,134</sup> (unlike the 1+1 dimensional case). However “hedgehog” space-time singularities<sup>133</sup> give non-trivial Berry phases. Read and Sachdev found that the closely related instantons of the effective  $U(1)$  gauge theory described before<sup>m</sup> also play a crucial role in the physics of the  $Sp(N)$  (as well as  $SU(N)$ ) spin models.

The Berry phase associated to such a singular configuration depends on details of the lattice geometry. In the short-range ordered  $(\pi, \pi)$  phase of the square lattice antiferromagnet this Berry phase is a multiple of  $in_c\pi/2$ . Although dealing with a gas of interacting ( $1/r$  Coulomb-like potential) instantons is a difficult problem (see Ref. <sup>119</sup> and references therein), we can guess that the physics will depend on  $n_c \bmod 4$ . A detailed analysis<sup>119</sup> shows that when  $n_c \neq 0 \bmod 4$  the instantons condense and *spontaneously break the lattice translation symmetry*. This generates a static electric field for the  $U(1)$  gauge field. Since the electric field is coupled to the difference of amplitudes of the bond variables, such state acquires spatially inhomogeneous expectation values of the bond variables, *it is a VBC and spinons are confined in pairs*. In the  $J_1$ – $J_2$  model around  $J_2/J_1 \simeq 0.5$  the mean-field state is short-range ordered with correlations peaked at  $(\pi, \pi)$ . A columnar dimerized state is predicted by Read and Sachdev from this analysis of the

<sup>m</sup>In that gauge theory associated to the phases of the link variables an instanton corresponds to a tunneling event during which the total magnetic field piercing the lattice is changed by  $\pm 2\pi$ .

fluctuations, in agreement with a number of numerical works on the  $SU(2)$   $J_1$ - $J_2$  spin- $\frac{1}{2}$  model.

In a recent work by Harada, Kawashima and Troyer<sup>135</sup> the phase diagram of the (first neighbor - unfrustrated)  $SU(N)$  antiferromagnet on the square lattice with  $n_c = 1$  was found to be in complete agreement with Read and Sachdev's predictions. They showed by quantum Monte Carlo simulations that for  $N \leq 4$  the system is Néel ordered whereas it is a columnar VBC for  $N > 5$ . This provides an additional support to the field theory arguments described above. It also underlines that the mechanism of spontaneous symmetry breaking and formation of a VBC may come from quantum fluctuations only and that frustration is not always required (although it clearly enhances quantum fluctuations).

On the other hand when  $n_c = 0 \bmod 4$  the analysis of Read and Sachdev shows that fluctuations should not bring any broken lattice symmetry. Spinons are also confined and this state closely resembles the valence-bond solid (VBS) proposed by Affleck *et al.*<sup>61</sup> as a possible ground-state when the spin  $S$  matches the coordination number  $z$  according to  $2S = 0 \bmod z$  (see §3.3).

#### 4.3.5. Deconfined phases

Now we suppose that, starting from a mean-field solution with collinear correlations (case i), a parameter of the original spin model is varied so that the mean field solution is changed and some bonds  $Q_{ii'}$  ( $i$  and  $i'$  belong to the same sublattice) acquire a non zero expectation value (case ii). In the framework of square lattice antiferromagnets, a finite third-neighbor coupling ( $J_3$ ) would be needed.<sup>120</sup> From the point of view of the long-wavelength gauge fluctuations (related to the continuum limit of the phases  $\theta_{ij}$ ) discussed above, the appearance of  $\bar{Q}_{ii'} \neq 0$  is equivalent to the condensation of a (Higgs) boson of charge 2. This is a spontaneous break down of the global  $U(1)$  staggered symmetry of Eqs. 26–28 down to a  $\mathbb{Z}_2$  one since the field  $Q_{ii}$  is not invariant under Eq. 27 except if  $\phi = 0$  or  $\pi$ . Based on results of Fradkin and Shenker<sup>136</sup> concerning confinement in compact lattice gauge theories coupled to matter, Read and Sachdev argued that this Higgs mechanism suppresses the low-energy gauge fluctuations and liberate the spinons. This confinement transition is described by a  $\mathbb{Z}_2$  gauge theory. The suppression of the  $U(1)$  gauge fluctuations also forbids the condensation of

instantons discussed above and the ground-state remains unique<sup>n</sup> and *bond variables have uniform expectation values. It is a genuine SL without any broken symmetry and deconfined spinons.*

## 5. Quantum Dimer Models

In a previous section (§3) we showed that pairing spins- $\frac{1}{2}$  into singlets at short distances is a rather natural way to overcome frustration in Heisenberg antiferromagnets. QDM are defined in the Hilbert space of nearest-neighbor valence-bond (or dimer) coverings of the lattice. By construction these models focus on the dynamics in the singlet space and ignore magnetic (gapped magnons or gapped spinons) excitations. For this reason they are (a priori) not appropriate to describe the physics of spin systems where magnetic excitations are gapless.

The Hamiltonian of a QDM usually contains kinetic as well as potential energy terms for these dimers. Such Hamiltonians can often be simpler than their spin parents and are amenable to several analytic treatments because of their close relations to classical dimer problems,<sup>137,138,139</sup> Ising models and  $\mathbb{Z}_2$  gauge theory.<sup>140,141,142</sup> These models can offer simple descriptions of VBC<sup>143</sup> as well as RVB liquids.<sup>144,141</sup> It is in particular possible to write down some QDM that have a simple and exact VBC ground-state with spontaneous broken symmetries (such as Rokhsar and Kivelson's model on the square lattice<sup>143</sup> with attractive potential energy only - in which case the exact ground-state is very simple). Simple solvable QDM which have a dimer-liquid ground-state can also be constructed.<sup>141</sup>

### 5.1. Hamiltonian

The first QDM was introduced by Rokhsar and Kivelson.<sup>143</sup> It is defined by an Hamiltonian acting in the Hilbert space of first-neighbor dimer (valence-bonds) coverings of the square lattice and reads:

$$\mathcal{H} = \sum_{\text{Plaquette}} [-J (|\uparrow\uparrow\rangle\langle\downarrow\downarrow| + \text{H.c.}) + V (|\uparrow\uparrow\rangle\langle\uparrow\uparrow| + |\downarrow\downarrow\rangle\langle\downarrow\downarrow|)] \quad (29)$$

Flipping two parallel dimers around a square plaquette is the simplest dimer move on the square lattice and the  $J$  terms precisely represent such dynamics. The  $V$  terms are diagonal in the dimer basis and account for an attraction or repulsion between nearest-neighbor dimers. These are the two

<sup>n</sup>Except for a discrete topological degeneracy.

most *local* terms (respecting all lattice symmetries) which can be considered.<sup>a</sup>

## 5.2. Relation with spin- $\frac{1}{2}$ models

There exists different interesting mappings between frustrated Ising models and QDM.<sup>145,142</sup> Here, however, we focus on the relations between QDM and  $SU(N)$  (or  $Sp(N)$ ) spin models in which dimers are related to singlet valence-bonds.

*Overlap expansion.* — A valence-bond state (product of two-spin singlets - belongs to the spin- $\frac{1}{2}$  Hilbert space) can be associated to any dimer covering.<sup>b</sup> Two such valence-bond states  $|a\rangle$  and  $|b\rangle$  are not orthogonal but, as first discussed by Sutherland<sup>146</sup> their overlap decays exponentially with the length  $L$  of the loops of their transition graphs (defined in §5.3.1) as  $|\langle a|b\rangle| = 2^{1-L/2}$ . Rokhsar and Kivelson<sup>143</sup> introduced a formal expansion parameter  $x$  and replaced  $|\langle a|b\rangle|$  by  $2x^L$ . Their idea is that although  $x = \frac{1}{\sqrt{2}}$  for physical  $SU(2)$  spins, the physics of some models may be captured by the first orders of a small  $x$  expansion. Truncating this expansion to order  $x^n$  gives an effective Hamiltonian which contains *local* terms involving at most  $n$  dimers.<sup>c</sup> In this approach the dimer states of the QDM are in one-to-one correspondence with *orthogonalized* valence-bonds in the spin Hilbert space.<sup>d</sup>

*Fluctuations about large- $N$  saddle points.* — From the argument above it could seem that the connection between spin- $\frac{1}{2}$  models and QDM relies on a variational approximation: the spin Hilbert space is restricted to the nearest-neighbor valence-bond subspace. This connection is in fact probably deeper, as some theories describing fluctuations about some large- $N$

<sup>a</sup>They were originally derived<sup>143</sup> as the lowest order terms of a formal overlap expansion (see §5.2 below) of the Heisenberg. In that calculation  $J \sim x^4$  and  $V \sim x^8$ . Notice that a three-dimer kinetic term (extending over two neighboring plaquettes) is generated at order  $x^6$  and is not included in Eq. 29.

<sup>b</sup>There is however a sign ambiguity (a valence-bond is antisymmetric under the exchange of both spins) that can be fixed by choosing an orientation on every bond.

<sup>c</sup>The *signs* of the non-diagonal (kinetic) terms of the effective QDM obtained by such small  $x$  expansion depends on the sign convention which was chosen to map valence-bonds to dimers. An important question is to know whether, at least at the lowest non-trivial order, a sign convention giving the same sign for all kinetic terms exists (as in Eq. 29). This is the case on the square<sup>143</sup> and triangular lattices.<sup>144</sup>

<sup>d</sup>This implicitly assumes that the valence-bond states are linearly independent. This can be demonstrated on the square lattice and appears to be the case on the triangular and kagome lattices for large enough sizes. The operator which orthogonalizes the valence-bond basis into the dimer basis is  $\Omega^{-1/2}$  where  $\Omega_{a,b} = \langle a|b\rangle$  is the overlap matrix.

saddle points ( $1/N$  corrections) are equivalent to (generalized) QDM. This mapping was discussed by Read and Sachdev<sup>123</sup> for representation with  $m = 1$  (number of rows in the Young tableau of the  $SU(N)$  representation),  $N \rightarrow \infty$  and  $n_c \sim \mathcal{O}(1)$ , it leads to a *generalized* QDM where  $n_c$  dimers emanate from each site. A QDM also describes  $1/N$  corrections in the case of the fermionic<sup>e</sup>  $SU(N)$  generalization<sup>116,124</sup> of the Heisenberg model:

$$\begin{aligned}\mathcal{H} &= \frac{1}{N} \sum_{ij} J_{ij} : B_{ij}^\dagger B_{ij} : \\ &= -\frac{1}{N} \sum_{ij} J_{ij} B_{ij}^\dagger B_{ij} + \text{cst}\end{aligned}\quad (30)$$

$$\text{where } B_{ij} = \sum_{\sigma=1}^N c_{j\sigma}^\dagger c_{i\sigma} \quad (31)$$

and where the  $c_{i\sigma}$  are  $N$  flavors of fermions satisfying a constraint similar to Eq. 15 :

$$\sum_{\sigma=1}^N c_{i\sigma}^\dagger c_{i\sigma} = N/2 \quad (32)$$

Rokhsar showed<sup>124</sup> that in the  $N \rightarrow \infty$  limit “dimerized states” (or Peierls states) becomes exact ground-states of Eq. 30 for a large class of models.<sup>f</sup> Quite naturally,  $1/N$  corrections will induce a dynamics into this subspace of dimerized states; it can be described by a QDM (with kinetic energy terms only at this order). At lowest order, on the square lattice, a kinetic term identical to the  $J$  term in Eq. 29 is generated and naturally favors a columnar or resonating-plaquette crystal (in agreement with a number of works on the spin- $\frac{1}{2}$  model). The same arguments were discussed for the kagome lattice.<sup>147</sup> In that case the leading  $1/N$  corrections to the fermionic saddle point generate three-dimer moves around hexagons and stabilize a

<sup>e</sup>Young tableau with  $n_c = 1$  column and  $m = N/2$  rows.

<sup>f</sup>Let  $J_0$  be the largest value of the  $J_{ij}$ . Each dimerization (no site is left empty) where only bonds where  $J_{ij} = J_0$  are occupied is a ground-state. Here a “dimer” between to neighbors  $i$  and  $j$  consists of a  $SU(N)$  singlet made with  $N$  fermions (one of each flavor) hopping back and forth between  $i$  and  $j$ . It is constructed from  $\prod_{\sigma=1}^N (c_{i\sigma}^\dagger + c_{j\sigma}^\dagger) |0\rangle$ , by projecting out the components which do not satisfy Eq. 32. Notice however that in the  $N \rightarrow \infty$  limit the relative fluctuations of the total number of fermion on each site are of order  $1/\sqrt{N}$  and can be neglected.



crystal of resonating hexagons.<sup>g</sup> This formalism was also applied to the checkerboard model<sup>98</sup> to conclude to the presence of a VBC phase.

### 5.3. Square lattice

The phase diagram of the Rokhsar and Kivelson's square lattice QDM is shown Fig. 3. Since a change in the signs of the basis dimer configurations can change  $J$  into  $-J$  (see Ref. <sup>143</sup>) we will choose  $J > 0$  without loss of generality.

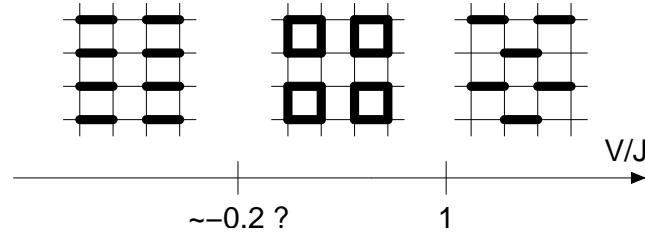


Fig. 3. Schematic phase diagram of the the square lattice QDM. The possible location of an intermediate plaquette phase is taken from the work of Leung *et al.*<sup>148</sup>

#### 5.3.1. Transition graphs and topological sectors

In order to understand the particularities of QDM on bipartite lattices it is useful to describe how the set of dimer coverings splits into *topological sectors*. To do so we first have to define transition graphs: the transition graph of two dimer coverings  $c$  and  $c'$  is obtained by superimposing  $c$  and  $c'$  on the top of each other; it defines a set of non-intersecting loops covering the lattice. On each bond where the dimers of  $c$  and  $c'$  match, a trivial loop of length 2 is obtained. When the lattice is bipartite (two sublattices  $A$  and  $B$ ) these loops can be *oriented* in the following way: any dimer belonging to  $c$  is oriented from  $A$  to  $B$  and dimers of  $c'$  are oriented  $B \rightarrow A$ . The transition graph is then made of loops of the type  $A \rightarrow B \rightarrow A \rightarrow B \dots$ . With periodic boundary conditions two winding numbers<sup>143</sup>  $-L/2 \leq \Omega_x, \Omega_y \leq L/2$  are associated to such a transition graph ( $L \times L$  sites).  $\Omega_x$  (resp.  $\Omega_y$ ) is the net number of topologically non-trivial loops

<sup>g</sup>To our knowledge however there is no clear evidence of such ordering in the spin- $\frac{1}{2}$  case.

(clockwise minus counterclockwise) encircling the torus in the  $x$  (resp.  $y$ ) direction.

Dimer coverings can be grouped into different *topological sectors*. By definition two dimer coverings belong to the same sector if they can be transformed into each other by repeated actions of *local* dimer moves (the transition graph associated to each movement does not wind around the whole system if it has periodic boundary conditions). On the square lattice two-dimer moves are sufficient to connect any two states in the same sector; that is the Hamiltonian Eq. 29 is ergodic within each topological sector. In a torus geometry,  $c$  and  $c'$  belongs to the same sector if and only if their transition graph has winding numbers  $\Omega_x = \Omega_y = 0$ . The different topological sectors can be labeled by their winding numbers with respect to some reference columnar configuration. Their number is of order  $\mathcal{O}(L^2)$  for a system of linear size  $L$ .

### 5.3.2. Staggered VBC for $V/J > 1$

When  $V$  is sufficiently large the system tries to minimize the number of parallel dimers. The staggered configuration shown Fig. 3 has no such *flip-pable plaquette*. It is always a zero-energy eigenstate of Eq. 29 and becomes a ground-state for  $J \geq V$ . It breaks several lattice symmetries (four-fold degenerate) and is a VBC.

The expectation value of the energy per plaquette satisfies  $\min(0, V - J) \leq E_0/N_p \leq \max(0, V + J)$ . For  $V/J > 1$  this gives  $0 \leq E_0/N_p$  and any zero-energy state saturates this lower bound and is therefore a ground-state. One should however notice that it is possible to make zero-energy domain walls in this VBC since the state shown Fig. 4 is also annihilated by the Hamiltonian. No local dimer movement can take place in the staggered VBC (with or without domain walls). Each of these states form a topological sector with a single configuration which has  $|\Omega_x| + |\Omega_y| = L/2$  with respect to a columnar state.

### 5.3.3. Columnar crystal for $V < 0$

When parallel dimers attract each other the system tries to maximize the number of flippable plaquettes. Columnar configurations as shown on the left side of Fig. 3 do maximize this number. Such a VBC is exactly realized for  $V < 0$  and  $J = 0$ . Elementary excitations consist of a pair of (say) vertical dimers in a background of vertical columns of horizontal dimers. Such excitations are gapped ( $\Delta E = 2|V|$ ) and this VBC phase will survive

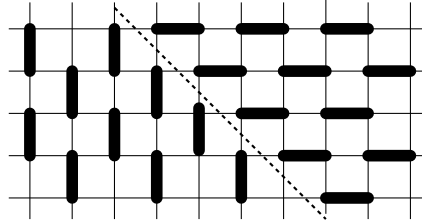


Fig. 4. Domain wall in a staggered VBC.

to the inclusion of a finite  $J$  term. Notice that unlike the staggered VBC presented in the previous paragraph the columnar dimer configuration is not an exact eigenstate when  $J \neq 0$ . The exact diagonalizations data of Leung *et al*<sup>148</sup> suggest that the columnar phase may disappear around a critical value  $V/J \simeq -0.2$ .

#### 5.3.4. Plaquette phase

When the kinetic energy dominates ( $|V| \ll J$ ) the system will try to maximize the number of resonating plaquettes  $||\rangle + |=\rangle$ . This can be achieved through the resonating plaquette crystal shown Fig. 3 and the numerical work (exact diagonalizations up to  $8 \times 8$  sites) of Leung *et al*<sup>148</sup> suggest that this phase is realized in an interval  $-0.2 \leq V/J \leq 1$ . Although this model would not suffer from the fermion sign problem we are not aware of any QMC simulation on this model.

#### 5.3.5. Rokhsar-Kivelson point

The point  $J = V$  (Rokhsar-Kivelson (RK) point) plays a special role. As remarked by Rokhsar and Kivelson<sup>143</sup> the equal-amplitude superposition of all dimerizations in a given topological sector is an exact ground-state. When  $J = V$  the Hamiltonian can be written as a sum of projectors:

$$\mathcal{H}_{J=V=1} = \sum_p |\Psi_p\rangle \langle \Psi_p| \quad (33)$$

$$|\Psi_p\rangle = |\text{I I}\rangle - |\text{II}\rangle \quad (34)$$

The linear superposition of all dimer coverings belonging to a given sector  $\Omega$

$$|0\rangle = \sum_{c \in \Omega} |c\rangle \quad (35)$$

is annihilated by Eq. 33 and is therefore a ground-state. The argument is the following. Consider a plaquette  $p$  and a configuration  $|c\rangle$ . If  $|c\rangle$  has one or no dimer at all on the edges of  $p$  we have  $\langle\Psi_p|c\rangle = 0$ . If two dimers are present, then there exists a configuration  $|c'\rangle$  in the same sector which only differ from  $|c\rangle$  by a two-dimer flip on  $p$ . In such a case the combination  $|c\rangle + |c'\rangle$  is again orthogonal to  $|\Psi_p\rangle$ . This shows that  $H|0\rangle = 0$ .

When open boundary conditions are considered (this restricts the topological sector to  $\Omega_x = \Omega_y = 0$ ) the RK state is the linear combination of an exponential number of configurations.<sup>h</sup> This is very different from the crystalline states considered so far where some periodic configurations were favored and it closely resembles Anderson's RVB picture. As we shall see this RK state is not a "true" liquid on the square lattice since dimer-dimer correlations are not short-ranged but algebraically decaying ( $\sim 1/r^2$ ) with distance. The calculation of dimer-dimer correlations in the RK state (Eq. 35) maps onto a *classical* dimer problem solved by Kasteleyn,<sup>137,139</sup> Fisher<sup>138</sup> and Fisher and Stephenson.<sup>149</sup> From this Rokhsar and Kivelson<sup>143</sup> constructed gapless excitations (in single-mode approximation) which dispersion relation vanishes as  $\mathbf{k}^2$  at small momentum (the origin is taken at  $(\pi, \pi)$ ). Quoting Rokhsar and Kivelson,<sup>143</sup> these excitations (dubbed "resonons") are the *Goldstone mode of the gauge symmetry which allows the phases of the different topological sectors to be varied without changing the energy*. Another mode of gapless excitations (around  $(\pi, 0)$  and  $(0, \pi)$  in the Brillouin zone), specific to the fact that the ground-state has critical (algebraic) dimer-dimer correlations, was recently discovered.<sup>150</sup>

The QDM on the square lattice is thus believed to be ordered (VBC) everywhere except at the RK point ( $J = V$ ) where it has quasi long-ranged (critical) dimer-dimer correlations.

#### 5.4. Hexagonal lattice

The QDM on the honeycomb lattice was studied by Moessner, Sondhi and Chandra,<sup>151</sup> in particular with Monte Carlo simulations. The phase diagram is very similar to the square lattice-case discussed above. It possesses three crystalline phases (Fig. 5) and has algebraically decaying dimer-dimer correlations at the Rokhsar Kivelson point (where the ground-state in each sector has the same form as Eq. 35). The absence of liquid phase (with exponentially decaying  $2n$ -mer- $2n$ -mer correlations) is believed to prevail in bipar-

<sup>h</sup>This is also true for periodic boundary conditions provided the two winding numbers do not scale like the linear size  $L$ .

tite lattices. This relation between the absence of a deconfined dimer liquid phase<sup>i</sup> and the bipartite character of the lattice as been discussed by several authors<sup>152</sup> and is related to the possibility of a *height representation*<sup>153</sup> of dimer coverings when the lattice is bipartite.<sup>j</sup>

$$\mathcal{H} = -J \sum_h \left( \left| \begin{array}{c} \bullet \quad \bullet \quad \bullet \\ \diagup \quad \diagdown \quad \diagup \\ \bullet \quad \bullet \quad \bullet \end{array} \right\rangle \left\langle \begin{array}{c} \bullet \quad \bullet \quad \bullet \\ \diagdown \quad \diagup \quad \diagdown \\ \bullet \quad \bullet \quad \bullet \end{array} \right| + \text{H.c.} \right) \\ + V \sum_h \left( \left| \begin{array}{c} \bullet \quad \bullet \quad \bullet \\ \diagup \quad \diagdown \quad \diagup \\ \bullet \quad \bullet \quad \bullet \end{array} \right\rangle \left\langle \begin{array}{c} \bullet \quad \bullet \quad \bullet \\ \diagup \quad \diagdown \quad \diagup \\ \bullet \quad \bullet \quad \bullet \end{array} \right| + \left| \begin{array}{c} \bullet \quad \bullet \quad \bullet \\ \diagdown \quad \diagup \quad \diagdown \\ \bullet \quad \bullet \quad \bullet \end{array} \right\rangle \left\langle \begin{array}{c} \bullet \quad \bullet \quad \bullet \\ \diagdown \quad \diagup \quad \diagdown \\ \bullet \quad \bullet \quad \bullet \end{array} \right| \right) \quad (36)$$

Fouet *et al.*<sup>97</sup> studied the spin- $\frac{1}{2}$   $J_1$ - $J_2$ - $J_3$  model on the hexagonal lattice by exact diagonalizations and found evidences of a staggered VBC of the type predicted for  $V/J > 1$  by Moessner *et al.*<sup>151</sup> in the QDM. Other phases (Néel ordered phase and a possible short-range RVB SL) are also present in the spin- $\frac{1}{2}$  model.<sup>97</sup>

### 5.5. Triangular lattice

The most local dimer Hamiltonian on the triangular lattice contains kinetic and potential two-dimer terms on each rhombus; it was studied by Moessner

<sup>i</sup>Bipartiteness seems to forbid deconfinement but not short-ranged dimer-dimer correlations. The 4-8 lattice (squares and octagons) is an example where dimer-dimer correlations are short-ranged. We thank R. Moessner for pointing this to us. On this lattice the equal-amplitude superposition of all coverings would be similar to an explicit VBC wave-function (thus confining). Such situations are only possible when the number of sites is even in the unit cell.

<sup>j</sup>Consider a bipartite lattice with coordination number  $z$ . For each dimer covering we can associate integers (heights) on the dual lattice by the following rule. Set the height to be zero on a plaquette at the origin. The height is then defined on the whole lattice by turning clockwise (resp. counterclockwise) around sites of the  $A$ -sublattice (resp.  $B$ -sublattice) and changing the height by  $z-1$  when crossing a dimer and by  $-1$  when crossing an empty bond. It is simple to check the difference of heights  $\delta h(x) = h_1(x) - h_2(x)$  between two dimerizations is constant inside each loop of their transition graph. Notice that the loops of a transition graph can be naturally oriented on a bipartite lattice. Then,  $\delta h(x)$  changes by  $+z$  (resp.  $-z$ ) when crossing a clockwise (resp. counterclockwise) loop of the transition graph. Columnar dimerizations have an averaged height which is flat and staggered ones have the maximum tilt. The winding numbers  $(\Omega_x, \Omega_y)$  correspond to the average height difference between both sides of the sample. The kinetic energy terms of Eqs. 29 and 36 change the height of the corresponding plaquette by  $\pm z$  and the potential terms ( $V > 0$ ) favor tilted configurations.

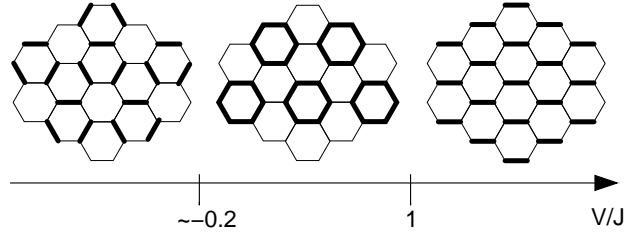


Fig. 5. Phase diagram of the hexagonal QDM obtained by Moessner *et al.*<sup>151</sup> Although the VBC shown for  $V < 0$  do not have all dimers parallel to the same direction it is equivalent to the columnar VBC found in the square lattice QDM because it maximizes the number of flippable plaquettes. It also corresponds to the ordering pattern predicted in the large- $N$  theory of Ref.<sup>119</sup> As for the VBC obtained for  $V/J > 1$ , it is the hexagonal counterpart of the *staggered* VBC of the square lattice (no flippable plaquette, exact eigenstate and maximum tilt in a height representation).

and Sondhi:<sup>144</sup>

$$\begin{aligned} \mathcal{H} = & -J \sum_r \left( \left| \begin{array}{c} \bullet \\ \diagup \quad \diagdown \\ \bullet \end{array} \right\rangle \left\langle \begin{array}{c} \bullet \\ \diagdown \quad \diagup \\ \bullet \end{array} \right| + \text{H.c.} \right) \\ & + V \sum_r \left( \left| \begin{array}{c} \bullet \\ \diagup \quad \diagdown \\ \bullet \end{array} \right\rangle \left\langle \begin{array}{c} \bullet \\ \diagup \quad \diagdown \\ \bullet \end{array} \right| + \left| \begin{array}{c} \bullet \\ \diagdown \quad \diagup \\ \bullet \end{array} \right\rangle \left\langle \begin{array}{c} \bullet \\ \diagdown \quad \diagup \\ \bullet \end{array} \right| \right) \end{aligned} \quad (37)$$

where the sums run over all rhombi  $r$  of the lattice (with three possible orientations). This model was shown to possess (at least) three crystalline phases, including a columnar and staggered one (Fig. 6) as in the two previous examples. An additional VBC (with resonating diamonds plaquettes) with a large unit cell (12 sites) was also predicted around  $V = 0$ . When  $V < 0$  and  $J = 0$  the ground-state is highly degenerate since it is possible, from an ordered columnar configuration, to shift all the dimers along any straight line without changing the number of flippable plaquettes (contrary to the square lattice case). However, an infinitesimal  $J$  is expected to lift this degeneracy and to order the ground-state in a columnar way.

The phenomenology of these ordered phases is that of usual VBC and we refer to the original paper<sup>144</sup> for details.

### 5.5.1. RVB liquid at the RK point

The new physics of this model appears through the existence of a *liquid* phase in the interval  $0.7 \lesssim V/J \leq 1$ . As for the two previous QDM the ground-states are exactly known at the RK point  $J = V$ . As before dimer-dimer correlations are obtained exactly at this point by a Pfaffian

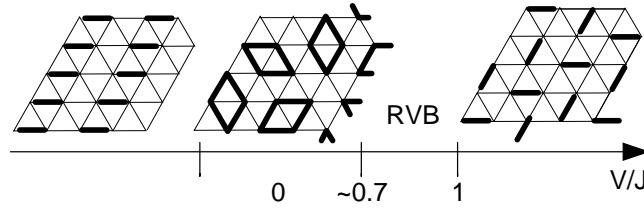


Fig. 6. Phase diagram of the triangular lattice QDM obtained by Moessner and Sondhi.<sup>144</sup>

calculation<sup>144,154,155</sup> but the result shows a *finite* correlation length. From their Monte Carlo simulations Moessner *et al.*<sup>144</sup> argued that the spectrum is gapped at the RK point and that this gap persists down to  $V/J \simeq 2/3$ , that is over a finite range of coupling. This picture is consistent with the exact diagonalizations performed on this model.<sup>156,157</sup>

### 5.5.2. Topological order

When the lattice is not bipartite the loops of a transition graph can no longer be oriented. The winding numbers  $\Omega_x$  and  $\Omega_y$  are now defined as the (positive) number of non-trivial loop around  $x$  and  $y$  in the transition graph with a reference configuration (say columnar). These two integers are not conserved by local dimer moves. They are however *conserved modulo two*, which leaves only four sectors.<sup>k</sup> Consequently *the dimer liquid ground-state is four-fold degenerate* at the RK point. This degeneracy holds exactly at the RK point even on finite-size samples but it is expected to hold in the thermodynamic limit in the whole liquid phase ( $0.7 \lesssim V/J \leq 1$ ).

Conventional orders are often associated to a spontaneously broken symmetry and lead to ground-state degeneracies in the thermodynamic limit. The four-fold degeneracy discussed above is the signature of some kind of order, called topological order.<sup>158</sup> The peculiarity of this order is that it is not associated to any local order parameter: a local observable cannot decide whether a given dimerization is in one sector or another. The existence of topological order is intimately associated to the fractionalized nature of the elementary excitations (see below). In the case of a RVB dimer liquid

<sup>k</sup>The two-dimer moves included in Eq. 37 are not sufficient to guaranty ergodicity with each of the four sectors. Staggered states (12-fold degenerate - not  $\mathcal{O}(L)$  like on the square lattice) have no flippable plaquette but can be connected to other states with four-dimer moves.<sup>144</sup>

these excitations have been known to be *Ising vortices* for a long time<sup>159,160</sup> (dubbed *visons* in the recent literature<sup>161,162</sup>). We will now discuss these excitations in more details in the framework of a QDM which realizes the same dimer liquid phase but for which not only the ground-state but all the eigenstates are known exactly.

### 5.6. Solvable QDM on the kagome lattice

An exactly solvable QDM on the kagome lattice was introduced by D. Serban, V. Pasquier and one of us<sup>141</sup>. It offers a very simple and explicit realization of the ideas discussed above (visons, topological order etc.).

#### 5.6.1. Hamiltonian

The kagome lattice QDM introduced in Ref. <sup>141</sup> contains only kinetic terms and has no external parameter. The Hamiltonian reads:

$$\mathcal{H} = - \sum_h \sigma^x(h) \quad (38)$$

$$\text{where } \sigma^x(h) = \sum_{\alpha=1}^{32} |d_\alpha(h)\rangle \langle \bar{d}_\alpha(h)| + \text{H.c} \quad (39)$$

The sum runs over the 32 loops on the lattice which enclose a single hexagon and around which dimers can be moved (see Table 1 for the 8 inequivalent loops). The shortest loop is the hexagon itself, it involves 3 dimers. 4, 5 and 6-dimers moves are also possible by including 2, 4 and 6 additional triangles (the loop length must be even). The largest loop is the star. For each loop  $\alpha$  we associate the two ways dimers can be placed along that loop:  $|d_\alpha(h)\rangle$  and  $|\bar{d}_\alpha(h)\rangle$ . Notice that  $\sigma^x(h)$  measures the relative phases of dimer configurations displaying respectively the  $d_\alpha(h)$  and  $\bar{d}_\alpha(h)$  patterns in the wave function.





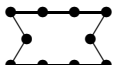


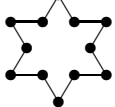
#### 5.6.2. RK ground-state

As for the QDM discussed previously the ground-state of this Hamiltonian is the equal amplitude superposition of all dimer coverings belonging to a given topological sector (as on the triangular lattice there are four sectors). This can be readily shown by writing  $\mathcal{H}$  as a sum of projectors:

$$\mathcal{H} = -N_h + \sum_h \sum_{\alpha=1}^{32} [ |d_\alpha(h)\rangle - |\bar{d}_\alpha(h)\rangle ] [ \langle d_\alpha(h)| - \langle \bar{d}_\alpha(h)| ] \quad (40)$$



Table 1. The 8 different classes of loops which can surround an hexagon of the kagome lattice. Including all possible symmetries we find 32 possible loops. The first column indicates the number of dimers involved in the coherent motion around the hexagon.

3			
4			
5			
6			

where  $N_h$  is the number of hexagons on the lattice. When expanding the products the diagonal terms give a simple constant since

$$\sum_{\alpha=1}^{32} |d_{\alpha}\rangle \langle d_{\alpha}| + |\bar{d}_{\alpha}\rangle \langle \bar{d}_{\alpha}| = 1 \quad (41)$$

This reflects the fact that, for any dimerization, the dimers on hexagon  $h$  match *one and only one* of the  $2 \times 32$  patterns  $\{d_{\alpha}, \bar{d}_{\alpha}\}$ .

Unlike the square or triangular case, the RK ground-states  $|0\rangle = \sum_{c \in \Omega} |c\rangle$  are not degenerate with some staggered VBC.<sup>1</sup> This means that the Hamiltonian of Eq. 38 is not at a phase transition to a VBC. As we will explain it is *inside* a liquid RVB phase.

The RK wave-function can be viewed as dimer condensate. It is similar to the ground-state of liquid  $^4\text{He}$  which has the same positive amplitude for any configuration and its permuted images.<sup>163</sup> An important difference, however, is that the QDM state is incompressible and cannot sustain acoustic phonons. This can be related to the fact that the  $U(1)$  symmetry of the Bose liquid is absent in the QDM on non-bipartite lattices. It is replaced

<sup>1</sup>Because resonances loops of length up to 12 are present the dynamics is ergodic in each of the four topological sectors.<sup>141</sup>

instead by a discrete  $\mathbb{Z}_2$  gauge symmetry (see §5.6.7 below).

### 5.6.3. Ising pseudo-spin variables

The kinetic energy operators  $\sigma^x$  defined in Eq. 39 commute with each other. This is obvious when two such operators act on remote hexagons but it also holds for neighboring ones. This property can easily be demonstrated with the help of the arrow representation of dimer coverings introduced by Zeng and Elser.<sup>164</sup> This mapping of kagome dimerizations to arrows on the bonds of the honeycomb lattice is illustrated Fig. 7. Each arrow has two possible directions: it points toward the interior of one of the two neighboring triangles. If site  $i$  belongs to a dimer  $(i, j)$  its arrow must point toward the triangle the site  $j$  belongs to. A dimer covering can be constructed from any arrow configuration provided that the number of outgoing arrows is odd (1 or 3) on every triangle.

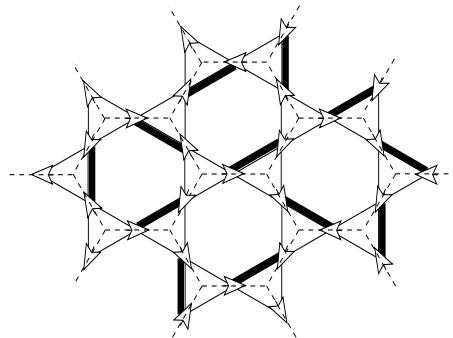


Fig. 7. A dimer covering on the kagome lattice and the corresponding arrows. Dashed lines: honeycomb lattice.

The operators  $\sigma^x$  have a particularly simple meaning in terms of the arrow degrees of freedom:  $\sigma^x(h)$  flips the 6 arrows sitting on  $h$ .<sup>m</sup> It is then clear that the  $\sigma^x$  commute and that  $\sigma^x(h)^2 = 1$ . In fact these operators can be used as Ising pseudo-spin variables and the Hamiltonian now describes non-interacting pseudo-spins in a uniform magnetic field pointing in the  $x$  direction. In the ground-state we have  $\sigma^x(h) = 1$  on every hexagon.

<sup>m</sup>Flipping all the arrows around any closed loop (such as around an hexagon) preserves the local constraint imposed on arrow configurations. Flipping the arrows around a topologically non-trivial loop changes the topological sector.

#### 5.6.4. Dimer-dimer correlations

The ground-state is the most possible disordered dimer liquid as the dimer-dimer correlations strictly vanish beyond a few lattice spacings. Such correlations can be computed by the Pfaffian method. On the kagome lattice the determinant of the Kasteleyn matrix (which is directly related to the partition function of the classical dimers problem) is exactly constant in Fourier space.<sup>165</sup> Since dimer-dimer correlations are obtained from the Fourier transform of the inverse of this determinant, they turn out to be strictly zero beyond a few lattice spacings (as soon as the two bonds do not touch a common triangle).<sup>141</sup> This result can also be obtained by a simpler argument<sup>141,166</sup> using the  $\sigma^x$  operators. This result is related to the kagome geometry.<sup>n</sup> This absence of long-ranged dimer-dimer correlations demonstrates that the RK state is a dimer liquid and that it breaks no lattice symmetry.

On the triangular lattice, even at high temperature, dimer-dimer correlations decay exponentially with distance but these correlations remain *finite* at any distance. On the square lattice such correlations are even larger because they decay only as a power law. This means that the infinite hardcore dimer repulsion makes QDM non-trivial even at infinite temperature; dimers cannot be free when they are fully-packed. From this point of view we see that the kagome lattice is particular: it is as close as possible to a free dimer gas, except for non-trivial correlations over a few lattice spacings. This is a reason why dimer coverings on the kagome lattice can be handled with independent pseudo-spin variables and why the RK state on this lattice is the most possible disordered RVB liquid.

#### 5.6.5. Visons excitations

The  $\sigma^x$  operators can be simultaneously diagonalized but they must satisfy the global constraint  $\prod_h \sigma^x(h) = 1$  since this product flips every arrow *twice*. It must therefore leave all dimerizations unchanged. The lowest excitations have therefore an energy 4 above the ground-state and they are made of a *pair* of hexagons  $a$  and  $b$  in a  $\sigma^x(a) = \sigma^x(b) = -1$  state.  $a$  and  $b$  are the locations of two Ising vortices (or *visons*<sup>161,162</sup>). As remarked before this means that the relative phases of the configurations with  $d_\alpha(h)$  and  $\bar{d}_\alpha(h)$  patterns have now changed sign. The corresponding wave-function is

<sup>n</sup>The model of Eq. 38 can be generalized to any lattice made of corner-sharing triangles.<sup>141</sup>

obtained in the following way. Consider a string  $\Omega$  which goes from  $a$  to  $b$  (see Fig. 8) and let  $\Omega(a, b)$  be the operator which measures the parity  $\pm 1$  of the number of dimers crossing that string.  $\Omega(a, b)$  commutes with all  $\sigma^x(h)$ , except for the ends of the string:  $\sigma^x(a)\Omega(a, b) = -\Omega(a, b)\sigma^x(a)$ . A dimer move changes the sign of  $\Omega(a, b)$  if and only if the associated loop crosses the string an odd number of times, which can only be done by surrounding one end of the string. This shows that  $\Omega(a, b)$  flips the  $\sigma^x$  in  $a$  and  $b$ .<sup>o</sup> As the RK ground state  $|0\rangle$ ,  $\Omega(a, b)|0\rangle$  is a linear combination of all dimer configurations belonging to one sector. However the amplitudes are now 1 and  $-1$  depending on the number of dimers crossing  $\Omega$ . This wave-function therefore has nodes, it is an excited state of energy 4 with two vortices in  $a$  and  $b$ . It is easy to see that a different choice  $\Omega'$  for the string connecting  $a$  and  $b$  gives the same state up to a global sign which depends on the parity of the number of kagome sites enclosed by  $\Omega \cup \Omega'$ .

These vortex excitations carry a  $\mathbb{Z}_2$  charge since attempting to put two vortices on the same hexagon does not change the state. Such excitations are not local in terms of the dimer degrees of freedom. Indeed, determining the sign of a given dimerization in a state with two visons which are far apart requires the knowledge of the dimer locations along the whole string connecting the two vortex cores. In this model the visons appear to be static and non-interacting. This is a particularity of this solvable model but the existence of gapped vison excitations is believed to be a robust property of RVB liquids. In more realistic models the visons will acquire a dynamics and a dispersion relation but will remain gapped.<sup>p</sup> They will also have some interactions with each other but should remain *deconfined*. This property is particularly clear in the kagome QDM: visons are necessarily created by pairs but the energy is independent of their relative distances.

The Ising vortices also offer a simple picture of the topological degeneracy. Consider a ground-state  $|+\rangle$  of the model which lives in the sector where the winding number  $\Omega_y$  (with respect to some arbitrary but fixed dimerization) is even. Another ground-state  $|-\rangle$  is obtained in the odd- $\Omega_y$  sector. Now consider the combination  $|0\rangle = |+\rangle + |-\rangle$  and apply the operator  $\Omega(0, L_x)$  corresponding to a closed loop surrounding the torus in the  $x$  direction. This amounts to creating a pair of nearby visons at the origin, taking one of them around the torus in the  $x$  direction and annihilating them.

<sup>o</sup>Up to a global sign (reference dependent)  $\Omega(a, b)$  is equal to  $\sigma^z(a)\sigma^z(b)$  where the  $\sigma^z$  operators are those introduced by Zeng and Elser.

<sup>p</sup>It is possible to add potential energy terms to Eq. 38 to drive the system outside of the liquid phase and this transition corresponds to a vison condensation.

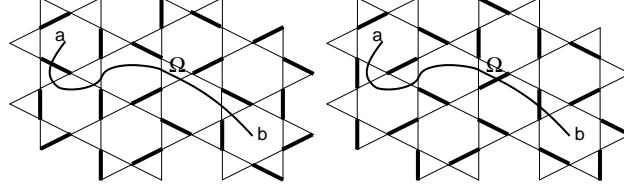


Fig. 8. A pair of visons (located in  $a$  and  $b$ ) is created by applying to the RK wavefunction a factor  $(-1)$  for each dimer crossing the string  $\Omega$ . The dimerization shown there on the left appears in the linear superposition of the two-vison state with the sign  $-1$  whereas the one on the right has the sign  $+1$ .

This can also be viewed as the creation of a vison in one hole of the torus (with no energy cost). It is simple to check that  $\Omega(0, L_x)|0\rangle = |+\rangle - |-\rangle$  (up to an irrelevant global sign). This provides a simple relation between the vison-pair creation operator and the existence of two topologically distinct ground-states  $|+\rangle + |-\rangle$  and  $|+\rangle - |-\rangle$ .

#### 5.6.6. Spinons deconfinement

We assume that dimers represent “dressed” singlet valence-bonds, as in the overlap expansion (§5.2). Since the Hilbert space is made of fully-packed dimer coverings the model of Eq. 38 only describes spin-singlet states. However, as any QDM, it can be extended to include static holes or spinons. Configurations with unpaired sites (spinon or holon) are now allowed but the kinetic terms of the original Hamiltonian which loop passes on an empty site gives zero. Consider a system with two static spinons in  $x$  and  $y$ . As on the square<sup>143</sup> and triangular lattices<sup>144</sup> at the RK point the exact ground-state  $|x, y\rangle$  remains the sum of all dimer coverings and the ground-state energy is independent of the distance between the two spinons (except at very short distance if they belong to a common hexagon). This is a first indication that RVB *spin* liquid has deconfined spin- $\frac{1}{2}$  excitations (spinons). In the QDM language these excitations are simply unpaired sites in a dimer liquid background. Such unpaired sites are necessarily created by pairs but they can then propagate freely (no attractive potential) when they are sufficiently far apart.

Another calculation allows to test the deconfinement properties of a dimer liquid. We consider the state  $|\psi\rangle = \sum_{\mathbf{r} \neq 0} |0, \mathbf{r}\rangle$  where  $|0, \mathbf{r}\rangle$  is the (un-normalized) state with two spinons in  $0$  and  $\mathbf{r}$ . The probability to find a spinon in  $\mathbf{r}$  in the  $|\psi\rangle$  can be obtained by the relatively involved calculation

of the monomer correlation<sup>a</sup> with Pfaffians. On the square lattice this probability goes to zero as  $1/\sqrt{r}$ .<sup>149</sup> This shows that the second spinon is (quasi-) confined in the vicinity of the first one on the square lattice because escaping far away represents a large “entropy” cost in the dimer background. On the triangular lattice it goes exponentially to a constant.<sup>154</sup> This result is a signature of deconfinement. In fact the same signature can be obtained on the kagome lattice without any technical calculation since the monomer correlation is exactly  $1/4$  at any distance.<sup>167</sup>

If unpaired sites are allowed one can describe spinons or holons. Unfortunately in the presence of simple kinetic energy terms for these objects the model can no longer be solved. However one can consider a static spinon and its interaction with visons: when the spinon is adiabatically taken around a vison the dimers are shifted along a path encircling the vison. Because the vison wave-function is particularly simple in this model it is easy to check that this multiplies the wave-function by a factor  $-1$ . This is the signature of a long-ranged statistical interaction<sup>160,159</sup> between visons and spinons (or holons). In more realistic models, as long as the visons are gapped excitations the spinons are expected to be deconfined. On the other hand if the visons condense their long-ranged statistical interaction with spinons frustrates their motion. This is no longer true if they propagate in *pairs*, in which case they are not sensitive any more to visons (see Ref. <sup>141</sup> for an extension of the present QDM with a vison condensation). This simple physical picture illustrates the relation between vison condensation and spinon confinement.

### 5.6.7. $\mathbb{Z}_2$ gauge theory

The forces responsible for confinement are usually associated to gauge fields and their fluctuations. Whereas  $U(1)$  compact gauge theories are generically confining in  $2+1$  dimensions,<sup>168,136</sup>  $\mathbb{Z}_2$  gauge theories are known to possess deconfined phases.<sup>169</sup> For this reason some attention has been paid to the connexions between  $\mathbb{Z}_2$  theories and fractionalized phases in 2D electronic systems.<sup>161</sup>

It is known<sup>140</sup> that QDM can be obtained as special limits of  $\mathbb{Z}_2$  gauge theories, the gauge variable being the dimer number on a bond. However, on the kagome lattice this connexion can be made exact and completely

<sup>a</sup>Ratio of number of dimer coverings with two holes in  $0$  and  $\mathbf{r}$  to the number without hole.

explicit since there is a one to one correspondence between dimer coverings and physical states (*i.e.* gauge-invariant) of a  $\mathbb{Z}_2$  gauge theory.<sup>141</sup> In this mapping the gauge fields are Ising variables living on the link of the honeycomb lattice (*i.e.* kagome sites) and are constructed from the arrows described previously. As for the constraints of gauge invariance they correspond to the odd parity of the number of outgoing arrows on every triangles. The  $\sigma^x$  operator used to define a solvable QDM translate into a gauge-invariant plaquette operator for the gauge degrees of freedom (product of the Ising gauge variables around an hexagon). With this mapping the visons appear to be vortices in the  $\mathbb{Z}_2$  gauge field and the solvable model of Eq. 38 maps to the deconfined phase of the gauge theory.

### 5.7. A QDM with an extensive ground-state entropy

So far we have discussed QDM that realize either spontaneous VBC, critical states or RVB liquids. We wish to mention here that these three scenarios may not be the only possible ground-states for QDM. In particular, a QDM on the kagome lattice with an extensive ground-state entropy was recently discussed.<sup>170</sup> This model was introduced from the observation that the dimer kinetic energy terms arising from an overlap expansion (§5.2) generally have non trivial *signs* as soon as resonance loops of *different lengths* are considered. It was then realized that such signs (which make the QDM no longer appropriate for QMC simulations) can lead to qualitatively new phases, different from VBC or RVB liquids. The Hamiltonian introduced in Ref. <sup>170</sup> is similar to that of Eqs. 38-39 except that each resonance loop  $\alpha$  is now included with a *sign*  $(-1)^{n_\alpha}$  where  $n_\alpha = 3, \dots, 6$  is the number of dimers involved:

$$\mathcal{H} = \sum_h (-1)^{n_\alpha} [ |d_\alpha(h)\rangle \langle \bar{d}_\alpha(h)| + | \bar{d}_\alpha(h)\rangle \langle d_\alpha(h)| ] \quad (42)$$

These signs are precisely those appearing in the overlap expansion (at the order of one hexagon) of the Heisenberg model on the kagome lattice. This expansion was carried out by Zeng and Elser<sup>171</sup> in an insightful paper which laid the basis of the analysis of the kagome antiferromagnet in the first neighbor valence-bonds subspace.

Although not exactly solvable, the Hamiltonian of Eq. 42 was shown to be a dimer liquid (short-ranged dimer-dimer correlation) and to have a huge ground-state degeneracy  $\sim 2^{N/6} = 1.122^N$  ( $N$  is the number of kagome sites). In addition, several numerical indications pointed to a critical behavior of this system,<sup>170</sup> with a possible algebraic decay of energy-energy

correlations.<sup>r</sup> It was argued that the effective QDM describing the singlet dynamics of the spin- $\frac{1}{2}$  Heisenberg antiferromagnet on the kagome lattice could be *close* (in parameter space) to Eq. 42. If correct, this sheds light on the very large density of singlet states observed at low energy in the numerical spectra of that spin model (see Sec. 7).

## 6. Multiple-spin exchange models

### 6.1. Physical realizations of multiple-spin interactions

#### 6.1.1. Nuclear magnetism of solid $^3\text{He}$

Solid  $^3\text{He}$  was the first magnetic system in which the importance of MSE interactions was recognized.<sup>172,173,174</sup> Due to the large zero-point motion of the atoms about their mean positions, tunneling events during which 2, 3 or 4 atoms exchange their positions in a cyclic way are frequent. These processes generate an effective interaction between the (nuclear) spins which can be written

$$\mathcal{H} = \sum_P -J_P (-1)^P (P_{spin} + P_{spin}^{-1}) \quad (43)$$

where the sum runs over permutations  $P$ ,  $J_P > 0$  is the exchange frequency of the associated tunneling process (in real space) and  $P_{spin}$  acts on the Hilbert space of spin- $\frac{1}{2}$  located on the site of the crystal. The sign  $-(-1)^P$  depends of the signature of the permutation  $P$  and is a consequence of the Pauli principle. For a *cyclic* permutation involving  $n$  spins this sign is just  $(-1)^n$  and is responsible for the ferromagnetic character of processes involving an odd number of spins. For spin- $\frac{1}{2}$  particles, two and three-spin exchange terms reduce to the familiar Heisenberg interaction:

$$P_{12} = 2\vec{S}_1 \cdot \vec{S}_2 + \frac{1}{2} \quad (44)$$

$$P_{123} + P_{321} = P_{12} + P_{23} + P_{31} - 1 \quad (45)$$

but this is no longer true for  $n \geq 4$ :

$$P_{1234} + P_{4321} = P_{12}P_{34} + P_{14}P_{23} - P_{13}P_{24} + P_{13} + P_{24} - 1 \quad (46)$$

which can be expressed (thanks to Eq. 44) as a sum of terms with two and four Pauli matrices.

<sup>r</sup>Notice that a one-dimensional analog of Eq. 42 can be defined and exactly maps onto the Ising chain in transverse field at its critical point.



$^3\text{He}$  can form solid atomic mono-layers with a triangular geometry when adsorbed on a graphite substrate at ultra low temperatures (milli Kelvin range). This 2D magnet has been studied for a long time (see Refs. <sup>175,176</sup> and references therein) and the importance of MSE interactions involving up to six atoms has now been recognized.<sup>177,178</sup> The exchange frequencies of the most important processes have been computed by Path Integral Monte Carlo (PIMC)<sup>179,180,181,182</sup> (analytic WKB calculations have also been carried out<sup>177,183</sup>) as a function of the density. The proposed MSE Hamiltonian describing the magnetic properties of this 2D quantum crystal reads

$$\mathcal{H} = (J_2 - 2J_3) \sum_{\text{---}} P_{12} + J_4 \sum_{\text{---}} (P_{1\dots 4} + \text{H.c}) \quad (47)$$

$$- J_5 \sum_{\text{---}} (P_{1\dots 5} + \text{H.c}) + J_6 \sum_{\text{---}} (P_{1\dots 6} + \text{H.c})$$

where Eq. 45 was used to absorb the three-spin terms into an effective first-neighbor Heisenberg exchange  $J_2^{\text{eff}} = J_2 - 2J_3$ . At high density the hard-core potential between Helium atoms only leaves three-body exchanges possible ( $J_3 \gg J_{n \neq 3}$ ) and Eq. 48 reduces to a first neighbor Heisenberg *ferromagnet*,<sup>184</sup> as observed experimentally for the first time by Franco *et al.*<sup>185</sup> in high-density layers. On the other hand the second layer solidifies at lower density and higher order exchange terms cannot be ignored.<sup>s</sup> PIMC simulations<sup>182</sup> and high-temperature fits of the experimental data<sup>178</sup> showed that the relative strength of two- and four-spin terms is roughly  $J_2^{\text{eff}}/J_4 \sim -2$  in the low-density second layer solid. The  $J_2$ - $J_4$  model was studied by exact diagonalizations in this region of parameter space and evidences for a short-ranged RVB SL phase with no broken symmetry were obtained.<sup>186,114,187</sup> The ultra-low temperature measurements of specific heat<sup>188</sup> and uniform susceptibility<sup>189</sup> are not incompatible with such a spin liquid phase but the spin gap, if any, has not yet been observed and should be smaller than  $100\mu\text{K}$ .

<sup>s</sup>The first layer is then so dense that exchange is strongly suppressed. The first layer can also be replaced by an  $^4\text{He}$  or HD mono-layer.

### 6.1.2. Wigner crystal

The Wigner crystal is another fermionic solid with a triangular geometry where MSE interactions can play an important role. At very low density the Coulomb energy dominates, the crystal is almost classical and MSE interactions are very small. Exchange frequencies  $J_P$  can be computed in this regime by a semi-classical (WKB) approximation<sup>177,190,191</sup> and, as for the high density solid of  $^3\text{He}$ , three-body exchanges dominate and give rise to ferromagnetism. However, at higher density and close to melting, PIMC calculations of the exchange frequency<sup>192</sup> showed that the magnetism may be described by a MSE model with parameters ( $J_2^{\text{eff}}$  and  $J_4$ ) close to those where the triangular MSE model is expected to be a RVB SL. Unlike the  $^3\text{He}$  case, the particles (electrons) are charged and an external magnetic field has also an orbital effect, it introduces complex phases in the exchange energies:  $P + P^{-1} \rightarrow e^{i\alpha}P + e^{-i\alpha}P^{-1}$  where the angle  $\alpha = 2\pi\phi/\phi_0$  is proportional to the magnetic flux  $\phi$  passing through the area enclosed by the exchange trajectory and  $\phi_0$  is the unit flux quantum. This can give rise to very rich phase diagrams<sup>192,191</sup> where complex MSE terms compete with the Zeeman effect (see Ref. <sup>193</sup> for some early experimental attempts to explore this physics).

### 6.1.3. Cuprates

The possibility of significant four-spin exchange around square Cu plaquettes in copper oxide compounds was first suggested by Roger and Delrieu.<sup>194</sup> They interpreted the anomalously large width of Raman scattering spectra as a signature of four-spin exchange in this copper oxide superconductor. The importance of these MSE interactions in  $\text{CuO}_2$  planes ( $J_4 \sim 0.25J_2$ ) has then been emphasized by a number of groups and in different materials and by different experimental and theoretical approaches.<sup>195,196,197,198</sup> Four-spin plaquette ring exchange also plays a significant role in ladder compounds.<sup>199,200,201,202</sup> For instance, exchange parameters with values  $J_{\text{rung}} = J_{\text{leg}} = 110$  meV and  $J_{\text{ring}} = 16.5$  meV were proposed for  $\text{La}_6\text{Ca}_8\text{Cu}_{24}\text{O}_{41}$  based on the dispersion relation of magnetic excitations.<sup>199,200</sup>

## 6.2. Two-leg ladders

Numerous works were devoted to ladder models with four-spin interactions. These include general bi-quadratic interactions as well as models with ring-

exchange terms. We will only discuss here the simplest of these MSE models:

$$\mathcal{H} = J \sum_n \left( \vec{S}_{n,1} \cdot \vec{S}_{n,2} + \vec{S}_{n,1} \cdot \vec{S}_{n+1,1} + \vec{S}_{n,2} \cdot \vec{S}_{n+1,2} \right) + K \sum_{\square} (P_{1234} + H.c) \quad (48)$$

Thanks to several studies<sup>200,203,204,205</sup> the phase diagram of this Hamiltonian is now rather well understood and five different phases were identified.

- **Ferromagnetic phase.** The ground-state is fully polarized. This phase includes the  $(J = -1, K = 0)$  and the  $(J = 0, K = -1)$  points.
- **Rung-singlet phase.** This phase includes the ground-state of the ladder without MSE term  $(J = 1, K = 0)$ . The spectrum is gapped and the ground-state is unique. A moderate  $K/J \gtrsim 0.23 \pm 0.03$  destroys this phase<sup>200,206,207,205</sup> in favor of the VBC below.
- **Staggered VBC** with dimers on the legs. In one of the two degenerate ground-states the dimerized bonds are  $(2n, 1) - (2n+1, 1)$  and  $(2n+1, 2) - (2n+2, 2)$ . The VBC disappears for  $K/J \gtrsim 0.5$ .<sup>205</sup> Such a staggered VBC was first predicted in the framework of a ladder with bi-quadratic interaction by Nersesyan and Tsvelik.<sup>59</sup> Using Matrix-Product Ansatz, Kolezhuk and Mikeska<sup>60</sup> constructed models which are generalizations of Eq. 48 and which have exact ground-state with long-ranged staggered dimer correlations. In this phase the magnetic excitations are very different from the magnon excitations of the rung-singlet phase above. Here the excitations do not form well-defined quasi-particles but a continuum made of pairs of domain walls connecting two dimerized ground-states.<sup>59,60</sup>
- **Scalar chirality phase.** The order parameter is  $\langle \vec{S}_{n,1} \cdot (\vec{S}_{n,2} \times \vec{S}_{n+1,2}) \rangle$  and it spontaneously breaks the time-reversal symmetry and translation invariance. The ground-state is two-fold degenerate up to the next transition at  $K/J \simeq 2.8 \pm 0.3$ .<sup>205</sup> There exists a duality transformation<sup>204,208</sup> which maps the scalar chirality order parameter onto the dimer order parameter of the VBC above.<sup>t</sup> Applying such a transformation to the exact VBC ground-states mentioned above, models with an exactly known ground-state and scalar chirality LRO can be constructed.<sup>204,208</sup> Although chiral SL have been much discussed in the literature, this is to our knowledge

<sup>t</sup>The Hamiltonian of Eq. 48 is self-dual at  $2K = J$ .

the first realization of such a phase in a  $SU(2)$  symmetric spin- $\frac{1}{2}$  model.

- **Short-ranged ordered phase with vector-chirality** correlations. The strongest correlations are  $\langle (\vec{S}_{n,1} \times \vec{S}_{n,2}) \cdot (\vec{S}_{n',1} \times \vec{S}_{n',2}) \rangle$  but they remain short-ranged. The spectrum is gapped and the ground-state is unique. This phase includes the pure  $K = 1$  model where  $J = 0$ . This phase is related by the duality transformation discussed above to the rung-singlet phase.<sup>208</sup> This transformation indeed relates the Néel correlations  $\langle (\vec{S}_{n,1} - \vec{S}_{n,2}) \cdot (\vec{S}_{n',1} - \vec{S}_{n',2}) \rangle$  (which are the strongest ones in the rung-singlet phase) to the vector-chirality correlations. Close to the ferromagnetic phase ( $J < 0$ ) one observes a crossover to a region where the strongest correlations are ferromagnetic spin-spin correlations along the legs and antiferromagnetic along the rungs.<sup>205</sup>

### 6.3. MSE model on the square lattice

The phase diagram of the Hamiltonian 48 on the *two-dimensional square-lattice* has been recently studied by Läuchli<sup>209</sup> by exact diagonalizations. Néel, ferromagnetic, columnar VBC and staggered VBC phases were identified, as in the ladder model above. In addition, a nematic phase characterized by long-ranged vector chirality correlations (alternating spin currents) was found around the  $K = 1$ ,  $J = 0$  point. To our knowledge this is the first microscopic realization of a nematic order in a two-dimensional spin- $\frac{1}{2}$  model.

### 6.4. RVB phase of the triangular $J_2$ - $J_4$ MSE

Because of its relevance to solid  $^3\text{He}$  films and Wigner crystals, the MSE model on the triangular lattice has been the subject of many studies.<sup>210,211,212,213,186,114,187</sup> We will discuss here some properties of the simplest MSE model with up to four-spin cyclic exchange interactions ( $J_2 - 2J_3$  and  $J_4$  only in Eq. 48). The classical phase diagram (Fig. 9) of this model has been studied by Kubo and collaborators<sup>210,211</sup> and the quantum one has been roughly scanned in Ref.<sup>187</sup>: we will mainly focus on the short-ranged RVB spin liquid (see Fig. 9), which is probably *the first RVB SL encountered in an  $SU(2)$ -symmetric spin model*.

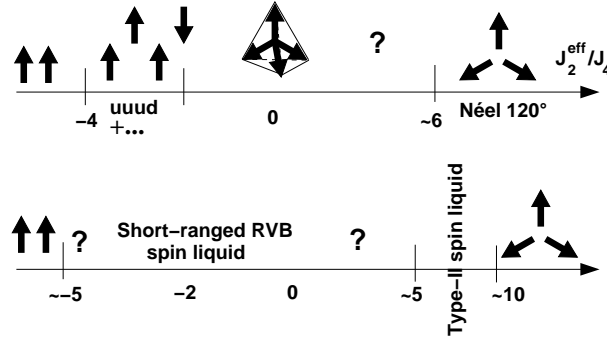


Fig. 9. Classical (top) and quantum (bottom) phases of the  $J_2 - J_4$  MSE Hamiltonian. The classical model was studied by Kubo and Momoi<sup>210</sup> and is based on a variational approach. The quantum phase diagram is the simplest scenario compatible with the exact diagonalizations data of Refs. <sup>186,114,187</sup>. While not completely understood, in the type-II spin-liquid region the spectra are characterized by a very large number of singlet excitations below the first triplet state. This is not the case in the RVB phase.

#### 6.4.1. Non-planar classical ground-states

It is well-known that an Heisenberg model (with possible second-neighbors, third-neighbors, ... interactions) on a Bravais lattice always admits a planar helical ground-state at the classical level. This is no longer true when MSE are present and finding the classical ground-state for arbitrary  $J_2$  and  $J_4$  is an unsolved problem. A mean-field phase diagram was obtained for the classical model<sup>210</sup> but very few exact results are known. In the neighborhood of  $J_4 = 1$   $J_2 = 0$  the classical ground-state is known to be a four-sublattice configurations with magnetizations pointing toward the vertices of a regular tetrahedron.<sup>210</sup> This is a quite interesting model where the ground-state spontaneously breaks a discrete Ising symmetry associated to the sign of the triple product  $\vec{S}_1 \cdot (\vec{S}_2 \times \vec{S}_3)$  around a triangle. This broken symmetry gives rise to a finite-temperature phase transition which has been observed in Monte Carlo simulations.<sup>211</sup> This phenomena is similar to the transition predicted in the  $(\pi, 0)$  phase of the  $J_1$ - $J_2$  model on the square lattice.<sup>14</sup>

#### 6.4.2. Absence of Néel LRO

The classical ground-states at  $J_4 = 1$ ,  $J_2 = 0$  are tetrahedral configurations. Although this phase appears to be stable within the framework of linear spin-wave calculations<sup>211</sup> or Schwinger-Boson mean-field theory,<sup>212</sup> exact diagonalizations indicate that the magnetic LRO is washed out by quantum

fluctuations.<sup>211,114</sup> The chiral order predicted to survive at long distances and finite temperatures<sup>211</sup> in the classical system for  $J_2 = 0$  is also likely to be washed out by quantum fluctuations.<sup>114</sup>

When  $J_2 = 1$  a relatively small amount of  $J_4 \sim 0.1$  is sufficient to destroy the three-sublattice Néel LRO realized by the first-neighbor Heisenberg model.<sup>187</sup> The nature of the phase on the other side of this transition is not settled but the finite-size spectra display a large density of singlet excitations at low energy which could be reminiscent of the kagome situation.<sup>187</sup>

From exact diagonalizations (up to 36 sites) no sign of Néel LRO could be found at  $J_4 = 1, J_2 = -2$ .<sup>186,114</sup> In addition, the finite-size analysis showed that the spin-spin correlation length is quite short at  $J_2 = -2$  and  $J_4 = 1$  and a spin gap of the order of  $\Delta \sim 0.8$  exists at this point. Much of the numerical effort to elucidate the nature of the MSE ground-state was concentrated on this point because it is close to the parameters realized in low-density  $^3\text{He}$  films (when higher order exchanges are neglected).

#### 6.4.3. *Local singlet-singlet correlations - absence of lattice symmetry breaking*

Having excluded the possibility of a Néel ordered ground-state at  $J_4 = 1, J_2 = -2$  it is natural to look for a possible VBC. Because of the complexity of the MSE Hamiltonian it is not clear what kind of spatial order should be favored. From the analysis of dimer-dimer correlations (see Fig. 10) it appears that parallel valence-bonds repel each-other at short distance. This is similar to what is observed in the staggered phase of the  $J_2$ - $J_4$  MSE ladder and square-lattice models. For this reason it appears that a plausible VBC would be the staggered VBC encountered in the triangular QDM for  $V > J$  (§5.5). However this scenario seems difficult to reconcile with the weakness of dimer-dimer correlations.<sup>114</sup> In addition, the low-energy singlet states and their quantum numbers<sup>214</sup> do not reflect the 12-fold quasi-degeneracy that should be present if the system was to spontaneously break some lattice symmetry according to a staggered VBC pattern. Small systems usually *favor* ordered phases because low-energy and long-wavelength fluctuations that could destabilize an ordered state are reduced compared to larger systems. From the fact that the finite-size spectra do not show the signatures of a staggered VBC symmetry breaking it is unlikely that the MSE model could develop a VBC of this kind in the thermodynamic limit.

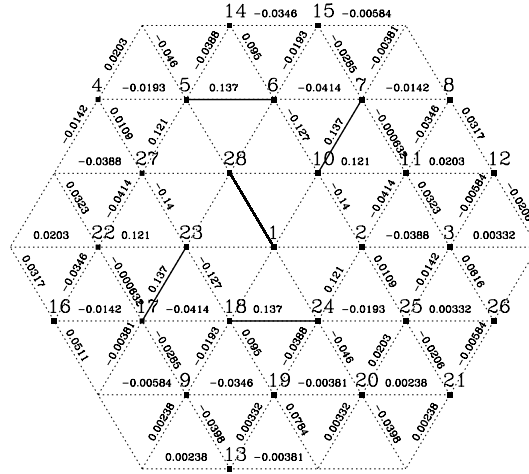


Fig. 10. Dimer-dimer correlations in the ground-state of the  $J_2$ - $J_4$  MSE model on the triangular lattice (28 sites) at  $J_2 = -2$ ,  $J_4 = 1$  (from Ref. <sup>114</sup>). Numbers are proportional to  $\langle \hat{d}_0 \hat{d}_x \rangle - \langle \hat{d}_0 \rangle \langle \hat{d}_x \rangle$  where the operator  $\hat{d}_x$  projects onto the singlet space of the bond  $x$  and  $\hat{d}_0$  refers to the reference bond (1,28). These results shows a clear tendency for repulsion between parallel dimers.

#### 6.4.4. Topological degeneracy and Lieb-Schultz-Mattis Theorem

Because no VBC phase could be identified in the MSE model at  $J_4 = 1$ ,  $J_2 = -2$  the numerical data were compared with the predictions of an RVB liquid scenario.

In one dimension a famous theorem due to Lieb, Schultz and Mattis<sup>215</sup> (LSM) states that in a one-dimensional spin system with an half-integer spin in the unit cell there is at least one excited state collapsing to the ground-state in the thermodynamic limit (periodic boundary conditions). There are in fact several arguments suggesting that this theorem might, at least to some extent, also apply to higher dimensions.<sup>216,217,157,218,219</sup> If that is the case a gapped system with an odd integer spin in the unit cell must have a degenerate ground-state. The simplest scenario to explain this degeneracy is a translation symmetry breaking. One could think that this would rule out the possibility of any (translation invariant) RVB liquid in such models. This is incorrect because a ground-state degeneracy can have

a topological origin on a system with periodic boundary conditions, as we discussed in the framework of QDM (§5). Such a phase is characterized by a four-fold topological ground-state degeneracy when the system is on a torus. That degeneracy allows the system to fulfill LSM's requirement without any spontaneous translation symmetry breaking.<sup>157</sup>

On a finite-size system the topological degeneracy is only approximate but some constraints exist for the quantum numbers (momentum in particular) of the quasi-degenerate multiplet.<sup>157</sup> A system with periodic boundary conditions with an even number of sites but an *odd number of rows* is expected to have two ground-states with differ by a momentum  $\pi$  in the direction parallel to the rows, in close analogy to the the LSM theorem in dimension one. The numerical spectra of the MSE model exhibit a set of three singlet energy levels collapsing onto the ground-state when the system size is increased<sup>114</sup> and their quantum number turn out to be consistent with the constraints derived from the general RVB picture.<sup>157</sup>

#### 6.4.5. Deconfined spinons

The SL phase described above is expected to have deconfined spinons ( $S = \frac{1}{2}$  excitations). These excitations should show up as an incoherent continuum in the spin-spin dynamical structure factor. However such a feature would probably be rather difficult to observe on small 2D lattices, in particular due to the small number of inequivalent  $\mathbf{k}$ -vectors in the Brillouin zone. On the other hand, the binding energy of two spinons can be evaluated by comparing the ground-state energy and the first magnetic excitation energy on even and odd samples. In the case of the MSE model at  $J_4 = 1, J_2 = -2$  the results show the existence of a bound-state (it is more favorable to put two spinons in the same small sample than in separate ones, which is not surprising) but this *does not mean that the spinons are confined* (contrary to the conclusions of Ref. <sup>114</sup>). Interestingly this binding energy seems to go to zero for the largest available sizes (Fig. 11): this might indicate the absence of attraction between spinons for large enough separation and an asymptotic deconfinement.

It is important to stress here that the RVB SL phase discussed here (and its QDM counterparts of §5.5 and §5.6) is not the only way to spinon deconfinement in 2D. There is at least another scenario, inherited from one dimension, which is the *sliding Luttinger liquid*. Indeed, the Luttinger liquid behavior and the one-dimensional critical behavior of magnetic chains seem to be robust to small (or moderate) *frustrating transverse couplings between*



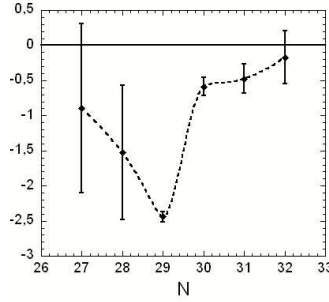


Fig. 11. Spinons binding energy as a function of the system size in the MSE model at  $J_2 = -2$  and  $J_4 = 1$ . The vertical bars correspond to the range of values found for different sample shapes.

*chains*, as observed both in theoretical<sup>220,221,222,223,224,225,226</sup> and numerical approaches.<sup>100</sup> This regime between one and two dimensions which may have been observed in  $\text{Cs}_2\text{CuCl}_4$ <sup>227</sup> is the subject of a number of recent studies.<sup>223,224</sup>

### 6.5. Other models with MSE interactions

Multiple-spin interactions are present in a number of models that were found to exhibit fractionalization or an RVB liquid ground-state. Well known examples of MSE interactions with an Ising symmetry are  $\mathbb{Z}_2$  gauge theories, where the gauge invariant plaquette term is a product of Pauli matrices  $\prod_i \sigma_i^z$ . Such theories have a deconfined phase in 2+1 dimension<sup>169</sup> and their relevance to fractionalized phases of 2D electronic systems has been pointed out by Senthil and Fisher.<sup>161</sup> The connexion between  $\mathbb{Z}_2$  gauge theories and QDM was mentioned in §5.6.7. Some MSE spin models with an Ising symmetry and a fractionalized ground-state were discussed by Kitaev,<sup>228</sup> Nayak and Shtengel.<sup>229</sup> In the other limit of a  $U(1)$  (or  $XY$ ) symmetry several models have been studied. Recent examples are based upon the spin- $\frac{1}{2}$  four-spin  $XY$  ring exchange interaction<sup>230,231,232,233</sup>

$$\mathcal{H} = -K \sum_{\langle ijkl \rangle} (S_i^+ S_j^- S_k^+ S_l^- + \text{H.c.}) \quad (49)$$

which is the  $XY$  analog of the  $SU(2)$  MSE interaction  $P_{1234} + \text{H.c.}$

## 7. Antiferromagnets on the kagome (and related) lattices

In RVB SL phases described in §5.5, §5.6 and §6.4 *singlet excitations (visons) are gapped*. In the  $\mathbb{Z}_2$  gauge theory approach this gap is essential for the consistency of the theory.<sup>161,162</sup> The gauge-field quasi particles are vortices of the gauge field and carry a unit  $\mathbb{Z}_2$  gauge flux but no spin. As illustrated in §5.6.6 in the framework of a simple QDM, visons have long-ranged interaction with spinons. If the spectrum of these visons has a gap then the spinons are unconfined and the phase is “fractionalized”. If they condense, the long range interaction between them and the spinons frustrate the motions of the latter which remained confined. The gap in the singlet sector (above the topological degeneracy) is thus a crucial ingredient of these RVB SL. At the end of this section we will show how the spin- $\frac{1}{2}$  first-neighbor Heisenberg model on the kagome lattice represents an enigma with respect to this scheme (as well as the QDM described in Sec. 5.7). We begin the section by a review of the properties of various models on the kagome lattice, which topology is the source of an extreme frustration, and, in many models, source of an extensive degeneracy of the ground-state.

### 7.1. Miscellaneous models on the kagome lattice

There has been a large number of studies devoted to different antiferromagnetic models on the kagome lattice. The next neighbor Ising model on such a lattice is disordered, its entropy per site is very large  $S_{\text{kag}}^{\text{Ising}} = 0.502$ , more than half the independent spin value, much larger than the triangular lattice value  $S_{\text{tri}}^{\text{Ising}} = 0.323$  and of the order of Pauling approximation for independent triangles  $S_{\text{Pauling}} = 0.501$ .<sup>234</sup> This suggests that the correlations in this system are very weak: the model remains disordered at all temperatures.<sup>235,236</sup> Moessner and Sondhi have studied this Ising model in a transverse magnetic field (the simplest way to include some quantum fluctuations in the model): the model fails to order for any transverse field, at any temperature.<sup>145,237</sup>

The nearest neighbor classical Heisenberg model on the kagome lattice has also a huge ground-state degeneracy. This property is easy to understand and holds on different lattices with corner sharing units such as the checkerboard lattice or the three dimensional pyrochlore lattice (Moessner and Chalker<sup>106,107</sup>). On all these lattices the nearest neighbor Heisenberg Hamiltonian can be written as the sum of the square of the total spin  $\vec{S}_\alpha$  of individual units  $\alpha$  (a tetrahedron in the 2-d and 3-d pyrochlore cases and

a triangle for the kagome lattice), which share only one vertex. Classical ground-states are obtained whenever  $\forall \alpha \vec{S}_\alpha = \vec{0}$ . This condition fixes the relative positions of the three classical spins of a triangle at 120 degrees from each other in a plane. But it does not fix the relative orientation of the plane of a triad with respect to the planes of triads on corner sharing triangles: the model has a continuous local degeneracy<sup>238,236</sup> at  $T = 0$ .<sup>u</sup> Thermal fluctuations select coplanar configurations.<sup>238,236,240</sup> The possibility of long-range order in spin-spin correlations at very low temperature has been discussed without any definitive conclusion.<sup>236,241</sup> The order parameter of the planar phase is defined by the local helicity (sometimes called vectorial chirality) :

$$\vec{\zeta} = \vec{S}_1 \times \vec{S}_2 + \vec{S}_2 \times \vec{S}_3 + \vec{S}_3 \times \vec{S}_1 \quad (50)$$

where the three sites define a triangle. This kind of order is sometimes called *nematic* by analogy to liquid crystals. The existence of such an order parameter might be related to the instability of the classical Heisenberg model on the kagome lattice to Dzyaloshinsky-Moriya interactions.<sup>242,243</sup> The classical model has a large density of low-lying excitations at low temperature.<sup>244</sup>

## 7.2. Spin- $\frac{1}{2}$ Heisenberg model on the kagome lattice: an extreme play-ground for “quantum fluctuations”

The nearest neighbor spin- $\frac{1}{2}$  quantum Heisenberg model on the kagome lattice has equally been the object of many studies<sup>245,246,247,248,171,249,250,251,252,253,254</sup> From these studies the following important facts have emerged :

### 7.2.1. Ground-state energy per spin

The Heisenberg model on the kagome lattice has an extremely low energy per bond ( $\langle \mathbf{S}_i \cdot \mathbf{S}_j \rangle \simeq -0.44$ )  $\sim 87\%$  of the energy per bond in an isolated triangle. On this lattice the energy per bond of the spin- $\frac{1}{2}$  system is much lower than the classical energy  $\frac{E_{qu.}}{E_{cl.}} \sim 1.74$ , a ratio much larger than in any other 2D magnet, that can only be compared to the value obtained for the Bethe chain (1.77). The kagome lattice is the 2D lattice which offers the largest stabilization due to quantum fluctuations.

<sup>u</sup>Counting the *planar* ground-states amounts to determine in how many ways one can associate one of the three letters *A*, *B* and *C* to each site so that each triangle has spins along the three different orientations. This already represents an extensive entropy.<sup>239,236</sup>

### 7.2.2. Correlations

The ground-state is disordered.<sup>255</sup> Within accuracy of the finite-size numerical computations, spin-spin correlations,<sup>248</sup> dimer-dimer correlations (Fig. 12), chirality-chirality correlations<sup>246</sup> are short-ranged, which is consistent with the previous point and series expansion results.<sup>256</sup>

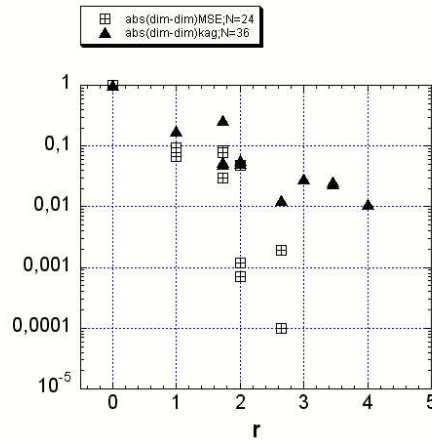


Fig. 12. Dimer-dimer correlations in the ground-state of the kagome Heisenberg model (black triangles) and in the MSE model discussed in §6.4 (open symbols) versus distance. Although the decrease of these correlations is weaker in the KH model than in the MSE model, it seems nevertheless roughly exponential in the first two decades, as the spin-spin correlations are.<sup>246,248</sup>

### 7.2.3. Spin-gap

There is plausibly a spin-gap of the order of  $1/20^{\text{th}}$  of the coupling constant.<sup>250</sup> In view of the smallness of this spin-gap with regards to the available sizes caution is necessary. The above conclusion was drawn from the value of the *microscopic* spin gap  $E_0(S = S_{\min} + 1) - E_0(S = S_{\min})$  on exact spectra of samples with up to 36 spins,<sup>250</sup> where  $E_0(S)$  is the lowest energy in the  $S$  sector, and  $S_{\min} = 0$  or  $\frac{1}{2}$  depending on the parity of the total number of spins. The finite-size effects on these results are an order of magnitude smaller than in a Néel ordered antiferromagnet. Nevertheless they are still not negligible for these sizes. An alternative determination of the spin-gap can be obtained along the following line. The lowest exact

eigenstate in each total spin sector  $S$  of a  $N$  spins sample defines the energy per spin  $e$  at  $T = 0$  as a function of its magnetization  $m = S/(N/2)$ . For low positive values of the magnetization, one can fit  $e(m)$  to the phenomenological law:<sup>v</sup>

$$e(m) = e(0) + am + bm^2/2 + \mathcal{O}(m^3) \quad (51)$$

$a$  and  $b$  are intensive quantities which depend on  $N$  but should converge to some (possibly zero) value when  $N \rightarrow \infty$ . This point of view is important because for an infinite system the thermodynamic function  $e(m) = \lim_{N \rightarrow \infty} E(S = mN/2)/N$  can be measured (through the zero temperature magnetization curve), but not  $E(S \sim \mathcal{O}(1))$ . The physical significance of Eq. 51 is clear:  $a$  measures half the spin gap (in a thermodynamic sense, that is the magnetic field  $H_c$  required to magnetize the system at zero temperature) and

$$b = \frac{\partial^2 e}{\partial m^2} = \chi^{-1} \quad (52)$$

where  $\chi$  is the homogeneous susceptibility of the medium for fields larger than the critical field  $H_c = a$ . This determination of the *thermodynamic* spin gap leads to a renormalization of the raw data<sup>250</sup> for small sizes (see Fig. 13). A linear extrapolation versus  $1/N$  (which should give a lower bound of the spin-gap) leads to the value 0.06 for the spin gap ( $e_\infty = -0.4365$  and  $\chi_\infty = 0.34$ ). This determination is in agreement with the direct extrapolation of the microscopic gap  $E_0(S = S_{min} + 1) - E_0(S = S_{min})$ . For  $N = 36$  at the smallest non-zero magnetization, the linear term of equation (51) is 90% of the quadratic term: this is an estimate of the degree of confidence on the existence of a spin-gap.

#### 7.2.4. *An exceptional density of low lying excitations in the singlet sector*

Whatever the ultimate fate of the spin gap a big surprise emerges from the exact spectra: the probable absence of gap in the singlet sector and the anomalous density of low energy states adjacent to the ground-state. Let us first comment the second point in details: even on the smallest size spectra the low lying states appear contiguous to the ground-state and the spectra

<sup>v</sup>This phenomenological form cannot extend below  $m = 0$  and beyond  $m = 1/3$  because at both magnetizations an angular point appears in  $e(m)$  with a discontinuity of the first derivative signaling a magnetization plateau.<sup>257,258</sup> This is discussed in more details in our lectures notes.<sup>95</sup>

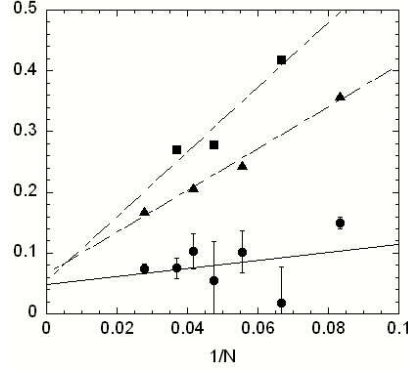


Fig. 13. Finite size scaling of the spin gap in the spin- $\frac{1}{2}$  Heisenberg model  $\mathcal{H} = \sum_{\langle i,j \rangle} \mathbf{S}_i \cdot \mathbf{S}_j$  on the kagome lattice. Triangles (resp. squares) are the raw results of the microscopic spin gap in the even (resp. odd) samples. Bullets represent the “thermodynamic” spin gap, they are obtained by the procedure described in the text (errors bars come from the rms uncertainty in the fits).

are extremely dense. The number of singlet levels in the spin-gap (taken as a natural energy band-width of the problem) increases exponentially fast with  $N$  as  $\sim 1.15^N$  as far as the  $N \leq 36$  systems are concerned (see Fig. 14). This property remains (and can be checked on larger systems) when the Hilbert space is restricted to that of first-neighbor valence-bond coverings.<sup>253,170</sup>

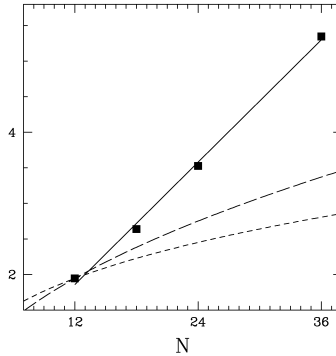


Fig. 14. Logarithm of the number of singlet states in the spin gap versus sample size (black squares). The short dashed and long dashed curves display the theoretical law (Eq. 54 with  $d = 2$ ) (short dashes:  $p = 1$ , long dashes:  $p = 2$ ).

Some remarks are necessary to fully appreciate this property. The  $2^N$  states of the system are stretched on an energy scale of the order of  $NJ$  where  $J$  is the coupling constant of the Hamiltonian. This implies that on most of the spectrum the density of states increases exponentially with  $N$ . If we specialize to the  $S = 0$  sector as we will do below, the picture is not very different: the number of states is  $C_{\frac{N}{2}}^N - C_{\frac{N}{2}-1}^N \sim \mathcal{O}(\frac{2^N}{N})$  and here too, in most of the spectrum the density is exponentially increasing with  $N$ . But in all the phases that we have studied up to now, the nature of the ground-state and of the low lying excitations leads to a different behavior at the bottom of the spectrum. The ground-state degeneracy is  $\mathcal{O}(1)$  in VBC, VBS and in the RVB SL (of the type discussed in §5.6 and §6.4 for instance) and it is  $\mathcal{O}(N^p)$  in Néel ordered states with  $p$  sublattices. In all these situations the low-lying excitations are described as modes or quasi-particles. Let us suppose that single-particle excitations have a dispersion law:

$$\omega(\mathbf{k}) \sim k^p. \quad (53)$$

In a  $d$ -dimensional system the total internal energy increases with temperature as  $E \sim NT^{(p+d)/p}$ , the specific heat as  $C_v \sim NT^{d/p}$  as well as the entropy  $\mathcal{S} \sim NT^{d/p}$ . In a micro-canonical point of view the density of states  $\rho(E)$  or a large enough system is simply related to the entropy by  $\mathcal{S} = \log(\rho(E))$ . Since  $\mathcal{S} \sim NT^{d/p} = N(E/N)^{d/(p+d)}$  we obtain

$$\log(\rho(E)) \propto N^{\frac{p}{p+d}} \quad (54)$$

As an example, let us consider the Rokhsar Kivelson QDM on the square lattice at the quantum critical point (Sec. 5): the dispersion law of the so-called resonons is quadratic around  $\mathbf{Q} = (\pi, \pi)$ , the logarithm of the number of states increases as  $N^{1/2}$  (long dashes of Fig. 14).

Even with such many-particle excitations one would expect a number of levels increasing more slowly than in the numerical spectra. Infinitely soft low-energy modes ( $p \rightarrow \infty$ ), are necessary to recover a density of low-lying levels growing as  $\sim \alpha^N$ . It is still unclear if we can do a connection between the “zero modes” of the classical model at  $T = 0$  and this picture. And we cannot completely indulge ourselves in saying that quantum fluctuations are unable to lift the classical degeneracy as quantum fluctuations seem to open a spin gap.

A physical consequence of this exceptional density of low lying singlets can be observed in the specific heat: at low temperature the specific heat of this spin system is unusually large, with a double peak

structure,<sup>255,259,260,261</sup> insensitive to relatively large magnetic fields.<sup>252</sup> This is easily understood if we suppose that in this energy range there is a large density of singlet states.<sup>252</sup> This result is to be compared to the experimental results of Ramirez *et al.*<sup>262</sup> on  $\text{SrCr}_9\text{Ga}_{12-9p}\text{O}_{19}$  (notice however that it is a spin- $\frac{3}{2}$  compound and that numerical calculations were performed on the spin- $\frac{1}{2}$  model) where the specific heat around 5 K has an extremely low sensitivity to magnetic fields up to 10 Tesla, whereas the homogeneous susceptibility in this range of temperature is probably very low if we notice that it turns down around 50K.<sup>263</sup>

#### 7.2.5. Absence of gap in the singlet sector

Up to  $N = 36$  sites there is no evidence of a possible gap in the singlet spectrum: this is an exceptional phenomenon in quantum mechanics of small systems where discretization is usually the rule.

It has been advocated in recent papers<sup>264,265</sup> that the ground-state of this model could break the translational symmetry and be a VBC. The first proposed crystal<sup>264</sup> is made of resonating *stars* with 6 dimers. The corresponding unit cell has 12 spins. The second VBC<sup>265</sup> is made of resonating (trimerized) *hexagons* and was already discussed as the most reasonable crystal (if any is realized in this system, which we think is not clear at all) by Marston and Zeng<sup>147</sup> and Zeng and Elser.<sup>171</sup> This later VBC has a unit cell with 36 sites. In both scenarios it is the energy gain obtained by *local resonances* (involving respectively 6 and 3 valence-bonds) which drives the system toward a VBC. From the energy point of view the star VBC is (by far) less realistic since it involves a much longer resonance loop.<sup>w</sup> This resonance loop involving 6 valence-bonds around a star has a vanishing amplitude at the lowest non-trivial order of the overlap expansion in the RVB subspace, as was shown by Zeng and Elser<sup>171</sup>. To our opinion there is no reason to think that the physics of the kagome model can be described from the limit of weakly coupled stars. On the other hand, in the approximation where only the shortest resonance loops are present, the model was indeed found to be in the *hexagon* VBC phase, as re-discovered recently from a different point of view.<sup>265</sup> A crucial (numerical) result of Zeng and Elser<sup>171</sup> is however that this VBC *melts* when higher order resonances loops are included.

<sup>w</sup>Notice also that the gap associated to the star VBC is predicted to be of the order of  $1/10$  of  $J$ ,<sup>264</sup> which is 10 times larger than the largest distance between two consecutive levels in the spectrum of the  $N = 36$  sample.



We have studied the 36-sites sample which can accommodate these two VBC: the low-lying levels of the spectrum do not give a clear picture of the supposed to be VBC. The eigenstates with the quantum numbers corresponding to these two VBC are not the lowest energy levels in the spectrum. No gap is seen in the spectrum, the largest distance between two consecutive states is  $10^{-2}$  and seems distributed at random, whereas the average distance between two consecutive states in the 50 first states is:  $2.5 \cdot 10^{-3}$ . It has been argued that long wave-length quantum fluctuations (almost absent in the  $N = 36$  sample which contains only two resonating hexagons or three stars) could eventually restore the order. We think that this is incorrect. In a VBC it is *local resonances* which favor the crystal and longer resonances which tend to reduce the order parameter and which could eventually destabilize it. Long-wavelength will tend to restore a larger ground-state symmetry (reducing the degeneracy). From this point of view it is unlikely that a VBC pattern will appear in larger systems if it is not apparent in the smallest systems (provided that boundary conditions do not frustrate the corresponding VBC). We thus consider that up to now numerical results do not support the claims of a star or hexagon VBC ground-state in this model.

If the hexagon VBC was however realized the important question would probably be why the associated gap is so tiny, certainly smaller than  $10^{-3}$ . A natural scenario would be that of a very close proximity to a quantum critical point, but that critical point remains to be identified. A third possibility would be that of a system with a true extensive entropy at zero temperature. This is less likely in our opinion since (up to now) only models with simple (if not trivial) local symmetries were found to have such ground-state entropy (Ising antiferromagnet on the triangular lattice for instance or the QDM of §5.7) and this entropy is usually sent to (possibly small but) finite temperatures by almost any perturbation.

#### 7.2.6. Anomalous density of states in other spin sectors

An anomalous density of low lying states is equally observed in the spin  $\frac{1}{2}$  sector (where the law could be fitted to  $N^{1.15^N}$ ), in the spin 1 sector as well as in other sectors with larger total spin. It should be noticed that such a density of states implies the absence of an intrinsic energy scale for the low lying excitations: a phenomenon that has been observed in inelastic neutron scattering (Ref. <sup>266</sup> and Refs. therein) and theoretically in the imaginary part of the dynamic susceptibility calculated within the dynamical mean

field theory (Georges *et al.*<sup>267</sup>). A high spin susceptibility just above the spin gap is not excluded in the spin- $\frac{1}{2}$ .<sup>268</sup>

The global picture of this phase is thus that of a SL with no long-ranged correlations in any local observable, and an large entropy of singlets at  $T \ll J$ , which is a manifestation of the extraordinary large density of states in each  $S$  subspace.

### 7.3. *Next-neighbor RVB description of the spin- $\frac{1}{2}$ kagome antiferromagnet*

Considering a supposed-to-be large spin-gap, Zeng and Elser<sup>171</sup> proposed a description of the ground-state and low-lying excitations of the kagome model in the basis of next neighbor valence bonds. They analyzed in this context the dimer dynamics and showed on a  $N = 36$  sample that the hexagon VBC –favored by the shortest (three-)dimer moves– melts when introducing higher order tunneling. Mila and Mambrini<sup>251,253</sup> confirmed that this reduced Hilbert space of next neighbor valence bonds captures some of the most perplexing features of this magnet and specifically the absence of (measurable) gap in the singlet sector and the exponential number of singlets. One of us, D. Serban and V. Pasquier<sup>170</sup> have elaborated on this work and on Zeng and Elser’s approach and proposed a QDM with an extensive zero-point entropy and critical (energy-energy<sup>x</sup>) correlations (see §5.7). All these results point to an absence of an intrinsic low-energy scale. This feature is typical of a critical state, but as seen in the above discussion, the simple RK picture does not seem to fit nicely to the exact diagonalization data: may be the available sizes are too small or the behavior of this quantum system corresponds to something completely new. Some recent numerical results<sup>254</sup> (in the full spin- $\frac{1}{2}$  Hilbert space as well as in the RVB subspace) showed that (static) non-magnetic impurities (holes) experience an unexpected *repulsion* in this system and that no significant magnetic moment is created in the vicinity of the impurities. It has been argued<sup>269</sup> that static non-magnetic impurities are useful to detect a possible spinon deconfinement in two-dimensional antiferromagnets. From this point of view the results mentioned above suggest such a deconfinement.

---

<sup>x</sup>Dimer-dimer correlations are short-ranged in this model.

#### 7.4. *Experiments in compounds with kagome-like lattices*

The low temperature specific heat of  $\text{SrCr}_9\text{Ga}_{12}\text{O}_{19}$  (the magnetic chromium ion has a spin  $3/2$ ) is apparently dominated by singlet states.<sup>262</sup> The magnetic excitations of this compound as seen by muons can be described as spins  $\frac{1}{2}$  itinerant in a sea of singlets.<sup>270</sup> The non-linear spin susceptibility of  $\text{SrCr}_9\text{Ga}_{12}\text{O}_{19}$  exhibits a very large increase at about 5 K, reminiscent of spin glasses,<sup>271</sup> but neutrons and muons show that a very significant fraction of the spins are not frozen below this temperature and exhibit still very rapid fluctuations.<sup>272</sup> The same phenomena have been observed in two jarosites that are equally good models of kagome antiferromagnets with half-odd-integer spin per unit cell.<sup>273,274</sup>

#### 7.5. *"Haldane's conjecture"*

Whereas the classical Heisenberg model on the kagome, checkerboard and pyrochlore lattices share the properties of local continuous degeneracy and disorder at  $T = 0$ , their quantum counterparts are quite different. As it has been explained in Sec. 3, the Heisenberg model on the checkerboard lattice has an ordered VBC with gaps to all excitations. In contrast to the case of the  $S = \frac{1}{2}$  Heisenberg model on the kagome lattice, recent results from Hida<sup>66</sup> show that there is a large gap to all excitations in the  $S = 1$  Heisenberg model on this same lattice, in agreement with experiments.<sup>275,276,277</sup>

Less is known on the ground-state of the Heisenberg model on the three-dimensional pyrochlore lattice: Canals and Lacroix<sup>278</sup> have shown that the spin-spin correlations are short ranged and they have observed that on a 16-sites spectrum the first excitations are singlet ones. Fouet *et al.* have computed the spectrum of a 32-sites pyrochlore sample<sup>99</sup>, this work confirms that the first excitations are still singlets for this size. There is plausibly a degeneracy of the ground-state in the thermodynamic limit but no evidence of a closing of the gap above: the system may therefore be a VBC. A first description of the singlet sector was proposed by Harris, Berlinsky and Bruder<sup>279</sup> and was developed further by Tsunetsugu<sup>280,281</sup>. It starts from the limit of weakly-coupled tetrahedron (and thus breaks some spatial symmetries). The ground-state of an isolated tetrahedron is two-fold degenerate and can be described by an Ising pseudo-spin. An effective Hamiltonian describing the interactions between these pseudo-spins was written<sup>279</sup> and analyzed in a semi-classical approximation. It was concluded that the system maybe a VBC. It was argued by Tsunetsugu that a soft mode could exist in the singlet sector.<sup>281</sup> The CORE approach of

Berg *et al.*<sup>102</sup> seems more appropriate to deal with these systems where dimerization is probably the dominant phenomenon. They treated larger units (block of four tetrahedron) and concludes to the existence of a VBC with a larger unit cell than the one predicted before<sup>279,280,281</sup> and a small singlet gap.

All these results seem to confirm a 2D version of Haldane's conjecture: among these frustrated systems with local continuous degeneracies in the classical limit, the spin- $\frac{1}{2}$  kagome antiferromagnet is the only system to have an half-odd integer spin in the unit cell. It is maybe not by chance that it is the only one with gapless excitations.<sup>y</sup> The spin- $\frac{1}{2}$  Heisenberg model on the checkerboard lattice or on the pyrochlore lattice and the spin-1 Heisenberg model on the kagome lattice have integer spins in the unit cell and quantum fluctuations lead to gapful excitations. It is also interesting to note that these results are consistent with a generalization of the LSM theorem in dimension two.<sup>216,217,157,218,219</sup>

An interesting analysis of Von Delft and Henley<sup>282</sup> supports this conjecture. These authors studied the collective tunneling of a small cluster of spins between two spin configurations that are degenerate in the classical limit. They found that for half-odd-integer spins the tunneling amplitude for a cluster of six spins around an hexagon (and on other larger loops) is exactly zero because of destructive interferences between different symmetry-related instantons. For small integer spins the interference is constructive and the tunnel amplitude and the tunnel splitting are large: this is consistent with numerical results which gives a large gap for the  $S = 1$  kagome antiferromagnet, and small gaps (if any) in the spin- $\frac{1}{2}$  system.

## 8. Conclusions

We conclude by summarizing some properties –and related open questions– of the different phases discussed in this review.

The properties of these phases are summarized in Table 2. Semi-classical phases with Néel long ranged order, magnons as gapless excitations, do exist in spin- $\frac{1}{2}$  2D systems with moderate frustration: the Heisenberg model on the triangular lattice is the most explicit example, with a sublattice magnetization about one half of the classical value.<sup>2</sup> The ground-state degeneracy is in the thermodynamic limit a power of  $N$ .

<sup>y</sup>The SCGO compound with 7 spins  $3/2$  by unit cell belongs to the same category and as also gapless excitations.<sup>262</sup>

An increased frustration, lower coordination number or smaller spin lead to quantum phases, with a ground-state of higher symmetry, no long ranged order in spin-spin correlations, a spin gap and the restored  $SU(2)$  symmetry. Two main alternatives are then opened: the VBC or VBS phases on one hand, the RVB SL on the other. RVB SL and VBC (as well as VBS) first requires the formation of local singlets. When a particular local resonance pattern dominates the dynamics of the Hamiltonian the system will try to maximize the number of occurrence of this pattern. This is usually achieved by a regular arrangement, that is a VBC. When no such pattern dominates the system may form a translation invariant RVB SL. In the first case the ground-state can be qualitatively described by one ordered configuration of singlets dressed by small fluctuations. In the RVB SL the amplitudes of the wave-function are distributed over an exponentially large number of configurations. These ground-states lead to very different excitations:  $\Delta S = 1$  gapped magnons in the first case (and  $\Delta S = 0$  domain-wall excitations), gapped  $\Delta S = 0$  visons and gapped  $\Delta S = \frac{1}{2}$  unconfined spinons in the second case.

In agreement with the large- $N$  results (Sec. 4), VBC or VBS phases appear in general in quantum situations where the large- $S$  classical limit displays collinear order <sup>a</sup>, whereas up to now RVB SL phases have only be encountered in range of parameters where the classical solutions are non collinear (MSE<sup>186,114</sup> and  $J_1$ - $J_2$  on the honeycomb lattice<sup>97</sup>).

These states obey the 2D extension of LSM theorem: if  $2S$  is odd in the unit cell and if excitations are gapped there is a ground-state degeneracy in the thermodynamic limit (with periodic boundary conditions). However the origin of the degeneracy differs in the two types of quantum phases. In the VBC phases the degeneracy is associated to spontaneously broken translation symmetry whereas in the RVB SL the degeneracy has a topological origin. In the VBS (or explicit VBC) the ground-state is unique but  $2S$  is even in the unit cell. As in one dimension the LSM theorem seems to play an important role and a formal proof of its validity in 2D is perhaps very close, if not achieved.<sup>218</sup> A RVB SL may have been observed numerically in a spin- $\frac{1}{2}$  model on the hexagonal lattice.<sup>97</sup> From the point of view of large- $N$  and QDM approaches a topological degeneracy is expected in such a SL. Interestingly that degeneracy is not imposed by the 2D extension of LSM's theorem and has not been detected.<sup>97</sup>

These paradigms are relatively well understood, at least on the qualita-

<sup>a</sup>We have discussed some possible counter examples in section 3. 6

tive level. They also appear naturally in the broader context of the classification of Mott insulators.<sup>283</sup> However several kinds of 2D frustrated magnets do not fall in these simple classes and many open questions remain.

This review was restricted to  $SU(2)$  invariant Hamiltonians. Whereas the Ising limit has been much studied, the differences between quantum XY and Heisenberg models have received much less attention.

Chiral SL have not been discussed in this review. They are characterized by a broken time-reversal symmetry. This possibility has been studied intensely since the 80's<sup>284,285,286,4</sup>. To the best of our knowledge it has not yet been identified in a realistic 2D model.<sup>b</sup>

The issue of quantum phase transitions in frustrated antiferromagnet is also an active topic that is not presented in this review. Many properties of these critical points are still unknown, not to mention the fascinating problems associated with (quenched) disorder.

Limited by place (and competence) we have not discussed in details the works done on spatially anisotropic models. This field which is in between one (review by P. Lecheminant in this book) and 2D is extremely flourishing tackled by bosonization and large- $N$  methods.

To conclude we would like to emphasize that new analytical and/or numerical methods are highly desirable to proceed in the analysis of the two emblematic problems by which we have opened and closed this review: the  $J_1$ - $J_2$  model on the square lattice and the spin- $\frac{1}{2}$  Heisenberg model on the kagome (and pyrochlore) lattices. In both of these problems a consensus remains to be obtained.

## 9. Acknowledgments

It would have been difficult to thank individually many of our colleagues cited in references with whom we had numerous and fruitful discussions – many thanks to all of them. It is also a pleasure to thank our close collaborators B. Bernu, V. Pasquier, D. Serban and P. Sindzingre, this review owes much to them. We are also grateful to C. Henley, A. Honecker, R. Moessner and O. Tchernyshyov for their insightful comments on the manuscript.

## References

1. E. Manousakis, Rev. Mod. Phys. **63**, 1 (1991).

<sup>b</sup>An example was recently discovered in one dimension: the scalar-chirality phase of the spin ladder model with 4-spin MSE interactions (see §6.2).

Table 2. Different phases encountered in  $SU(2)$ -symmetric frustrated models in 2D

Phase	$2S/\text{cell}$	Order	Degeneracy	Broken sym.	Excitations	Thermo.	Examples
Néel AF p-sublattice	any	spin-spin LRO	$\mathcal{O}(N^p)$	$SU(2)$ Translations Point group	Gapless magnons (spin waves)	$C_v \sim T^2$ $\chi \sim \text{cst}$	Spin- $\frac{1}{2}$ triangular Heisenberg AF
VBC (§3) (spontaneous)	odd	singlet-singlet LRO colli. spin-spin SRO	$> 1$	Translations Point group	Gapped magnons	$C_v$ and $\chi$ activated	Honeycomb $J_1$ - $J_2$ Checkerboard Square $J_1$ - $J_2$ ?
VBC (§3) (explicit)	even	None	1	None	Gapped magnons	$C_v$ and $\chi$ activated	$\text{SrCu}_2(\text{BO}_3)_2$ $\text{CaV}_4\text{O}_9$
VBS (§3.3)	even	“String” LRO	1	None	Gapped magnons Edge excitations	$C_v$ and $\chi$ activated	AKLT Hamiltonians $S = 1$ kagome AF ?
RVB SL (§5.5 §5.6, §6.4)	odd	Topological non-coli. SRO	4 (torus)	None	Gapped spinons Gapped visons	$C_v$ and $\chi$ activated	MSE (§6) QDM on triangular and kagome lattices
Kagome (§7) Heisenberg AF	3	None ?	$\sim 1.15^N$ ?	None ?	Gapped triplets ? Gapless singlets	$C_v \sim T^\alpha$ ? $\chi$ activated	

Two-dimensional quantum antiferromagnets

71

This table summarizes the properties of some important phases encountered in 2D frustrated magnets.  $S$  is the value of the spin on each site. “Order” refers to the nature of the long-ranged correlations (if any). The ground-state degeneracy in the limit of an infinite system (with periodic boundary conditions) is indicated in the fourth column, except for RVB SL it is related to the spontaneously broken symmetries mentioned in the next column. Elementary excitations and the low-temperature behavior of the specific heat ( $C_v$ ) and uniform susceptibility ( $\chi$ ) are given in column six. The last column gives some examples of theoretical or experimental realizations of these phases. The six families of systems presented here of course do not exhaust all possibilities. The results which are plausible but still debated (concerning the spin- $\frac{1}{2}$  Heisenberg antiferromagnet on the kagome lattice in particular) are indicated by question marks. Some authors classify all the systems with gapped excitations in a loose category of “quantum disordered systems”, alluding to the absence of Néel long-ranged order. It is a rather unhappy appellation for VBC (which obviously have some order) and in fact for most of the quantum systems with a gap. In classical statistical physics “disorder” is associated to entropy, which is not the case in these gapped systems at  $T = 0$ .

2. B. Bernu, P. Lecheminant, C. Lhuillier and L. Pierre, Phys. Rev. B **50**, 10048 (1994).
3. Proceedings of the *Highly Frustrated Magnetism 2000* conference, published in J. Can. Phys **79**, (2001).
4. E. Fradkin, *Field Theories of Condensed Matter Systems*, Addison-Wesley (1998).
5. A. Auerbach, *Interacting electrons and Quantum Magnetism*, Springer-Verlag, Berlin Heidelberg New York, 1994.
6. A. M. Tsvelik, *Quantum Field Theory in Condensed Matter Physics* Cambridge University Press (1996).
7. S. Sachdev, *Quantum Phase Transitions*, Cambridge U. Press, New York (1999).
8. J. M. Luttinger and L. Tisza, Phys. Rev. **70**, 954 (1946).
9. P. Chandra and B. Douçot, Phys. Rev. B **38**, 9335 (1988).
10. J. Villain, R. Bidaux, J. P. Carton and R. Conte, J. Phys. (Paris) **41**, 1263 (1980).
11. E. Shender, Sov. Phys. JETP **56**, 178 (1982).
12. C. L. Henley, Phys. Rev. Lett. **62**, 2056 (1989).
13. A. Moreo, E. Dagotto, T. Jolicœur and J. Riera, Phys. Rev. B **42**, 6283 (1990).
14. P. Chandra, P. Coleman, and A. Larkin, Phys. Rev. Lett. **64**, 88 (1990).
15. R. R. P. Singh, W. Zheng, J. Oitmaa, O. P. Sushkov, C. J. Hamer, cond-mat/0303075.
16. G. Misguich, B. Bernu and L. Pierre, Phys. Rev. B **68**, 113409 (2003).
17. C. Weber and F. Mila, private communication.
18. T. Jolicœur, E. Dagotto, E. Gagliano and S. Bacci, Phys. Rev. B **42**, 4800 (1990).
19. A. Chubukov and T. Jolicœur, Phys. Rev. B **46**, 11137 (1992).
20. S. E. Korshunov, Phys. Rev. B **47**, 6165 (1993).
21. P. Lecheminant, B. Bernu, C. Lhuillier and L. Pierre, Phys. Rev. B **52**, 6647 (1995).
22. R. Melzi *et al.*, Phys. Rev. Lett. **85**, 1318 (2000).
23. R. Melzi *et al.*, Phys. Rev. B **64**, 024409 (2001).
24. H. Rosner *et al.*, Phys. Rev. Lett. **88**, 186405 (2002).
25. H. Rosner *et al.*, Phys. Rev. B **67**, 014416 (2003).
26. D. J. Klein, J. Phys. A: Math. Gen. **15**, 661 (1982).
27. C. K. Majumdar and D. K. Ghosh, J. Math. Phys. **10**, 1399 (1969).
28. R. R. P. Singh, M. P. Gelfand and D. A. Huse, Phys. Rev. Lett. **61**, 2484 (1988).
29. M. P. Gelfand, R. R. P. Singh and D. A. Huse, J. Stat. Phys. **59**, 1093 (1990).
30. Zheng Weihong, J. Oitmaa, and C. J. Hamer, Phys. Rev. B **43**, 8321 (1991).
31. J. Oitmaa and Zheng Weihong, Phys. Rev. B **54**, 3022 (1996).
32. M. P. Gelfand, R. R. P. Singh and D. A. Huse, Phys. Rev. B **40**, 10801 (1989).
33. M. P. Gelfand. Phys. Rev. B **42**, 8206 (1990).



34. R. R. P. Singh, Zheng Weihong, C. J. Hamer, and J. Oitmaa, Phys. Rev. B **60**, 7278 (1999).
35. V. N. Kotov, J. Oitmaa, O. Sushkov and Zheng Weihong, Phil. Mag. B **80**, 1483 (2000).
36. M. E. Zhitomirsky and K. Ueda, Phys. Rev. B **54**, 9007 (1996).
37. L. Capriotti, F. Becca, A. Parola, and S. Sorella, Phys. Rev. Lett. **87**, 097201 (2001).
38. O. P. Sushkov, J. Oitmaa, and Zheng Weihong, Phys. Rev. B **66**, 054401 (2002).
39. O. P. Sushkov, J. Oitmaa, and Zheng Weihong, Phys. Rev. B **63**, 104420 (2001).
40. M. S. L. du Croo de Jongh, J. M. J. Van Leeuwen, and W. Van Saarloos, Phys. Rev. B **62**, 14844 (2000).
41. E. Dagotto and A. Moreo, Phys. Rev. B **39**, 4744 (1989), Phys. Rev. Lett. **63**, 2148 (1989).
42. F. Figueirido *et al.*, Phys. Rev. B **41**, 4619 (1990).
43. D. Poilblanc, E. Gagliano, S. Bacci and E. Dagotto, Phys. Rev. B, **43** 10970 (1991).
44. H. J. Schulz, T. A. L. Ziman, Europhys. Lett. **18**, 355 (1992). T. Einarsson and H. J. Schulz, Phys. Rev. B **51**, 6151 (1995).  
H. J. Schulz, T. A. L. Ziman, D. Poilblanc, J. Physique I **6**, 675 (1996).
45. S. Chakravarty, B. I. Halperin and D. R. Nelson, Phys. Rev. B **39**, 2344 (1989). H. Neuberger and T. Ziman, Phys. Rev. B **39**, 2608 (1989).  
D. Fisher, Phys. Rev. B **39**, 11783 (1989). T. Einarsson and H. Johannes-son, Phys. Rev. B **43**, 5867 (1991). P. Hasenfratz and F. Niedermayer, Z. Phys. B. Condens. Matter **92**, 91 (1993).
46. A. W. Sandvik, Phys. Rev. B **56**, 11678 (1997).
47. S. Sorella, Phys. Rev. Lett. **80**, 4558 (1998).
48. S. Sorella, Phys. Rev. B **64**, 024512 (2001).
49. S. White, Phys. Rev. Lett. **69**, 2863 (1992).
50. S. White, Phys. Rev. B **48**, 10345 (1993).
51. T. Giamarchi and C. Lhuillier, Phys. Rev. B **43**, 12943 (1991).
52. B. Shastry and B. Sutherland, Phys. Rev. Lett. **47**, 964 (1981).
53. F. Haldane, Phys. Rev. B **25**, 4925 (1982).
54. I. Affleck, J. Phys. Cond. Matt. **1**, 3047 (1989).
55. H. Yokoyama and Y. Saiga, J. Phys. Soc. Jpn. **66**, 3617 (1997).
56. T. Nakamura and S. Takada, Phys. Rev. B **55**, 14413 (1997).
57. D. Augier, E. Sorensen, J. Riera, and D. Poilblanc, Phys. Rev. B **60**, 1075 (1999).
58. E. Dagotto and T. M. Rice, Science **271**, 618 (1996).
59. A. A. Nersesyan and A. M. Tsvelik, Phys. Rev. Lett. **78**, 3939 (1997).
60. A. K. Kolezhuk and H.-J. Mikeska, Int. J. Mod. Phys. B **12**, 2325 (1998).  
Phys. Rev. Lett. **80**, 2709 (1998). Phys. Rev. B **56**, 11380 (1997).
61. I. Affleck, T. Kennedy, E. Lieb, and H. Tasaki, Phys. Rev. Lett. **59**, 799 (1987).
62. I. Affleck, T. Kennedy, E. H. Lieb, and H. Tasaki, Commun. Math. Phys.

- 115**, 477 (1988).
63. M. den Nijs and K. Rommelse, Phys. Rev. B **40**, 4709 (1989).
  64. T. Kennedy and H. Tasaki, Phys. Rev. B **45**, 304 (1992).
  65. T. Jolicœur, private communication.
  66. K. Hida, J. Phys. Soc. Jpn. **69**, 4003 (2000).
  67. Y. Yamashita and K. Ueda, Phys. Rev. Lett. **85**, 4960 (2000).
  68. N. Katoh and M. Imada, J. Phys. Soc. Jpn. **63**, 4529 (1994). M. Troyer, H. Tsunetsugu, and D. Wuertz, Phys. Rev. B **50**, 13515 (1994). S. Taniguchi *et al.*, J. Phys. Soc. Jpn. **64**, 2758 (1995). K. Kodama *et al.*, J. Phys. Soc. Jpn. **65**, 1941 (1996). Y. Fukumoto and A. Oguchi, J. Phys. Soc. Jpn. **65**, 1440 (1996). K. Kodama *et al.*, J. Phys. Soc. Jpn. **66**, 793 (1997). T. Miyasaka and D. Yoshioka, J. Phys. Soc. Jpn. **65**, 2370 (1996). T. Ohama, H. Yasuoka, M. Isobe, and Y. Ueda, J. Phys. Soc. Jpn. **66**, 23 (1997).
  69. K. Ueda, H. Kontani, M. Sigrist, and P. A. Lee, Phys. Rev. Lett. **76**, 1932 (1996).
  70. M. Albrecht and F. Mila, Phys. Rev. B **53**, 2945 (1996).
  71. M. Troyer, H. Kontani, and K. Ueda, Phys. Rev. Lett. **76**, 3822 (1996).
  72. S. Sachdev and N. Read, Phys. Rev. Lett. **77**, 4800 (1996).
  73. O. A. Starykh *et al.*, Phys. Rev. Lett. **77**, 2558 (1996).
  74. Zheng Weihong *et al.*, Phys. Rev. B **55**, 11377 (1997).
  75. H. Kageyama *et al.*, Phys. Rev. Lett. **82**, 3168 (1999).
  76. H. Nojiri *et al.*, J. Phys. Soc. Jpn. **68**, 2906 (1999).
  77. S. Miyahara and K. Ueda, Phys. Rev. Lett. **82**, 3701 (1999).
  78. H. Kageyama *et al.*, Phys. Rev. Lett. **84**, 5876 (2000).
  79. A. Koga and N. Kawakami, Phys. Rev. Lett. **84**, 4461 (2000).
  80. E. Müller-Hartmann, R. R. P. Singh, C. Knetter, and G. S. Uhrig, Phys. Rev. Lett. **84**, 1808 (2000).
  81. K. Totsuka, S. Miyahara, and K. Ueda, Phys. Rev. Lett. **86**, 520 (2001).
  82. A. Läuchli, S. Wessel, and M. Sigrist, Phys. Rev. B **66**, 014401 (2002).
  83. K. Kodama *et al.*, Science **298**, 395 (2002).
  84. S. Miyahara and K. Ueda, J. Phys.: Condens. Matter **15**, R327-R366 (2003).
  85. B. Shastry and B. Sutherland, Physica B (Amsterdam) **108**, 1069 (1981).
  86. O. Cepas, T. Ziman, Proceedings of the conference in Fukuoka, Nov. 2001, to appear in Fukuoka University Press [cond-mat/0207191]. O. Cepas, T. Sakai, T. Ziman, Progr. Theor. Phys. Suppl. **145**, 43 (2002).
  87. W. Zheng, J. Oitmaa, and C. J. Hamer Phys. Rev. B **65**, 014408 (2002).
  88. M. Albrecht and F. Mila, Europhys. Lett. **34**, 145 (1996).
  89. C. H. Chung, J. B. Marston, and S. Sachdev, Phys. Rev. B **64**, 134407 (2001).
  90. Y. Fukumoto and A. Oguchi, J. Phys. Soc. Jpn. **68**, 3655 (1999).
  91. T. Momoi and K. Totsuka, Phys. Rev. B **61**, 3231 (2000).
  92. T. Momoi and K. Totsuka, Phys. Rev. B **62**, 15067 (2000).
  93. S. Miyahara and K. Ueda, Phys. Rev. B **61**, 3417 (2000).
  94. G. Misguich, T. Jolicœur, and S. M. Girvin, Phys. Rev. Lett. **87**, 097203 (2001).
  95. C. Lhuillier and G. Misguich, in *High Magnetic Fields*, edited by C. Berthier,

- L. Levy, and G. Martinez (Springer, Berlin, 2002), pp. 161–190, cond-mat/0109146.
96. P. W. Leung and N. Lam, Phys. Rev. B **53**, 2213 (1996).
  97. J.-B. Fouet, P. Sindzingre, and C. Lhuillier, Eur. Phys. J. B **20**, 241 (2001).
  98. B. Canals, Phys. Rev. B **65**, 184408 (2002).
  99. J.-B. Fouet, M. Mambrini, P. Sindzingre, and C. Lhuillier, Phys. Rev. B **67**, 054411 (2003).
  100. P. Sindzingre, J. B. Fouet, and C. Lhuillier, Phys. Rev. B **66**, 174424 (2002).
  101. W. Brenig and A. Honecker, Phys. Rev. B **65**, 140407R (2002).
  102. E. Berg, E. Altman, and A. Auerbach, Phys. Rev. Lett. **90**, 147204 (2003).
  103. O. Tchernyshyov, O. A. Starykh, R. Moessner and A. G. Abanov, cond-mat/0301303.
  104. R. Moessner, Oleg Tchernyshyov and S. L. Sondhi, cond-mat/0106286.
  105. S. Palmer and J. T. Chalker, Phys. Rev. B **64**, 094412 (2002).
  106. R. Moessner and J. T. Chalker, Phys. Rev. B **58**, 12049 (1998).
  107. R. Moessner and J. T. Chalker, Phys. Rev. Lett. **80**, 2929 (1998).
  108. O. A. Petrenko and D. McK. Paul, Phys. Rev. B **63**, 024409 (2001).
  109. Hikaru Kawamura and Takuya Arimori, Phys. Rev. Lett. **88**, 077202 (2002).
  110. C. L. Henley, Can. J. Phys. (Canada) **79**, 1307 (2001). [cond-mat/0009130]
  111. J.-B. Fouet, Ph.D. thesis, Université Cergy Pontoise, 2003.
  112. M. P. Gelfand *et al.*, Phys. Rev. Lett. **77**, 2794 (1996).
  113. F. Becca and F. Mila, Phys. Rev. Lett. **89**, 037204 (2002).
  114. G. Misguich, C. Lhuillier, B. Bernu and C. Waldtmann, Phys. Rev. B **60**, 1064 (1999).
  115. I. Affleck, Phys. Rev. Lett. **54**, 966 (1985).
  116. I. Affleck and J. Marston, Phys. Rev. B **37**, 3774 (1988).
  117. D. Arovas and A. Auerbach, Phys. Rev. B **38**, 316 (1988).
  118. N. Read and S. Sachdev, Phys. Rev. Lett. **62**, 1694 (1989).
  119. N. Read and S. Sachdev, Phys. Rev. B **42**, 4568 (1990).
  120. N. Read and S. Sachdev, Phys. Rev. Lett. **66**, 1773 (1991).
  121. S. Sachdev and N. Read, Int. J. Mod. Phys. **5**, 219 (1991).
  122. S. Sachdev in *Low Dimensional Quantum Field Theories for Condensed Matter Physicists* edited by Y. Lu, S. Lundqvist, and G. Morandi, World Scientific, Singapore, 1995. cond-mat/9303014.
  123. N. Read and S. Sachdev, Nucl. Phys. B **316**, 609 (1989).
  124. D. Rokhsar, Phys. Rev. B **42**, 2526 (1991).
  125. K. G. Wilson, Phys. Rev. D **10**, 2445 (1974).
  126. R. Balian, J. M. Drouffe, and C. Itzykson, Phys. Rev. D **10**, 3376 (1974), Phys. Rev. D **11**, 2098 (1975), Phys. Rev. D **11**, 2098 (1975).
  127. D. P. Arovas and A. Auerbach, Phys. Rev. B **38**, 316 (1988). A. Auerbach and D. P. Arovas, Phys. Rev. Lett. **61**, 617 (1988). J. E. Hirsch and S. Tang, Phys. Rev. B **39**, 2850 (1989).
  128. H. A. Ceccatto, C. J. Gazza, and A. E. Trumper, Phys. Rev. B **47**, 12329 (1993). A. E. Trumper, L. O. Manuel, C. J. Gazza, and H. A. Ceccatto Phys. Rev. Lett. **78**, 2216 (1997).
  129. We thank O. Tchernyshyov for pointing us this physical interpretation of

the  $U(1)$  flux.

130. S. Sachdev, Phys. Rev. B **45**, 12377 (1992).
131. C. H. Chung and J. B. Marston and Ross H. McKenzie, J. Phys.: Condens. Matter **13**, 5159 (2001). [cond-mat/0012216]
132. F. D. M. Haldane, Phys. Lett. **93A**, 464 (1983);  
Phys. Rev. Lett. **50**, 1153 (1983).
133. F. D. M. Haldane, Phys. Rev. Lett. **61**, 1029 (1988).
134. X. G. Wen and A. Zee, Phys. Rev. Lett. **61**, 1025 (1988). E. Fradkin and M. Stone, Phys. Rev. B **38**, 7215 (1988). T. Dombre and N. Read, Phys. Rev. B **38**, 7181 (1988).
135. K. Harada, N. Kawashima, and M. Troyer, Phys. Rev. Lett. **90**, 117203 (2003).
136. E. Fradkin and S. H. Shenker, Phys. Rev. D **19**, 3682 (1979).
137. P. W. Kasteleyn, Physica **27**, 1209 (1961).
138. M. E. Fisher, Phys. Rev. **124**, 1664 (1961).
139. P. W. Kasteleyn, J. of Math. Phys. **4**, 287 (1963).
140. R. Moessner, S. L. Sondhi, E. Fradkin, Phys. Rev. B **65**, 024504 (2002).
141. G. Misguich, D. Serban, V. Pasquier, Phys. Rev. Lett. **89**, 137202 (2002).
142. R. Moessner, S. L. Sondhi, Phys. Rev. B **68**, 054405 (2003).
143. D. S. Rokhsar and S. A. Kivelson, Phys. Rev. Lett. **61**, 2376 (1988).
144. R. Moessner and S. L. Sondhi, Phys. Rev. Lett. **86**, 1881 (2001).
145. R. Moessner, S. L. Sondhi, and P. Chandra, Phys. Rev. Lett. **84**, 4457 (2000).
146. B. Sutherland, Phys. Rev. B **37**, 3786 (1988).
147. J. B. Marston, C. Zeng, J. Appl. Phys. **69**, 5962 (1991).
148. P. W. Leung, K. C. Chiu and K. J. Runge, Phys. Rev. B **54**, 12938 (1996).
149. M. E. Fisher and J. Stephenson Phys. Rev. **132**, 1411 (1963).
150. R. Moessner and S. L. Sondhi, cond-mat/0307592. See Appendix B concerning the square-lattice QDM .
151. R. Moessner, S. L. Sondhi and P. Chandra, Phys. Rev. B **64**, 144416 (2001).
152. D. A. Huse, W. Krauth, R. Moessner and S. L. Sondhi, cond-mat/0305318 and references therein.
153. L. S. Levitov, Phys. Rev. Lett. **64**, 92 (1990),  
C. L. Henley, J. Stat. Phys. **89**, 483 (1997).
154. P. Fendley, R. Moessner and S. L. Sondhi, Phys. Rev. B **66**, 214513 (2002).
155. A. Ioselevich, D. A. Ivanov and M. V. Feigelman, Phys. Rev. B **66**, 174405 (2002).
156. L. B. Ioffe, M. V. Feigel'man, A. Ioselevich, D. Ivanov, M. Troyer, G. Blatter, Nature **415**, 503 (2002).
157. G. Misguich, C. Lhuillier, M. Mambrini, P. Sindzingre, Eur. Phys. J. B **26**, 167 (2002).
158. X. G. Wen, Phys. Rev. B **44**, 2664 (1991).
159. S. Kivelson, Phys. Rev. B **39**, 259 (1989).
160. N. Read and B. Chakraborty, Phys. Rev. B **40**, 7133 (1989).
161. T. Senthil and M. P. A. Fisher, Phys. Rev. B **62**, 7850 (2000).
162. T. Senthil and M. P. A. Fisher, Phys. Rev. Lett. **86**, 292 (2001); Phys. Rev.

- B **63**, 134521 (2001).
163. R. P. Feynman, Phys. Rev. **90**, 1116 (1952), Phys. Rev. **91**, 1291 (1953).
  164. V. Elser and C. Zeng. Phys. Rev. B **48**, 13647 (1993).
  165. A. J. Phares and F. J. Wunderlich, Nuovo Cimento B **101**, 653 (1988).
  166. See §V.E.6 of Ref.<sup>170</sup>
  167. This follows from the independence of the arrow variables, see §V.B of Ref.<sup>170</sup>
  168. A. M. Polyakov, *Gauge Fields and Strings*, (Harwood Academic, New York, 1987).
  169. J. B. Kogut, Rev. Mod. Phys. **51**, 659 (1979).
  170. G. Misguich, D. Serban and V. Pasquier, Phys. Rev. B **67**, 214413 (2003).
  171. C. Zeng and V. Elser. Phys. Rev. B **51**, 8318 (1995).
  172. D. J. Thouless, Proc. Phys. Soc. London **86**, 893 (1965).
  173. M. Roger, J. H. Hetherington, and J. M. Delrieu, Rev. Mod. Phys. **55**, 1 (1983).
  174. M. C. Cross and D. S. Fisher, Rev. Mod. Phys. **57**, 881 (1985).
  175. D. S. Greywall and P. A. Busch, Phys. Rev. Lett. **62**, 1868 (1989).  
D. S. Greywall, Phys. Rev. B **41**, 1842 (1990).
  176. H. Godfrin and R. E. Rapp, Adv. Phys. **44**, 113 (1995).
  177. M. Roger, Phys. Rev. B **30**, 6432 (1984).
  178. M. Roger, C. Bäuerle, Yu. M. Bunkov, A.-S. Chen, and H. Godfrin, Phys. Rev. Lett. **80**, 1308 (1998).
  179. D. M. Ceperley and G. Jacucci, Phys. Rev. Lett. **58**, 1648 (1987).
  180. B. Bernu, D. Ceperley, and C. Lhuillier, J. Low Temp. Phys. **89**, 589 (1992).
  181. D. M. Ceperley, Rev. Mod. Phys. **67**, 279 (1995).
  182. B. Bernu and D. Ceperley, in *Quantum Monte Carlo Methods in Physics and Chemistry*, edited by M. P. Nightingale and C. J. Umrigar (Kluwer, Dordrecht, The Netherlands, 1999).
  183. H. Ashizawa and D. S. Hirashima, Phys. Rev. B **62**, 9413 (2000).
  184. J. M. Delrieu, M. Roger, J. H. Hetherington, J. Low Temp. Phys. **40**, 71 (1980).
  185. H. Franco, R. E. Rapp and H. Godfrin, Phys. Rev. Lett. **57**, 1161 (1986).
  186. G. Misguich, B. Bernu, C. Lhuillier, and C. Waldtmann, Phys. Rev. Lett. **81**, 1098 (1998).
  187. W. LiMing, G. Misguich, P. Sindzingre, and C. Lhuillier, Phys. Rev. B **62**, 6372 (2000).
  188. K. Ishida, M. Morishita, K. Yawata, and H. Fukuyama, Phys. Rev. Lett. **79**, 3451 (1997).
  189. E. Collin *et al.*, Phys. Rev. Lett. **86**, 2447 (2001).
  190. M. Katano and D. S. Hirashima, Phys. Rev. B **62**, 2573 (2000).
  191. D. S. Hirashima and K. Kubo, Phys. Rev. B **63**, 125340 (2001).
  192. B. Bernu, L. Candido, and D. M. Ceperley Phys. Rev. Lett. **86**, 870 (2001).
  193. T. Okamoto and S. Kawaji, Phys. Rev. B **57**, 9097 (1998).
  194. M. Roger and J. M. Delrieu, Phys. Rev. B **39**, 2299 (1989).
  195. S. Sugai *et al.*, Phys. Rev. B **42**, 1045 (1990).
  196. R. Coldea *et al.*, Phys. Rev. Lett. **86**, 5377 (2001).

197. E. Müller-Hartmann and A. Reischl, Eur. Phys. J. B **28**, 173 (2002).
198. A. A. Katanin, and A. P. Kampf, Phys. Rev. B **67**, 100404R (2003).
199. M. Matsuda *et al.*, Phys. Rev. B **62**, 8903 (2000).
200. S. Brehmer *et al.*, Phys. Rev. B **60**, 329 (1999).
201. K. P. Schmidt, C. Knetter and G. S. Uhrig, Europhys. Lett. **56**, 877 (2001).
202. A. Göling *et al.*, Phys. Rev. B **67**, 052403 (2003).
203. M. Müller, T. Vekua, and H.-J. Mikeska, Phys. Rev. B **66**, 134423 (2002).
204. T. Hikihara, T. Momoi, and X. Hu, Phys. Rev. Lett. **90**, 087204 (2003).
205. A. Läuchli, G. Schmid, and M. Troyer, Phys. Rev. B **67**, 100409R (2003).
206. Y. Honda and T. Horiguchi, cond-mat/0106426.
207. K. Hijii and K. Nomura Phys. Rev. B **65**, 104413 (2002).
208. T. Momoi, T. Hikihara, M. Nakamura, Xiao Hu, Phys. Rev. B **67**, 174410 (2003).
209. A. Läuchli, talk given at the *Highly Frustrated Magnetism 2003* conference, Grenoble, France (August 2003).
210. K. Kubo and T. Momoi, Z. Phys. B **103**, 485 (1997).
211. T. Momoi, K. Kubo, and K. Niki, Phys. Rev. Lett. **79**, 2081 (1997).
212. G. Misguich, B. Bernu, and C. Lhuillier, J. Low Temp. Phys. **110**, 327 (1998).
213. K. Kubo, H. Sakamoto, T. Momoi, and K. Niki, J. Low Temp. Phys. **111**, 583 (1998).
214. A 16- and a 32-site triangular lattices which do not frustrate the staggered VBC were investigated. In both cases some of the irreducible representations of the space group required to break the appropriate lattice symmetries are very high in the spectrum. C. Lhuillier and G. Misguich (unpublished).
215. E. H. Lieb, T. D. Schultz, D. C. Mattis., Ann. Phys. (N.Y) **16**, 407 (1961).
216. I. Affleck and E. Lieb, Lett. Math. Phys. **12**, 57 (1986).
217. M. Oshikawa, Phys. Rev. Lett. **84**, 1535 (2000).
218. M. B. Hastings, cond-mat/0305505.
219. M. Oshikawa, Phys. Rev. Lett. **90**, 236401 (2003).
220. A. A. Nersesyan, A. O. Gogolin, and F. H. L. Essler, Phys. Rev. Lett. **81**, 910 (1998).
221. P. Azaria *et al.*, Phys. Rev. Lett. **81**, 1694 (1998).
222. V. J. Emery, E. Fradkin, S. A. Kivelson and T. C. Lubensky, Phys. Rev. Lett. **85**, 2160 (2000).
223. M. Bocquet, F. Essler, A. M. Tsvelik and A. O. Gogolin, Phys. Rev. B **64**, 094425 (2001), M. Bocquet, Phys. Rev. B **65**, 1884415 (2001).
224. A. Vishwanath and D. Carpentier, Phys. Rev. Lett. **86**, 676 (2001).
225. S. Sachdev and K. Park, Annals of Physics (N.Y.), **58**, 298 (2002).
226. O. A. Starykh and R. R. P. Singh and G. C. Levine, Phys. Rev. Lett. **88**, 167203 (2002).
227. R. Coldea, D. A. Tennant, A. M. Tsvelik, and Z. Tylczynski, Phys. Rev. Lett. **86**, 1335 (2001).
228. A. Kitaev, Annals Phys. **303**, 2 (2003). [quant-ph/9707021]
229. C. Nayak and K. Shtengel, Phys. Rev. B **64**, 064422 (2001).
230. L. Balents, M. P. A. Fisher, and S. M. Girvin, Phys. Rev. B **65**, 224412

- (2002).
231. A. Paramekanti, L. Balents, and M. P. A. Fisher Phys. Rev. B **66**, 054526 (2002).
  232. A. W. Sandvik, S. Daul, R. R. P. Singh, and D. J. Scalapino, Phys. Rev. Lett. **89**, 247201 (2002).
  233. T. Senthil and O. Motrunich, Phys. Rev. B **66**, 205104 (2002).
  234. L. Pauling, in *The nature of the chemical bond* (Cornell University Press, Ithaca, 1938).
  235. K. Kano and S. Naya, Prog. in Theor. Phys. **10**, 158 (1953).
  236. D. Huse and A. Rutenberg, Phys. Rev. B **45**, 7536 (1992).
  237. R. Moessner and S. L. Sondhi, Phys. Rev. B **63**, 224401 (2001).
  238. J. Chalker, P. C. W. Holdsworth, and E. F. Shender, Phys. Rev. Lett. **68**, 855 (1992).
  239. R. J. Baxter, J. Math. Phys. **11**, 784 (1970).
  240. I. Richte, P. Chandra, and P. Coleman, Phys. Rev. B **47**, 15342 (1993).
  241. J. Reimers and A. Berlinsky, Phys. Rev. B **48**, 9539 (1993).
  242. M. Elhajal, Ph. D. thesis, Université Joseph Fourier. Grenoble. France, 2002.
  243. M. Elhajal, B. Canals, and C. Lacroix, Phys. Rev. B **66**, 014422 (2002).
  244. A. Keren, Phys. Rev. Lett. **72**, 3254 (1994).
  245. V. Elser, Phys. Rev. Lett. **62**, 2405 (1989).
  246. J. Chalker and J. Eastmond, Phys. Rev. B **46**, 14201 (1992).
  247. S. Sachdev, Phys. Rev. B **45**, 12377 (1992).
  248. P. Leung and V. Elser, Phys. Rev. B **47**, 5459 (1993).
  249. P. Lecheminant *et al.*, Phys. Rev. B **56**, 2521 (1997).
  250. C. Waldtmann *et al.*, Eur. Phys. J. B **2**, 501 (1998).
  251. F. Mila, Phys. Rev. Lett. **81**, 2356 (1998).
  252. P. Sindzingre *et al.*, Phys. Rev. Lett. **84**, 2953 (2000).
  253. M. Mambrini and F. Mila, Eur. Phys. J. B **17**, 651 (2001).
  254. S. Dommange, M. Mambrini, B. Normand and F. Mila, cond-mat/0306299.
  255. C. Zeng and V. Elser, Phys. Rev. B **42**, 8436 (1990).
  256. R. Singh and D. Huse, Phys. Rev. Lett. **68**, 1766 (1992).
  257. K. Hida, J. Phys. Soc. Jpn. **70**, 3673 (2001).
  258. D. C. Cabra, M. D. Grynberg, P. C. W. Holdsworth, P. Pujol, Phys. Rev. B **65**, 094418 (2002).
  259. N. Eltsner and A. P. Young, Phys. Rev. B **50**, 6871 (1994).
  260. T. Nakamura and S. Miyashita, Phys. Rev. B **52**, 9174 (1995).
  261. P. Tomczak and J. Richter, Phys. Rev. B **54**, 9004 (1996).
  262. A. P. Ramirez, B. Hessen, and M. Winkelman, Phys. Rev. Lett. **84**, 2957 (2000).
  263. P. Mendels *et al.*, Phys. Rev. Lett. **85**, 3496 (2000).
  264. A. V. Syromyatnikov and S. V. Maleyev, Phys. Rev. B **66**, 132408 (2002).
  265. P. Nikolic and T. Senthil, cond-mat/0305189.
  266. T. Mondelli *et al.*, Physica B **284**, 1371 (2000).
  267. A. Georges, R. Siddhant and S. Florens, Phys. Rev. Lett. **87**, 277203 (2001).
  268. C. Lhuillier and P. Sindzingre, in *Quantum properties of Low dimensional*

- antiferromagnets*, edited by Y. Ajiro and J. P. Boucher (Kyushu University Press, Fukuoka, Japan, 2002), p. 111.
269. S. Sachdev and M. Vojta, Proceedings of the XIII International Congress on Mathematical Physics, July 2000, London. A. Fokas, A. Grigoryan, T. Kibble, and B. Zegarlinski eds, International Press, Boston (2001) [cond-mat/0009202].
270. Y. Uemura *et al.*, Phys. Rev. Lett. **73**, 3306 (1994).
271. A. Ramirez, G. P. Espinosa, and A. S. Cooper, Phys. Rev. Lett. **64**, 2070 (1990).
272. S.-H. Lee *et al.*, Europhys. Lett. **35**, 127 (1996).
273. A. Keren *et al.*, Phys. Rev. B **53**, 6451 (1996).
274. A. S. Wills *et al.*, Europhys. Lett. **42**, 325 (1998).
275. K. Awaga *et al.*, Phys. Rev. B **49**, 3975 (1994).
276. N. Wada *et al.*, J. Phys. Soc. Jpn. **66**, 961 (1997).
277. I. Watanabe *et al.*, Phys. Rev. B **58**, 2438 (1998).
278. B. Canals and C. Lacroix, Phys. Rev. Lett. **80**, 2933 (1998).
279. A. B. Harris, A. J. Berlinsky and C. Bruder, J. Appl. Phys. **69**, 5200 (1991).
280. H. Tsunetsugu, J. Phys. Soc. Jpn. **70**, 640 (2001).
281. H. Tsunetsugu, Phys. Rev. B **65**, 024415 (2002).
282. J. V. Delft and C. L. Henley, Phys. Rev. Lett. **69**, 3236 (1992), Phys. Rev. B **48**, 965 (1993).
283. S. Sachdev, Annals Phys. **303**, 226 (2003) [cond-mat/0211027] and Rev. Mod. Phys. **75**, 913 (2003) [cond-mat/0211005].
284. X. Wen, F. Wilczek, and A. Zee, Phys. Rev. B **39**, 11413 (1989).
285. V. Kalmeyer and R. Laughlin, Phys. Rev. Lett. **59**, 2095 (1987), Phys. Rev. B **39**, 11879 (1989).
286. K. Yang, L. Warman, and S. M. Girvin, Phys. Rev. Lett. **70**, 2641 (1993).